AD_____

Award Number: DAMD17-01-1-0165

TITLE: Cripto: A target for breast cancer treatment

PRINCIPAL INVESTIGATOR: Eileen D. Adamson, Ph.D.

CONTRACTING ORGANIZATION: The Burnham Institute
La Jolla, California 92037

REPORT DATE: June 2004

TYPE OF REPORT: Final

PREPARED FOR: U.S. Army Medical Research and Materiel Command
Fort Detrick, Maryland 21702-5012

DISTRIBUTION STATEMENT: Approved for Public Release;
Distribution Unlimited

The views, opinions and/or findings contained in this report are those of the author(s) and should not be construed as an official Department of the Army position, policy or decision unless so designated by other documentation.

REPORT DOCUMENTATION PAGE

Form Approved
OMB No. 074-0188

1. AGENCY USE ONLY (Leave blank)	2. REPORT DATE	3. REPORT TYPE AND DATES COVERED
	June 2004	Final (1 Jun 01 - 31 May 04)

4. TITLE AND SUBTITLE
Cripto: A target for breast cancer treatment

5. FUNDING NUMBERS
DAMD17-01-1-0165

6. AUTHOR(S)
Eileen D. Adamson, Ph.D.

7. PERFORMING ORGANIZATION NAME(S) AND ADDRESS(ES)
The Burnham Institute
La Jolla, California 92037

E-Mail: eadamson@burnham.org

8. PERFORMING ORGANIZATION REPORT NUMBER

9. SPONSORING / MONITORING AGENCY NAME(S) AND ADDRESS(ES)
U.S. Army Medical Research and Materiel Command
Fort Detrick, Maryland 21702-5012

10. SPONSORING / MONITORING AGENCY REPORT NUMBER

11. SUPPLEMENTARY NOTES
Report contains color

12a. DISTRIBUTION / AVAILABILITY STATEMENT
Approved for Public Release; Distribution Unlimited

12b. DISTRIBUTION CODE

13. Abstract ***(Maximum 200 Words)*** *(abstract should contain no proprietary or confidential information)*

Cripto is a growth factor that is important in breast cancer, leading to increases in cell proliferation and to increased survival of cells. Specific receptors for this factor have not been defined for breast cells but there is evidence from published work that Cripto acts as a co-factor for the Nodal factor, previously thought to be present and active only in early embryonic development. This work will define the importance of this route of Cripto signaling in breast cells compared with the other known route involving Ras and the MAPK/Erk pathway. A number of possible ways that Cripto could effect a proliferative signal to breast cells has been described by the PI in a review article previously reported and published in J Cell Physiol. 190, 267-278. The experimental studies for exploring the mechanism of activation of breast cancer cells by Cripto is described for the first year of the experimental work, with the aim of making peptides that block Cripto and its tumorigenic effects.

14. SUBJECT TERMS
Growth factor, proliferation, mutation, signal blocking peptides

15. NUMBER OF PAGES
54

16. PRICE CODE

17. SECURITY CLASSIFICATION OF REPORT	18. SECURITY CLASSIFICATION OF THIS PAGE	19. SECURITY CLASSIFICATION OF ABSTRACT	20. LIMITATION OF ABSTRACT
Unclassified	Unclassified	Unclassified	Unlimited

Table of Contents

CRIPTO: A TARGET for BREAST CANCER TREATMENT

INTRODUCTION

This study was delayed in starting by one year because of lack of a suitable post-doctoral associate to perform the laboratory work. Dr Min Li has been working on the project since July, 2002, and we are now making the final report for June 30, 2004.

Cripto is a known requirement for development of the early embryo and for the development of the normal mammary gland. If this gene is reactivated aberrantly, it contributes to breast cancer cell growth and/or survival. This has been known for some time. But the receptor for Cripto remained unknown until recently and the mechanism of its interaction has just been evaluated through a study of the molecular structure of Cripto.

We reported last year that the literature meanwhile has described a few important advances of how Cripto interacts with the mammary and other cell types. Cripto (CR1 or Cr1 (mouse)) acts as both a ligand and a co-receptor in the stimulation of cells and the generation of a signal to redirect the behavior of breast cancer (and colon) cancer cells. With the cell line that we used we were not able to reproduce the published results showing that Cripto induced increased proliferation and/or survival in culture as described (Bianco et al., 2001; Wechselberger et al., 2001). We found that the cell line was heterogenous and discontinued its use. However, even for the cloned line that we obtained that was derived from the same NmuMG line, and also for the human breast cancer cell line,MCF7 cells, Dr Li was unable to find the same responses to over-expressed cripto and mutant cripto as published (De Luca et al., 1999). We reported last year these difficulties at length. Several excellent papers on Cripto have been published by other groups that have used different approaches to achieve similar goals. Therefore, we felt that it was not productive to continue this line of research. A summary of what we have done is described in part 1.

This year Dr Li was worried that his work was not producing consistent results and was anxious to do research that was advancing the field of cancer research as well as advancing his career. We agreed therefore that he should work on another topic of his choice. He chose to work on the gene GADD45A as a target of regulation of the transcription factor Egr1, and its role in survival and anti-apoptosis . We are reporting these studies now in part 2 of the Body of the report.

BODY OF REPORT-Part 1- Cripto

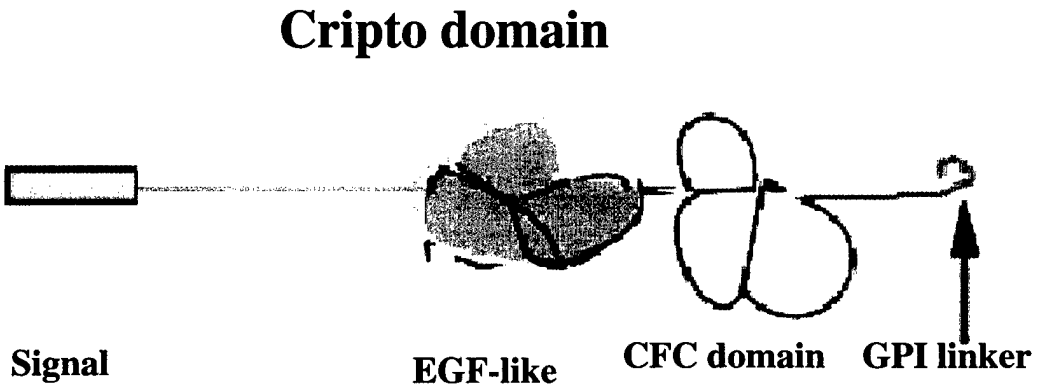

Cripto is a known requirement for development of the early embryo and for the development of the normal mammary gland. If this gene is reactivated aberrantly, it contributes to breast cancer cell growth and/or survival. This has been known for some time. But the receptor for Cripto remained unknown until recently and the mechanism of its interaction has just been evaluated through a study of the molecular structure of Cripto.

A new hypothesis that we suggested (Adamson et al., 2002) was that in breast cancer cells, the CR1/AKT/MAPK/ ERK pathway may also play a major role in the transformed character of the cells that leads to excess proliferation. This has proved to be correct and was published by a large collaborative group (Normanno et al., 2004). In addition, our hypothesis was that the CFC domain of Cripto was important in receptor binding was also proved correct by several groups in different systems. I have collaborated with colleagues in Italy to produce two papers published in J Cell Biology and in Development (see below).

The Aims of the idea grant were to investigate the possibility of making mutants of Cripto that would disable or activate the disulfide loop structures of the CFC domain of Cripto. This domain is known to be required for the binding of Cripto to **nodal** , a TGFβ family member that requires Cripto to act as its co-receptor.

Our suggested structure of mouse Cripto-CFC domain was:-

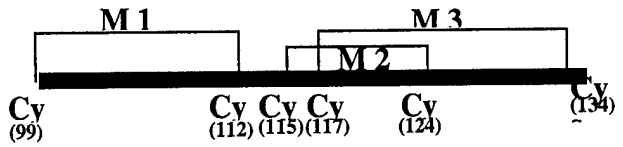

For each mutated Cripto (M1, M2 and M3), 2 Cys were replaced by Ala

The newly published structure (Foley et al., 2003) indicates that this is incorrect and this explains why our mutated versions of Cripto gave neutral or small effects on the growth or survival of the cells. The disulfide structure of the CRIPTO-CFC domain of **human** Cripto protein was determined by a combination of enzymatic and chemical fragmentation, followed by chromatographic separation of the fragments, and characterization by mass spectrometry and N-terminal sequencing. These studies showed that Cys115 forms a disulfide bond with Cys133, Cys128 with Cys149, and Cys131 with Cys140 in human Cripto.

The receptor of choice for Cripto was studied by Gray et al (Gray et al., 2003) who showed that Cripto binds to the activin and Type II activin receptor and ALK4 and can block activin binding to ALK4 in human liver cancer cells. But signaling by nodal or Vg1 requires a coreceptor from the epidermal growth factor-Cripto-FRL1-Cryptic protein family such as Cripto. Under some conditions, Cripto can block binding of activins (which are inhibitors of growth) thus accounting for the transforming action of Cripto. Another study using mammary cells confirmed this finding (Bianco et al., 2002). Signaling pathways used by Cripto have been reported (Yeo and Whitman, 2001). A review by Rosa et al summarizes these findings (Rosa, 2002).

To complicate matters more, Cripto can also act independently of Alk4 and nodal, through a pathway dependent on Glypican-1, a membrane-associated heparan sulfate proteoglycan, and activates the tyrosine kinase c-Src, triggering the mitogen-activated protein kinase and

Akt signaling pathways. An active Src kinase is necessary for Cripto to induce in vitro transformation and migration in mouse mammary epithelial cells (Bianco et al., 2003). This is another pathway that I suggested (or predicted) in my review (Adamson et al., 2002) which was published well ahead of this work.

One of the causes of the intense level of attention that was paid to Cripto in the last 2 years (Bhattacharya et al., 2004; Bianco et al., 2003; Harms and Chang, 2003; Normanno et al., 2004) was generated by our original findings that a) Cripto is an early growth factor required for the development of the embryo (Xu et al., 1999) and b) that Cripto is required for the differentiation of cardiomyocytes (Xu et al., 1998). Others have developed the idea that since stem cells express Cripto, it is likely to play a role in stem cell physiology. Thus the structure of Cripto and the nature of the Cripto receptor were rapidly discovered and characterized. Our plans that were innovative 3 years ago were suddenly inadequate and later shown to be redundant, mostly in the last year. I have continued to work with Italian collaborators and we have had exchange students and visits. We have produced two papers together describing i) the default differentiation pathway of Cripto -/- embryo stem cells. These cells spontaneously differentiate into neural cells at a high level and this is being tested in animal models along therapeutic treatment lines (Parisi et al., 2003). ii) the second paper concerned the high degree of anterior neural development that occurs in Cripto-/- mouse embryos even though they survive only for 8-9 days in the embryo stage (Liguori et al., 2003).

Part 2- GADD45A

Several researchers in my laboratory work on identifying the target genes regulated by Egr1 transcription factor. One of the genes identified as up-regulated by genotoxic stresses in both normal and cancer cell lines derived from breast and from prostate, was GADD45A. Dr Min Li decided to undertake the verification of this gene that was identified by our microarray technology. He has made the following progress that strongly indicates that Egr1 is a transcriptional activator of this important gene family. There are 3 members of the family, all are similar and we report only on GADD45A but all members play a role in DNA damage repair processes.

Genotoxic stresses such as gamma or Ultraviolet irradiation (IR and UV-C) or chemotherapy drugs such as Etoposide, damage DNA by strand breakage, and in order to repair the damage a large number of different genes are mobilized to stop further damage by DNA breakages and incorrect repairs before cell division could lead to genetic instability and multiple mutated genes. Egr1 is an immediate response gene that can rapidly activate a cohort of genes that are required for fast deployment. P53 also has this function, but is often already mutated or inactive in cancer cell lines. Egr1 regulates a very similar set of target genes to p53 and in fact, also up-regulates p53. The target genes include cell growth inhibitors such as p21/CIP1/WAF1 a gene that arrests the cell cycle at both G1 and G2. Slowing the growth prevents the cell from entering S phase, and allows time for the repair enzymes to assemble at breakage points and effect repairs. Many of these genes are likely to be targets of Egr1 transcriptional regulation, but this has not been ascertained for many genes yet, including GADD45A, All the GADD45 genes respond to stresses by elevation of transcript levels following stress and/or growth arrest conditions or treatment with DNA-damaging agents and p53 is thought to be the major transcriptional regulator. However, the DNA damage-induced transcription of these genes is mediated by both p53-dependent

(Kastan et al., 1992; Zhan et al., 1994). and p53-independent mechanisms (Taylor and Stark, 2001).

Dr Li has the following evidence:-

1. Egr1 is induced before GADD45A following UV-C irradiation

UV irradiation of DU145 prostate cancer cells leads to the rapid induction of Egr1 mRNA with a maximum 45 to 60 min later. GADD45A is induced to a similar degree but its induction is slower and reaches a maximum at 90min (**Figure 1A**). The level of Egr1 protein expression increased with the dose of UV-C in parallel with the expression of GADD45A (**Fig 1B**). For ionizing radiation, DU145 cells responded to give maximal Egr1 protein expression at 10Gy while 20Gy was less: GADD45A expression was maximal at 10 Gy also (**Fig 1C**). Similarly, in 293T cells except that the maximal GADD45A protein level was achieved at 40 J/m^2 (**Fig 1D**). Therefore, strong induction of Egr1 preceded that of GADD45A in a fashion that suggests that Egr1 could be regulating the DNA repair gene after DNA damaging stimuli.

To compare the effect of endogenous Egr1 induced by three different stimuli in three cell lines, a quantitative RT-PCR study was made (Table 1) of the induction of mRNA levels for Egr1 and GADD45A. The levels of Egr1 were highly elevated in all 3 cell types but to different levels with MCF7 (p53+) breast cancer cells were the most responsive. This indicates that the effect of Egr1 is common to several cell types, independent of their p53 status.

Egr1 is required for GADD45A expression

Mouse embryo fibroblasts that lack Egr1 expression were derived from Egr1 null mouse embryos (MEFs) and were tested for GADD45A inducibility after treatment of null and wild-type MEFs with the phorbol ester, TPA. **Figure 2A and B** shows that TPA induced Egr1 mRNA expression in wt-MEFs 3-fold, while Egr1-null MEFs were unable to induce GADD45A mRNA. We verified this by using the antisense Egr1 oligonucleotides that were designed to reduce the expression of either mouse or human Egr1 specifically (Virolle et al., 2003). **Figure 2C** shows that UV-induced Egr1 protein expression in DU145 prostate cells was reduced by AS-Egr1 in concert with GADD45A reduction. This result further supports the hypothesis that Egr1 is required for the UV induction of GADD45A.

Egr1 binds directly to the GADD45A promoter

Since GADD45A was originally identified by a promoter microarray study as a possible target gene regulated by Egr1 as evidenced by a positive signal for hybridization with Egr1-immunoprecipitated chromatin cross-linked DNA, we expected that we should be able to verify this finding by "conventional" ChIP. That is, amplification of the purified DNA fragments that were captured from TPA-induced DU145 cells should contain this promoter and by designing primers that span a portion of the promoter that contains the high-affinity Egr1 binding sites and performing PCR, the amplified DNA should be visible after electrophoresis on an agarose gel. **Figure 3** shows that the expected 264 bp DNA was recognized in UV and IR-induced cells but not in serum or untreated (NT) cells, indicating that induction with genotoxic stresses was required for Egr1 binding to the GADD45A promoter. More obviously, this result provides proof that Egr1 can bind to the activated GADD45A promoter.

Egr1 stimulates a GADD45A promoter-reporter construct

In order to delineate the Egr1 binding site (EBS) a mutation analysis was made to compare the full-length (2.3kb DNA) 5' regulatory sequence containing 29 bp of 5'UTR and 2kb of GADD45A promoter, ligated to luciferase using the expression plasmid pGL3-basic vector. The results of site-directed mutagenesis to change four nucleotides in the putative EBS are shown in **Figure 4A** (red sites). Using transfection into 293T cells with Renilla luciferase as an internal control the expression of pGL3-luciferase was measured and expressed as a fold-change of normal to mutated promoter activities, when Egr1 was expressed ectopically (middle group) or endogenously after Egr1 was induced by irradiation with UV-C at 40 J/m^2. The results in **Figure 4B** showed that very strong induction of the GADD45A promoter occurs by both forms of Egr1 expression. The mutant forms 1, 2 and 3 were the most affected binding sites when mutated, while site 4 (which contain a group of 3-4 putative EBS) is much less reduced in activity by mutation. We concluded that the most effective Egr1-activated sites are sites 1 and 2 in the 5'UTR of GADD45A. These sites are different from the sites that were found to be activated by WT1, therefore it seems likely that WT1 and Egr1 do not compete with each other because different specific binding sites occur.

In conclusion, Dr Li has good evidence that Egr1 plays a role in the recovery after DNA breaks. GADD45A (Gadd45), GADD45B (MyD118), and GADD45G (CR6) constitute a family of evolutionarily conserved, small, acidic, nuclear proteins, that have been implicated in terminal differentiation, growth suppression, and apoptosis. Published data indicate that the Gadd45 proteins may cooperate to activate cell cycle S and G2/M checkpoints following exposure of cells to UV irradiation (Vairapandi et al., 2002). GADD45B and GADD45G, as well as GADD45A, interact with both Cdk1 and cyclinB1, resulting in inhibition of the kinase activity of the Cdk1/cyclinB1 complex and the start of excision repair of DNA. They are important in the DNA repair and survival response of cells to DNA damage but are also involved in cell apoptosis. We are continuing with this investigation with the assistance of these funds from the DOD.

FIGURES AND TABLE

Figure 1A. The expression of Egr1 mRNA precedes GADD45A after UV irradiation of

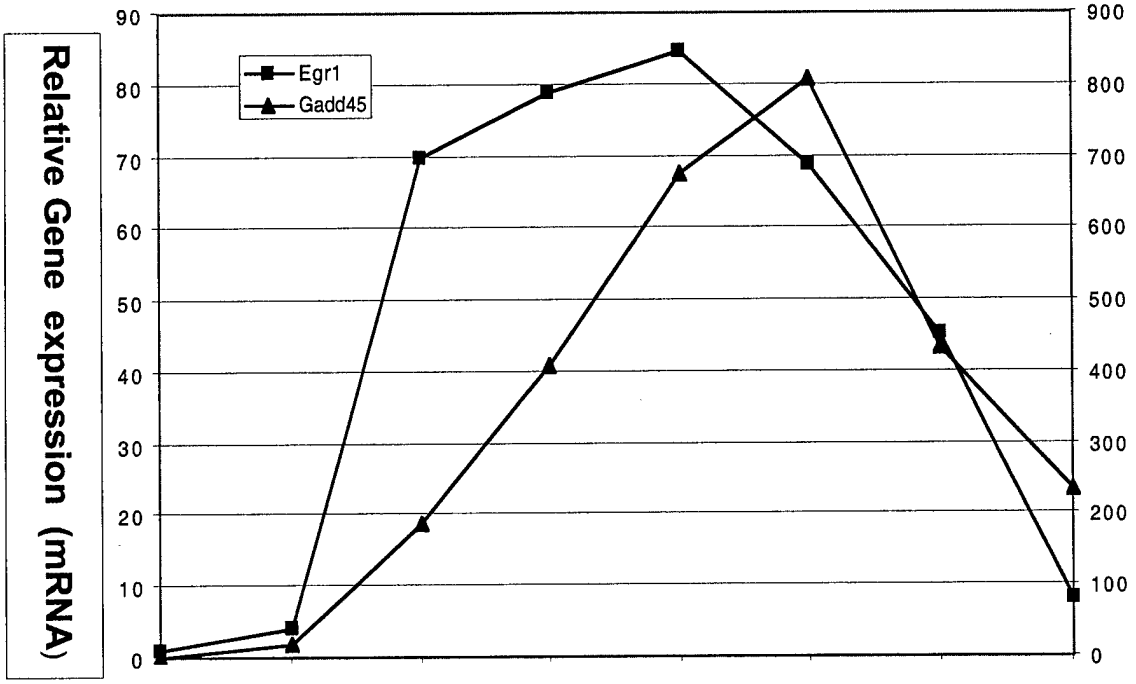

DU145 cells

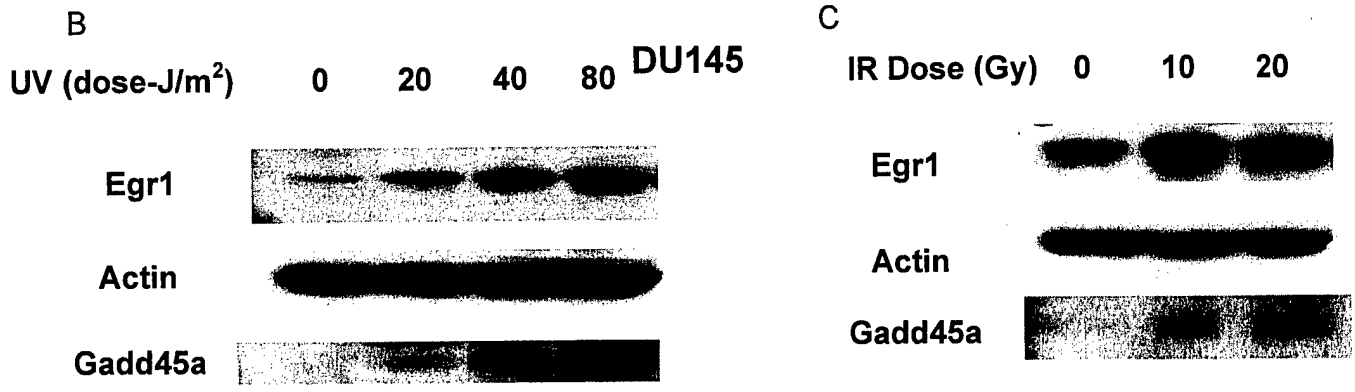

D

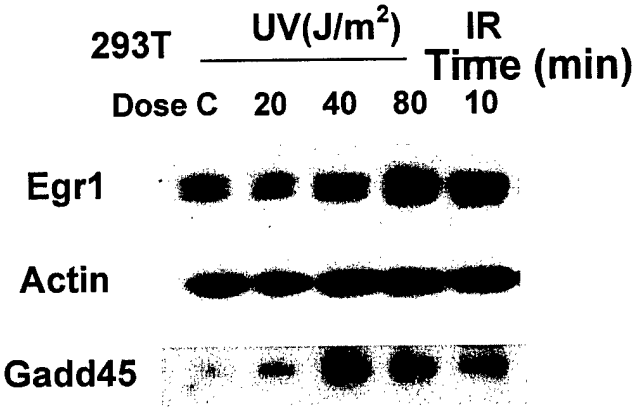

Figure 1. B, C, D, Dose response to irradiation in DU145 and 293T cells

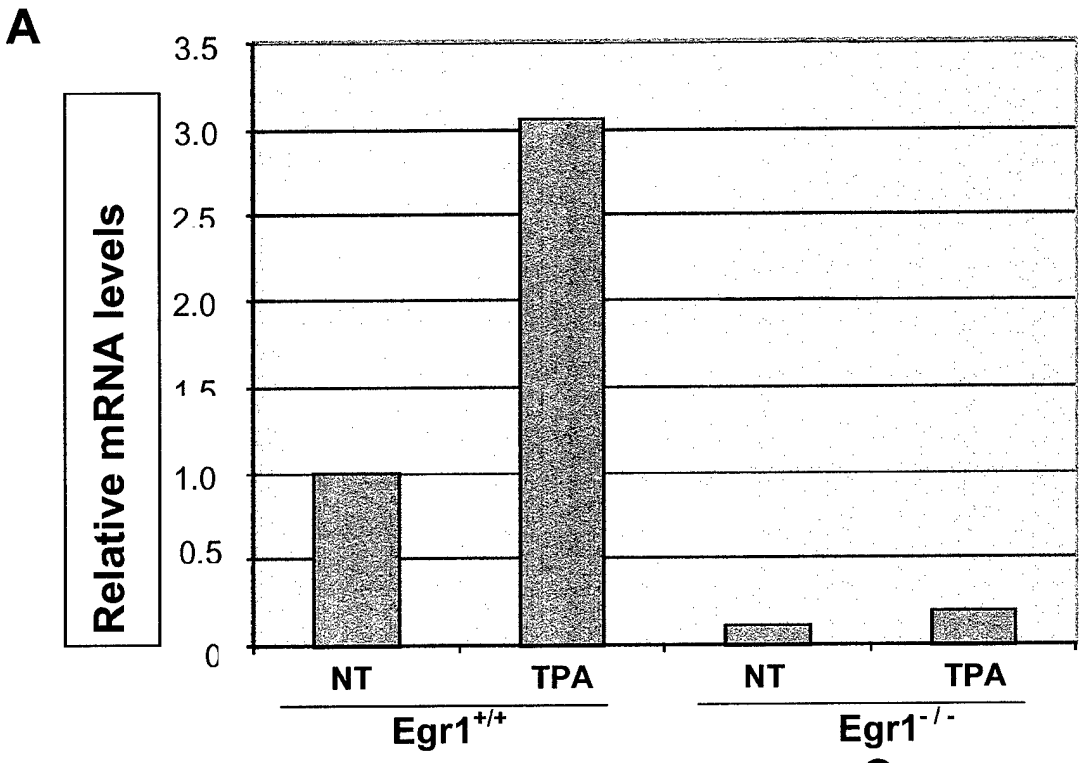

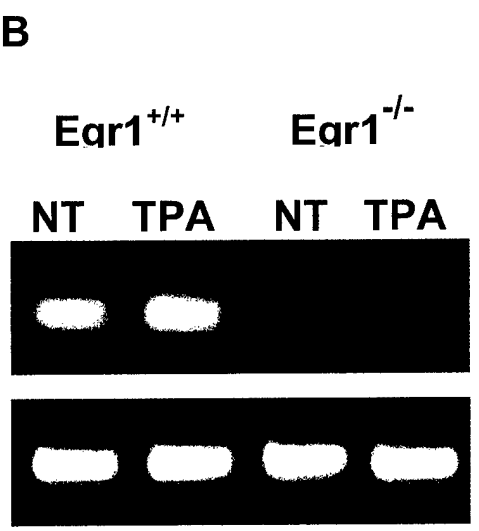

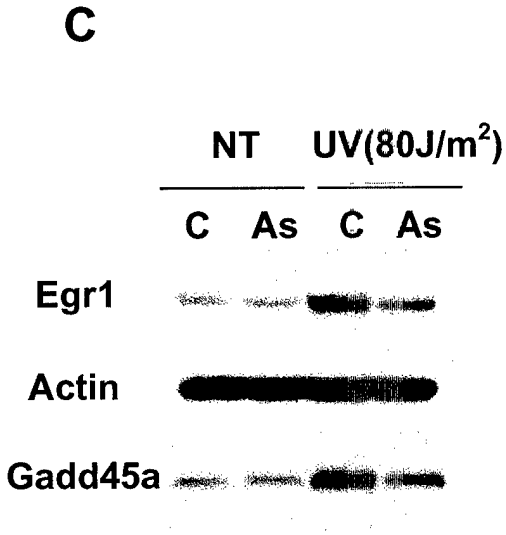

Figure 2 A, Egr1 is required for gadd45a expression. Egr1+/+ and Egr1-/- MEF cells were harvested 2 h after exposure to TPA (100 ng/ml), and Gadd45a mRNA (A) and protein levels (**B**) were assayed by semi-quantitative RT-PCR. **C, Egr1 antisense inhibits the expression of Gadd45a induced by UV in DU145 cells.**

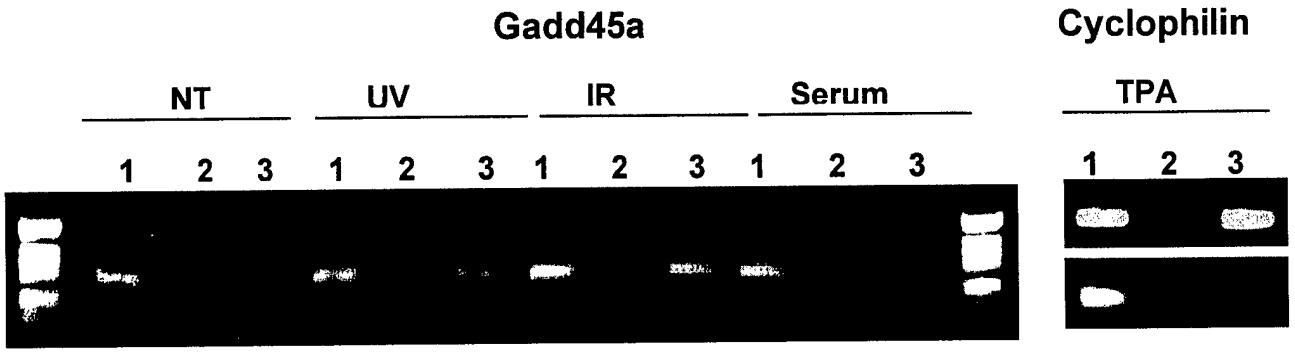

1. Total DNA input
2. non-immmune-control
3. Anti Egr1 ChIP

Fig. 3. Egr1 directly bound to Gadd45a regulatory sequence in vivo in UV and IR-treated cells shown by conventional ChIP. DU145 cells were treated with UV(40 J/m^2), IR(10 Gy), TPA(100 ng/ml) and serum, chromatin was crosslinked with formaldehyde and then immunoprecipitated with a specific Egr1 antibody or a nonimmune control. The detection of Gadd45a GC-rich fragment (264 bp) was performed by PCR as described in Methods.

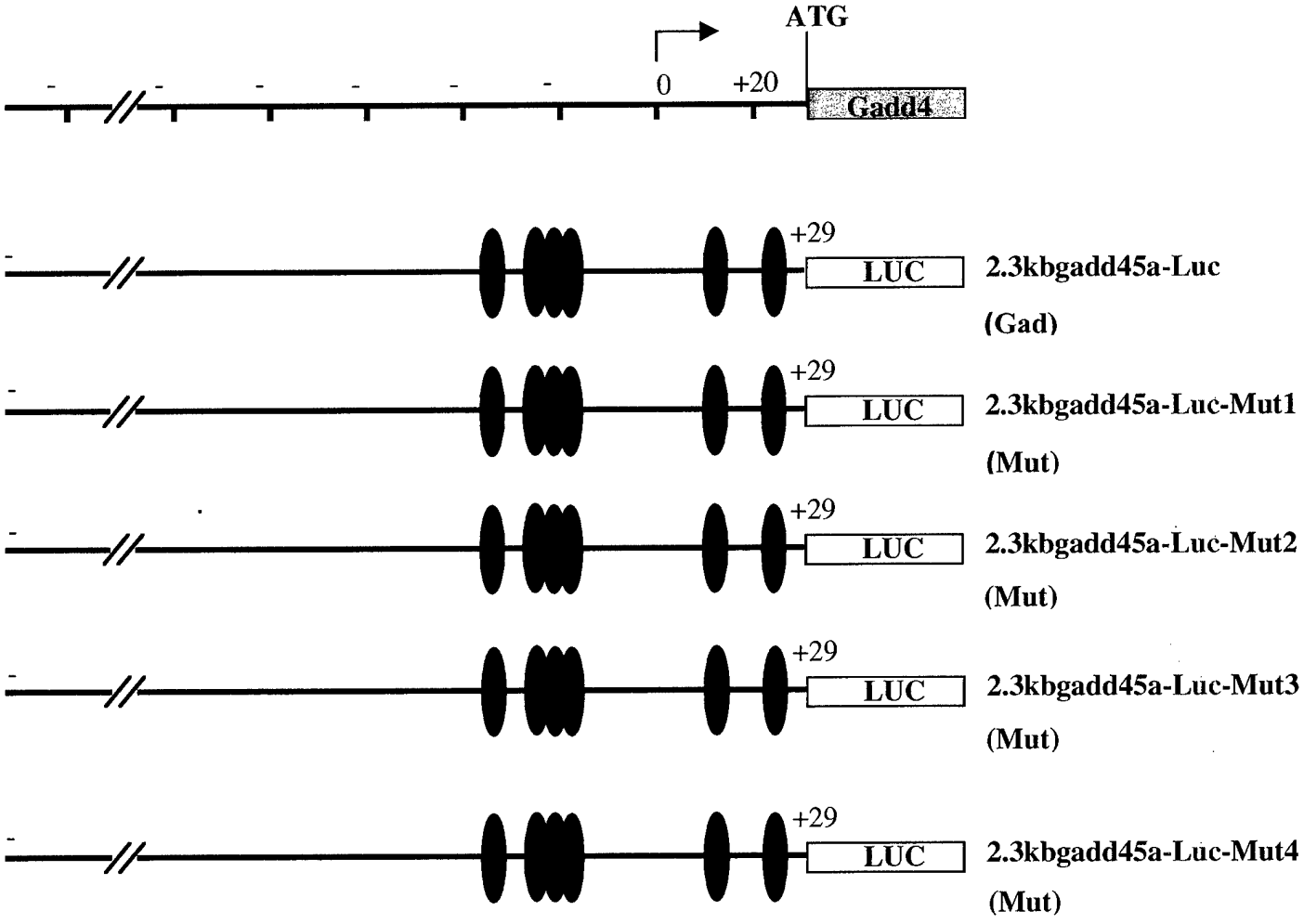

Figure 4A- The construction of Gadd45a promoter-luciferase vector. Cloning 2.3 kb promoter of Gadd45a gene into pGL3-Basic vector. As well as, site-direction mutation (red) of possible Egr-1 binding sites in Gadd45a promoter were carried out.

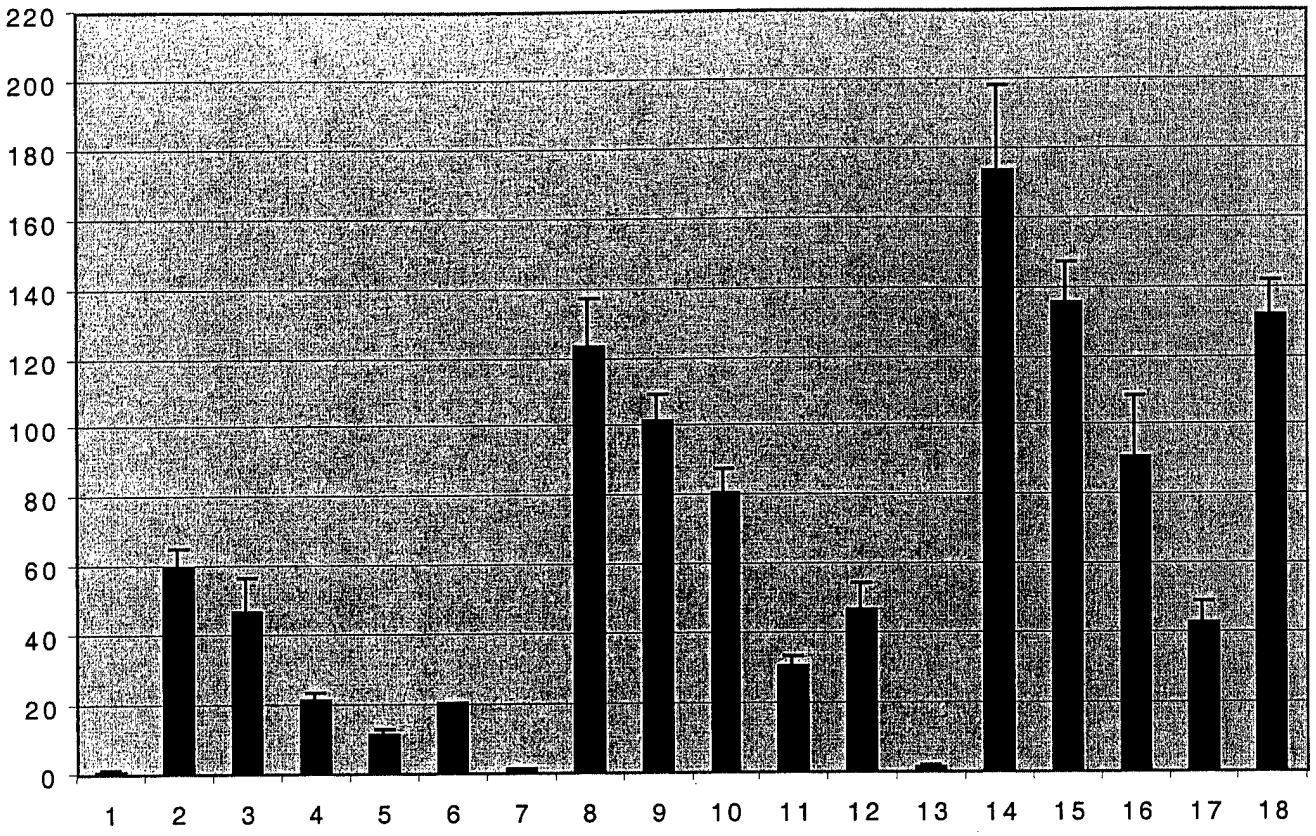

1 pGL3+pcDNA$_3$	**7 pGL3+Egr1**	**13 pGL3+pcDNA$_3$ (UV)**
2 Gadd+pcDNA$_3$	**8 Gadd+Egr1**	**14 Gadd+pcDNA$_3$ (UV)**
3 Mut1+ pcDNA$_3$	**9 Mut1+ Egr1**	**15 Mut1+ pcDNA$_3$ (UV)**
4 Mut2+ pcDNA$_3$	**10 Mut2+ Egr1**	**16 Mut2+ pcDNA$_3$ (UV)**
5 Mut3+ pcDNA$_3$	**11 Mut3+ Egr1**	**17 Mut3+ pcDNA$_3$ (UV)**
6 Mut4+ pcDNA$_3$	**12 Mut4+ Egr1**	**18 Mut4+ pcDNA$_3$ (UV)**

Fig 4B. Induction of Gadd45a promoter activity by Egr1 and UV treatment. The Gadd45a promoter-luciferase-reporter vector and EBS-mutated vector from Gadd45a promoter-luciferase-reporter vector were transfected into 293T cells. After 24 hours transfection, cells in 13-18 group were treated with UV (40J/m^2). Then 2 hours later the luciferase activity was measured according to manual.

Gadd45α mRNA expression by q-RT-PCR

Cell lines	Genes	mRNA level (fold)		
		TPA	ETO	UV
P69T	Egr1	14.8±8.2		
	Gadd45	2.2, 2.3		
DU145	Egr1	143.6 ±41.5	29.8±10.1	
	Gadd45	7.7	2.7	
MCF7	Egr1	6441		3.8
	Gadd45	35.8		29.0

TABLE 1

Partial verification of the mRNA levels induced by the elevation of Egr1 in 3 cells lines. In all cases, the levels of GADD45A are elevated but the specific level depends on the cell type.

Key research accomplishments

- The work that we proposed was an important aspect of breast cancer progression. The importance of Cripto is clearly increasing, and this line of research is worth supporting. However, our efforts were not productive and not for the lack of effort.
- The work on GADD45A is in a much better place with consistent and interesting results that are worth pursuing. This work needs several more experiments and some more studies that compare other transcription factors that might affect GADD45A regulation. This work will continue using any DOD funds that remain.

Reportable outcomes

1. The PI was invited to present the studies made on **Cripto** in her laboratory as well as one describing the work on Egr1 (also supported by the DOD) at the University of Texas at San Antonio. The former was a 2 hour teaching seminar to the graduate students and postdoctoral trainees at the Institute of Biotechnology.
2. A very favorable response was made to our published review reported last year.
3. Three publications on Cripto this year and last year by the PI are attached:-

   a) Adamson, E. D., Minchiotti, G., and Salomon, D. S. (2002). Cripto: a tumor growth factor and more. [Review] [74 refs]. Journal of Cellular Physiology *190*, 267-278.

   b) Parisi S. D'Andrea D. Lago CT. **Adamson** ED. Persico MG. Minchiotti G. (2003). Nodal-dependent Cripto signaling promotes cardiomyogenesis and redirects the neural fate of embryonic stem cells.(2003). J.Cell Biology. 163(2):303-14.

c) Liguori GL, Echevarria D, Improta R, Signore M, **Adamson E,** Martinez S, Persico MG. (2003) Anterior neural plate regionalization in cripto null mutant mouse embryos in the absence of node and primitive streak. Dev Biol. 264(2):537-49.

Conclusions

The structure of Cripto and especially the disulfide bridge loops were not known at the time and have recently been published. The educated prediction that we made was incorrect and the mutant forms of Cripto that we made were not useful. In this case, the collaboration of larger teams of workers in several different fields combined to make excellent advances on this important gene that we could not match. We therefore worked on another protein (GADD45a) that was also highly relevant to breast and prostate cancer. Publications resulting will acknowledge the support of the BCRP program of the DOD.

REFERENCES

Adamson, E. D., Minchiotti, G., and Salomon, D. S. (2002). Cripto: a tumor growth factor and more. [Review] [74 refs]. Journal of Cellular Physiology *190*, 267-278.

Bhattacharya, B., Miura, T., Brandenberger, R., Mejido, J., Luo, Y., Yang, A. X., Joshi, B. H., Ginis, I., Thies, R. S., Amit, M., *et al.* (2004). Gene expression in human embryonic stem cell lines: unique molecular signature. Blood *103*, 2956-2964. Epub 2003 Dec 2930.

Bianco, C., Adkins, H., Wechselberger, C., Seno, M., Normanno, N., De Luca, A., Sun, Y., Khan, N., N, K., Williams, K., *et al.* (2002). Cripto-1 activates Nodal and ALK4 dependent and independent signalling pathways in mammary epithelial cells. Mol Cell Biol. 2002 Apr;22(8):2586-97.

Bianco, C., Strizzi, L., Rehman, A., Normanno, N., Wechselberger, C., Sun, Y., Khan, N., Hirota, M., Adkins, H., Williams, K., *et al.* (2003). A Nodal- and ALK4-independent signaling pathway activated by Cripto-1 through Glypican-1 and c-Src. Cancer Res *63*, 1192-1197.

Bianco, C., Wechselberger, C., Ebert, A., Khan, N. I., Sun, Y. P., and Salomon, D. S. (2001). Identification of Cripto-1 in human milk. Breast Cancer Research & Treatment *66*, 1-7.

De Luca, A., Casamassimi, A., Selvam, M. P., Losito, S., Ciardiello, F., Agrawal, S., Salomon, D. S., and Normanno, N. (1999). EGF-related peptides are involved in the proliferation and survival of MDA-MB-468 human breast carcinoma cells. Int J Canc *80*, 589-594.

Foley, S., HW, v. V., RE, B., HB, A., AE, C., J, S., M, S., CN, Y., and D, W. (2003). The CRIPTO/FRL-1/CRYPTIC (CFC) domain of human Cripto. Functional and structural insights through disulfide structure analysis. Eur J Biochem *270*, 3610-3618.

Gray, P. C., Harrison, C. A., and Vale, W. (2003). Cripto forms a complex with activin and type II activin receptors and can block activin signaling. Proc Natl Acad Sci U S A *100*, 5193-5198. Epub 2003 Apr 5197.

Harms, P., and Chang, C. (2003). Tomoregulin-1 (TMEFF1) inhibits nodal signaling through direct binding to the nodal coreceptor Cripto. Genes Dev *17*, 2624-2629.

Kastan, M. B., Zhan, Q., el-Deiry, W. S., Carrier, F., Jacks, T., Walsh, W. V., Plunkett, B. S., Vogelstein, B., and Fornace, A. J., Jr. (1992). A mammalian cell cycle checkpoint pathway utilizing p53 and GADD45 is defective in ataxia-telangiectasia. Cell *71*, 587-597.

Liguori, G. L., Echevarria, D., Improta, R., Signore, M., Adamson, E., Martinez, S., and Persico, M. G. (2003). Anterior neural plate regionalization in cripto null mutant mouse embryos in the absence of node and primitive streak. Dev Biol *264*, 537-549.

Normanno, N., De Luca, A., Bianco, C., Maiello, M. R., Carriero, M. V., Rehman, A., Wechselberger, C., Arra, C., Strizzi, L., Sanicola, M., and Salomon, D. S. (2004). Cripto-1 overexpression leads to enhanced invasiveness and resistance to anoikis in human MCF-7 breast cancer cells. J Cell Physiol *198*, 31-39.

Parisi, S., D, D. A., CT, L., ED, A., MG, P., and G, M. (2003). Nodal-dependent Cripto signaling promotes cardiomyogenesis and redirects the neural fate of embryonic stem cells. J Cell Biol *163*, 303-314.

Rosa, F. M. (2002). Cripto, a multifunctional partner in signaling: molecular forms and activities. Sci STKE *2002*, PE47.

Taylor, W. R., and Stark, G. R. (2001). Regulation of the G2/M transition by p53 [Review]. Oncogene *20*, 1803-1815.

Vairapandi, M., Balliet, A. G., Hoffman, B., and Liebermann, D. A. (2002). GADD45b and GADD45g are cdc2/cyclinB1 kinase inhibitors with a role in S and G2/M cell cycle checkpoints induced by genotoxic stress. J Cell Physiol *192*, 327-338.

Virolle, T., Krones-Herzig, A., Baron, V., De Gregorio, G., Adamson , E. D., and Mercola, D. (2003). Egr1 promotes growth and survival of prostate cancer cells: identification of novel Egr1 target genes. J Biol Chem *278*, 11802-11810.

Wechselberger, C., Ebert, A. D., Bianco, C., Khan, N. I., Sun, Y., Wallace-Jones, B., Montesano, R., and Salomon, D. S. (2001). Cripto-1 enhances migration and branching morphogenesis of mouse mammary epithelial cells. Exp Cell Res *266*, 95-105.

Xu, C., Liguori, G., Adamson, E. D., and Persico, M. G. (1998). Cardiac differentiation is blocked in embryonic stem cells lacking Cripto-1. Dev Biol *196*, 237-247.

Xu, C., Liguori, G., Persico, M. G., and Adamson, E. D. (1999). Abrogation of the Cripto gene in mouse leads to failure of post-gastrulation morphogensis and lack of differentiation of cardiomyocytes. Development *126*, 483-494.

Yeo, C., and Whitman, M. (2001). Nodal signals to Smads through Cripto-dependent and Cripto-independent mechanisms. Mol Cell *7*, 949-957.

Zhan, Q., Bae, I., Kastan, M. B., and Fornace, A. J., Jr. (1994). The p53-dependent gamma-ray response of GADD45. Cancer Res *54*, 2755-2760.

Personnel receiving pay from the research effort.

PI. Eileen D, Adamson, Ph.D. 15-20% effort, three years
Post-doctoral Associate, Min Li Ph.D. 100% effort, two years

Appendices.

Copies of three papers on Cripto authored by the PI are attached

1. **Adamson ED**, Minchiotti G, Salomon DS. Cripto: a tumor growth factor and more. J Cell Physiol. 2002 Mar;190(3):267-78. Review.

2. Parisi S. D'Andrea D. Lago CT. **Adamson** ED. Persico MG. Minchiotti G. (2003) Nodal-dependent Cripto signaling promotes cardiomyogenesis and redirects the neural fate of embryonic stem cells.(2003). J.Cell Biology. 163(2):303-14,.

3. Liguori GL, Echevarria D, Improta R, Signore M, **Adamson E,** Martinez S, Persico MG. (2003) Anterior neural plate regionalization in cripto null mutant mouse embryos in the absence of node and primitive streak. Dev Biol. 264(2):537-49.

JOURNAL OF CELLULAR PHYSIOLOGY 190:267–278 (2002)
DOI 10.1002/jcp.10072

REVIEW ARTICLES

Cripto: A Tumor Growth Factor and More

EILEEN D. ADAMSON,[1]* GABRIELLA MINCHIOTTI,[2] AND DAVID S. SALOMON[3]

[1]*La Jolla Cancer Research Center, The Burnham Institute, La Jolla, California*
[2]*International Institute of Genetics and Biophysics, CNR, Via Pietro Castellino, Naples, Italy*
[3]*Tumor Growth Factor Section, Basic Research Laboratory, National Cancer Institute, NIH, Bldg 10, Rockville Pike, Bethesda, Maryland*

Cripto, a growth factor with an EGF-like domain, and the first member of the EGF-CFC family of genes to be sequenced and characterized, contributes to deregulated growth of cancer cells. A role for Cripto in tumor development has been described in the human and the mouse. Members of the EGF-CFC family are found only in vertebrates: CFC proteins in zebrafish, *Xenopus*, chick, mouse and human have been characterized and indicate some common general functions in development. Cripto expression was first found in human and mouse embryonal carcinoma cells and male teratocarcinomas, and was demonstrated to be over-expressed in breast, cervical, ovarian, gastric, lung, colon, and pancreatic carcinomas in contrast to normal tissues where Cripto expression was invariably low or absent. Cripto may play a role in mammary tumorigenesis, since in vitro, Cripto induces mammary cell proliferation, reduces apoptosis, increases cell migration, and inhibits milk protein expression. This prediction is strengthened by observations of Cripto expression in 80% of human and mouse mammary tumors. At least three important roles for Cripto in development have created considerable interest, and each activity may be distinct in its mechanism of receptor signaling. One role is in the patterning of the anterior–posterior axis of the early embryo, a second is a crucial role in the development of the heart, and a third is in potentiating branching morphogenesis and modulating differentiation in the developing mammary gland. Whether these properties are functions of different forms of Cripto, different Cripto receptors or the distinct domains within this 15–38 kDa glycoprotein are examined here, but much remains to be revealed about this evolutionarily conserved gene product. Since all Cripto receptors have not yet been determined with certainty, future possible uses as therapeutic targets remain to be developed. Cripto is released or shed from expressing cells and may serve as an accessible marker gene in the early to mid-progressive stages of breast and other cancers. Meanwhile some speculations on possible receptor complexes for Cripto signaling in mammary cells are offered here as a spur to further discoveries. J. Cell. Physiol. 190: 267–278, 2002. © 2002 Wiley-Liss, Inc.

CRIPTO IS THE FIRST MEMBER OF A FAMILY OF GENES NOW NAMED EGF-CFC

The Cripto gene (*CR1*), first cloned from a cDNA library derived from a human teratocarcinoma cell line was named accordingly as teratocarcinoma-derived growth factor-1 (*TDGF1* and maps to human chromosome 3p21.3 (Dono et al., 1991; Saccone et al., 1995). Mouse*Tdgf1* (encoding Cripto protein) has been isolated and characterized (Dono et al., 1993; Liguori et al., 1996). Mouse Cripto has 92% similarity to its human counterpart in the EGF-like domain, which is the most conserved of the domains. There is 83% homology in the EGF-like domains between the members of this family and 40% homology in the CFC domain. In all, seven related genes have been cloned, including mouse and human Cryptic (Ciccodicola et al., 1989; Shen et al., 1997; Bamford et al., 2000), *Xenopus* Frl-1(Kinoshita et al., 1995), Zebrafish one-eyed pinhead (*oep*) (Zhang et al., 1998), and chick-Cripto (Colas and Schoenwolf, 2000). The name CFC for the second conserved domain is derived from the combination Cripto/Frl/Cryptic. The sequence, alignments, and functions of the EGF-CFC gene family have been reviewed recently (Salomon et al., 1999, 2000).

Contract grant sponsor: Department of Defense; Contract grant number: DAMD17-01-1-0165.

*Correspondence to: Eileen D. Adamson, La Jolla Cancer Research Center, The Burnham Institute, 10901, N. Torrey Pines Rd., La Jolla, CA 92037. E-mail: eadamson@burnham.org

Received 2 October 2001; Accepted 9 November 2001

STRUCTURE OF CRIPTO PROTEIN

Mouse Cripto protein (Cr1) consists of 171 amino acids and unlike the human CR1 (188 amino acids) has a signal sequence, but both proteins can be secreted, #187 (Brandt et al., 1994) and #2384 (Normanno et al., 1995) (Ciccodicola et al., 1989; Dono et al., 1991; Normanno et al., 1994). The protein product of the *TDGF-1* gene in mouse and human will be denoted as Cripto here. The EGF-CFC family of proteins contain several domains (Fig. 1). The signal sequence allows the polypeptide to be processed through the Golgi body and secreted into the medium. In human Cripto, the hydrophobic domain is not large enough to act as a secretory signal, secretion does occur in human cells by an unknown mechanism. The core peptide is ~20 kDa and glycosylation and other post-translational modifications results in a product of Mr = 28–36 kDa. The Cripto produced by vector expression in chinese hamster ovary (CHO) cells is secreted as a 24–28 kDa protein (Brandt et al., 1994). The pattern of six cysteine residues of the EGF-like domain in Cripto is recognizable, but of the three disulfide loops in EGF, loop A is missing and loop B is truncated resulting in a structure that does not bind to the EGFR family of receptors (Bianco et al., 1999). The six cysteine residues of the EGF-like domain form similar disulfide bridges as in EGF, that is 2–4, 1–3, and 5–6 (Lohmeyer et al., 1997). Within the EGF-like domain, the sequence similarity between the seven members is is 60–70%. Next to the EGF-like domain of Cripto, an additional six-cysteine CFC domain is conserved in the analogous proteins at 35–48%. The CFC domain has unspecified, but crucial functions. It also has three disulfide bridges, whose exact disposition is currently unknown but the spacing of the cysteine residues bears some resemblance to the EGF-like domains found in laminin (Abe et al., 1998). The EGF-CFC proteins range from 171 to 202 amino acids with a core protein of 18–21 kDa and an overall sequence identity between these proteins of only 22–32%. Nevertheless, a high level of overlap has been observed in the interspecies developmental activities of family members, as described later. All the members of the EGF-CFC family, except for Oep in Zebrafish, are glycoproteins that contain a single *N*-glycosylation site and potential *O*-glycosylation sites. Recently, a single *O*-linked fucosylation site has been found between the second and third cysteines in the EGF-like domain of all the EGF-CFC proteins (human T88, mouse T72). Loss of this fucosyl residue by mutation of T88 to G, inhibited the ability of Cripto to interact with its cofactor, Nodal, to signal via Smad2 (Schiffer et al., 2001). This rare modification is also present in the EGF-modules of secreted proteins involved in blood coagulation, thus adding to the importance of glycosylation in the functionality of Cripto.

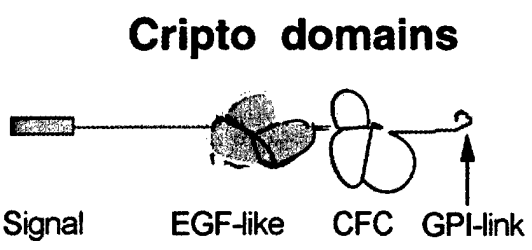

Fig. 1. Cripto protein domains: signal, EGF-like, CFC, and GPI linkage domains.

The hydrophobic domain of Cripto near the carboxy terminus, like other members of the family, has consensus sequences to form a glycerolphosphatidylinositol (GPI) linkage with the cell membrane (Minchiotti et al., 2000). This linkage ensures that secreted Cripto is inserted into the lipids of the plasma membrane perimeter of the cell to form a membrane-anchored extracellular polypeptide, where it could affect cell–cell and cell–matrix interactions. Here, it is likely also to interact with cofactors and receptor polypeptides as well as intracellular linking molecules in lipid rafts, where GPI-linked proteins tend to cluster to effect signaling to the nucleus. A soluble form of Cripto produced by experimental truncation of the carboxy-terminal 16 amino acids to remove the GPI-linkage, is active in growth assays and in null mutation rescue studies in zebrafish embryos (Minchiotti et al., 2001). Human tumors secrete a shortened form of Cripto with an amino-terminal deletion of 42 amino acids by translation from an alternative in frame CUG codon. This protein product likely has activity since it retains the EGF-like and the CFC motif (see below). (For more details on the sequences and roles of the EGF-CFC family of genes, see these reviews: Salomon et al., 1999, 2000.)

EXPRESSION OF CRIPTO IS RESTRICTED

Cripto is expressed early in development

Cripto is expressed early in development in the inner cell mass and the trophoblast cells of the mouse blastocyst (Johnson et al., 1994), in human NTERA2 embryonal carcinoma (EC) cells (Dono et al., 1991; Saccone et al., 1995), in mouse F9 EC cells (Dono et al., 1993; Liguori et al., 1996), and in mouse embryo stem (ES) cells (Xu et al., 1998), but is down-regulated in the first cell types to differentiate from ES cells, namely, visceral and parietal endoderm cells. In the embryo, Cripto is expressed in the E6.5 embryo in the epiblast, primitive streak and ectoplacental cone (Dono et al., 1993; Ding et al., 1998). At E8.5, Cripto is expressed in myocardium of the developing heart tube and in the conotruncus heart outflow region (Dono et al., 1993). Cripto$^{(-/-)}$ embryos die at this stage in utero, by failure to form the anterior–posterior axis and to make sufficient mesoderm, failure to form the primitive streak and to regulate the many genes that center on the activities of the Nodal gene (Ding et al., 1998; Xu et al., 1999; Reissmann et al., 2001; Schier, 2001; Yeo and Whitman, 2001), and see below. Cripto continues to be expressed in the myocardium and outflow region of normal embryos until E10 and then is no longer detected in development. This suggests that Cripto is involved in heart development, but this could not be determined in the Cripto null mouse, because heart-specific Cripto ablation is required for this, a study that awaits completion.

Expression of cripto is restricted after birth

Cripto mRNA is detected at low levels in spleen, testis, heart, lung, and brain (Dono et al., 1991) of the adult mouse, but no function has been described in any normal

tissue except for the mammary gland. Three weeks after birth, the mammary glands of the female mouse start to proliferate from the short ducts at the nipples that developed prenatally. Growth of the ducts becomes active under the influence of pubertal steroid hormones, estrogen, and progesterone. The mammary tree grows rapidly in the virgin into a multi-branched epithelial ductile system to fill the mammary fat pad that limits its further expansion. Cripto is expressed in all epithelial cells at increasing levels during this period. Upon pregnancy, terminal endbuds develop into ductal-alveolar lobules that synthesize milk proteins that enter the duct lumen together with Cripto itself (Bianco et al., 2001). Cripto expression increases during all these stages (Kenney et al., 1995), and starts to decline at the late lactation stage (De Santis et al., 1997) in keeping with the effect of Cripto on mammary epithelial cells described below. When Cripto was experimentally over-expressed in mammary epithelial cells, similar branching structures were formed in vitro and this turned into ductal hyperplasia when Cripto-transduced mammary epithelial cells were transferred to the mouse (Salomon et al., 1999; Wechselberger et al., 2001). It is possible that other tissues such as lung, kidney, and salivary gland form branching structures when stimulated by Cripto expression, but to date none have been reported.

ACTIVITIES OF CRIPTO

Cripto is a growth factor

The growth stimulatory properties of Cripto have been demonstrated on tumor cells of many kinds, pancreatic, ovarian, endometrial, intestinal, and mammary tumor cells. Normal human and mouse mammary epithelial cells also respond to Cripto and are good resources for receptor analysis (see below). The growth responses have been reviewed extensively (Salomon et al., 1999, 2000).

Cripto commonly supports cell survival

The intensity or duration of the Cripto signal or the conditions of treatment (i.e., growing vs. confluent static cells) may account for reports that Cripto stimulates either survival or apoptosis in related cell types CID-9 and HC-11, both derived from mouse mammary COMMA-D cells. These cells have characteristics typical of mid-pregnant mouse mammary gland cells from which they were derived (Medina et al., 1986). When Cripto was expressed constitutively in moderate amounts in CID-9 cells, increased survival was observed. Conversely, cells expressing an antisense (AS) Cripto version of the retroviral vector were retarded in growth and demonstrated increased levels of apoptosis (Niemeyer et al., 1998). Similarly, recombinant Cripto added to growing HC-11 cells stimulated survival (De Santis et al., 1997). However, recombinant Cripto can also induce apoptosis in confluent HC-11 mouse mammary epithelial cells under certain conditions. Culture of confluent cells for two days in the absence of the survival factors, EGF, and insulin, followed by exposure to Cripto caused maximal apoptosis at 3 days (De Santis et al., 2000). These conditions may mimic the regressing or involuting mammary gland, which undergoes apoptosis when lactation must be terminated and the gland returns to a resting condition with reduced size (see below).

Cripto inhibits the differentiation of mammary cells in culture

The synthesis of several milk proteins is stimulated by the culture of cells on a matrix and in the presence of a lactogenic hormone mixture consisting of prolactin, insulin, and dexamethasone (DIP). Using this system, the production of beta-casein and whey acidic protein was inhibited by the over-expression of endogenous Cripto or by the addition of exogenous Cripto to CID-9, HC-11 cells, or primary cultures of mouse mammary epithelial cells established from mid-pregnant mice (De Santis et al., 1997; Niemeyer et al., 1998). These responses agree with the rising expression levels of Cripto in the normal mammary gland during pregnancy and lactation, in parallel with rapid growth of the mammary ductal epithelium and later with milk protein production.

Cripto increases the migration of expressing cells and has a chemotactic effect on other cells

Cripto is over-expressed in cancer cells, and may contribute to metastatic progression by its effect on the shape, adhesivity, and migratory activity of cell. This was shown in CID-9 cells over- or under-expressing Cripto (Niemeyer et al., 1998) and in mouse embryo fibroblasts (MEFs) that were derived from knockout mice. The Cripto null cells attached poorly to fibronectin and collagen, but better to laminin than wild-type MEFs, suggesting that this population of cells could be more epithelial in type. Wild-type MEFs migrated through a porous membrane at a higher rate than $Cr^{(-/-)}$ cells, indicating that the expression of Cripto stimulates cell motility. Conditioned medium from Cripto-secreting cells also attracted higher rates of migration of cells towards it than medium lacking Cripto (Xu et al., 1999). Undoubtedly, these effects contributed to the early lethality (E8–9) of the developing embryo. When cervical carcinoma cells were experimentally induced to over-express Cripto, an increase in cell migration was observed, which correlated with an increase in the expression of vimentin compared to control cells, detected using microarray analyses of mRNA populations in the two cell types (Ebert et al., 2000). Therefore, like many other growth factors, Cripto can affect cell shape and cell migration by secondary effects on the cytoskeleton, as well as by increasing cell proliferation. In embryo cells, the induction of vimentin is indicative of mesodermalization of the epithelial layer and the migration of cells for morphogenesis. In cancer cells, vimentin expression similarly indicates the formation of more mesodermal-like cells with increased migratory activity. Likewise, overexpression of mouse Cripto in mouse mammary EpH4, NOG-8, NMuMG, and TAC-2 epithelial cells showed elevated migration and scattering (Wechselberger et al., 2001).

Cripto is essential for early embryonic development

Homologous recombination of the Cripto gene in ES cells produced normal heterozygous $Cr1^{(+/-)}$ animals. $Cr1^{(-/-)}$ embryos were abnormal on the seventh day of

gestation (E7) and failed to develop further than E9. Embryos failed to form the anterior–posterior axis and while embryonic mesoderm was sparse, extraembryonic mesoderm was present (Ding et al., 1998; Xu et al., 1999). Importantly, chimeric animals made by the injection of $Cr1^{(-/-)}$ ES cells into normal blastocysts were normal and had 50% incorporation of the Cripto null ES cells into all the tissues. Therefore, the wild-type cells were able to rescue the null cells, probably by a combination of juxtacrine and paracrine effects of the anchored and soluble forms of Cripto from the wild-type cells, respectively. This is a good illustration of the effectiveness of soluble Cripto even in embryos where tightly controlled morphogens must be orchestrated.

Cripto is required for cardiogenesis in culture

The development of the heart was shown to require Cripto at an early stage, using ES cells in which Cripto was inactivated by two rounds of targeting to produce $Cr1^{(-/-)}$ ES cells. ES cells normally differentiate as aggregates (embryoid bodies, EBs) to form cardiomyocytes that contract visibly starting at 7 days after the removal of leukemia inhibitory factor (LIF) from the culture medium. Cripto null EBs did not produce contracting cardiomyocytes even during extended culture periods. In these cultures, no cardiac muscle proteins were transcriptionally activated while the transcription factors (Gata4, Nkx2.5, and MEF2) that are known to be required for heart formation were expressed. The re-expression of Cripto sense, but not AS in the Cripto null ES cells rescued the ability of the cells to differentiate into cardiomyocytes, indicating that Cripto is required to activate a set of cardiac genes (Xu et al., 1998). The mechanism of the activity of Cripto in pre-cardiomyocytes is unknown, but these cells will be a good source to explore, for receptors that are specific to this stage of development and for the signaling mechanism.

Cripto plays a role in mammary gland development

Cripto is expressed in the developing mouse mammary gland at increasing levels from 3 weeks of age, under the influence of pubertal hormones. Both mRNA and protein have been observed and immunocytochemical staining showed Cripto protein in all epithelial cell types (Kenney et al., 1995; Niemeyer et al., 1998). Terminal end buds, ductal, and lobular–alveolar cells were all positive and expressed about four-fold higher levels during pregnancy and lactation compared to mature non-pregnant mammary glands. Cripto is released into the milk in the human (Bianco et al., 2001), where it may have some functions as a growth factor. Cripto expression declines rapidly at the end of lactation, and reverts to very low or no expression during involution of the mammary gland. However, in Balb/c mice that reach 2 years of age, the mammary glands re-express Cripto and can develop spontaneous adenocarcinomas (Herrington et al., 1997).

CRIPTO IS AN AUTOCRINE GROWTH FACTOR IN MAMMARY, COLON, PANCREATIC, AND OTHER TUMORS

As indicated above, mouse or human mammary cells over-expressing Cripto exhibit increased proliferation and transformed growth in vitro (Ciardello et al., 1991; Niemeyer et al., 1998). Cripto was detected in human breast cancers, accompanied by members of the EGF ligand family (Panico et al., 1996) and in the early invasive stage of cervical carcinoma (Ertoy et al., 2000). A recent review analyzes the incidence of immunoreactive Cripto in breast, colon, stomach, pancreas, lung, ovary, endometrium, testis, bladder, and prostate tumors (Salomon et al., 2000). The highest significant increase in expression of Cripto compared to non-involved epithelium was in colon, stomach, pancreas, breast, lung, and bladder carcinoma. It was noted that the level of expression increases with degree of dysplasia from pre-malignant to metastatic disease in gastric cancer. Given the common finding of the over-expression of several EGF-related growth factors simultaneously, together with receptor proteins, EGFR (HER1) and ErbB2 (HER2), the additive or synergistic effect may play a significant role in tumorigenesis. Cripto over-expression was shown to repress the expression of E-cadherin and other epithelial markers such that epithelial integrity was compromised. This indicates that Cripto over-expression could be tumorigenic in vivo.

Animal models have been useful in defining molecular interactions in the mammary glands of transgenic mice by over-expressing a transgene from a mammary-specific promoter such as the mouse mammary tumor virus-LTR (MMTV). To determine if Cripto over-expression alone can cause tumor formation, MMTV-CR-1 transgenic mice have been developed (Wechselberger et al., unpublished communications). The results so far show that mammary hyperplasias occur in multiparous females and about 35% of multiparous females develop papillary adenocarcinomas of the mammary gland. In virgin females, there is a dramatic increase in ductal morphogenesis (lateral side branching) and intraductal hyperplasia.

SIMILARITIES OF CRIPTO TO THE FIBROBLAST GROWTH FACTOR (FGF) FAMILY

The similarity of Cripto to FGF is not immediately obvious, but several features are shared. First, the frog *Xenopus laevis* EGF-CFC protein homologue, Frl-1, was cloned from its binding to the *Xenopus* FGF receptor using a functional screen in yeast (Kinoshita et al., 1995). Secondly, both have essential functions in mesoderm and axis formation and patterning in developing embryos. Thirdly, although Cripto does not bind to the FGFR-1 directly, it does have a common docking protein, FGFR substrate-2 (FRS2). FRS2 binds to activated FGFR1 via its phosphotyrosine-binding (PTB) domain, and activates Grb2 and Sos to signal through the RAS/MAPK pathway (Kouhara et al., 1997; Ong et al., 2000). FRS2 is able to attach to the plasma membrane through myristylation, thus bringing it (and the FGFR) close to lipid rafts where Cripto is anchored. Finally, a remarkable finding using three-dimensional

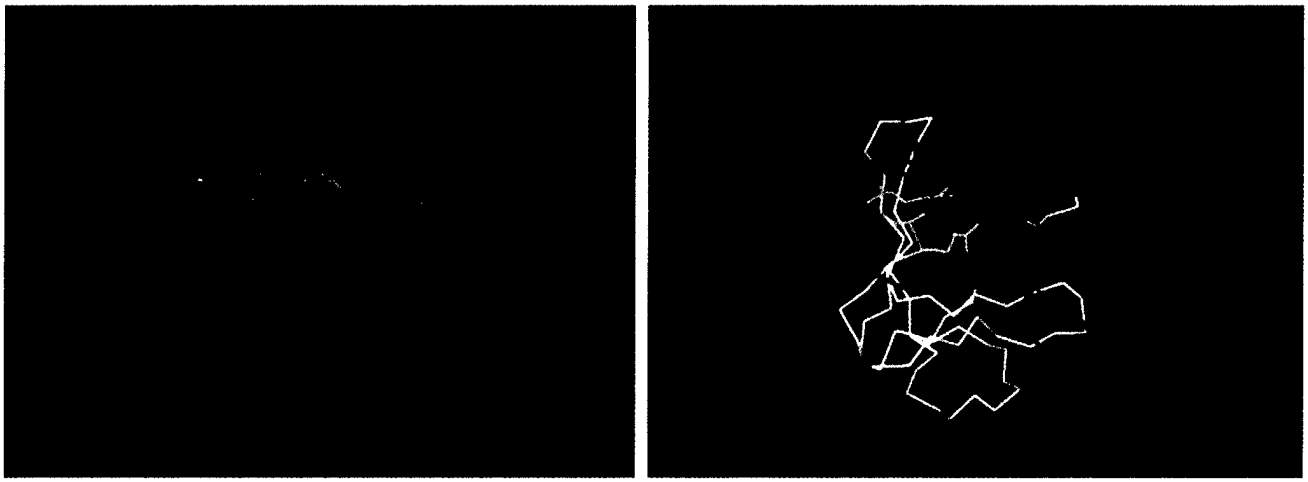

Fig. 2. Molecular structures. **A**: View of a model for Cripto superimposed onto the basic FGF structure (2bfh). The Cα traces are shown, Cripto in magenta; FGF in cyan. **B**: Cripto model with EGF-like domain in red and the CFC domain in blue. Disulfide bonds are shown in yellow. Reproduced from Minchiotti et al. (2001) by permission of the publisher.

protein structure searches produced a very distinct match between the folded structure of Cripto and the β-trefoil structure of FGF2 (Ponting and Russell, 2000; Minchiotti et al., 2001). The overlap in these structures is reproduced in Figure 2A, the resulting predicted structure of Cripto is shown in Figure 2B.

The β-trefoil structure is not restricted to the FGF family, but occurs widely in other factors such as the lymphokine, interleukin 1. A binding domain within this structure may contribute to the ability of FGFs and Cripto to bind to heparin sulfate proteoglycans (HSPG) on the cell surface and in the matrix of the basal lamina. Binding to matrix is thought to enhance the affinity of cell receptors for growth factors held within. These are important clues in predicting how Cripto could have distinct types of receptors for each type of activity (see below).

MECHANISMS UNDERLYING THE ACTIVITIES OF CRIPTO

Signaling pathway

See recent reviews for details of the developmental signaling pathways operating for the EGF-CFC family of ligands (Schier and Shen, 2000; Shen and Schier, 2000; Schier, 2001). Cripto was first assigned to the Epidermal Growth Factor (EGF)-like family of ligands, but the EGF-like domain is unable to bind to any of the EGFR family of receptors. However, it does cross-talk with the ErbB4 receptor and the FGFR-1 indirectly, stimulating the tyrosine phosphorylation of these receptors and contributing to the subsequent stimulation of growth (Bianco et al., 1999; Salomon et al., 1999). The first studies of the receptor in mammary epithelial and A431 cells using recombinant [^{125}I]-Cripto, found no binding to any ErbB receptors. ErbB4 was shown to be activated and tyrosine phosphorylated by Cripto, but not by binding directly. The activation occurred through crosstalk via unknown receptor/adapters, such as c-Src to the ErbB4 receptor. c-Src can activate Shc which then complexes with Grb2 and Sos, for subsequent activation of the Ras/Raf/MEK/MAPK pathway to stimulate transcription factor activity in the nucleus (Kannan et al., 1997). This pathway may explain the proliferative effect of Cripto, but how the signals are generated is still unclear. A further clue to the receptor moieties is that Cripto stimulates the rapid appearance of phosphorylated proteins of 185 kDa (likely ErbB4) and 120, 80, and 60 kDa and recently the possible identity of these intermediaries has been suggested (see below) In addition, PI3 kinase was shown to be activated by Cripto because treatment with the PI3Kinase inhibitor, LY294002 blocked PI3Kinase activation and the inhibitory effect of Cripto on β-casein protein synthesis in HC-11 cells. The data suggest that human Cripto can function as a survival factor through a PI3K-dependent signaling pathway involving AKT and GSK-3β. This pathway could also explain the effects of Cripto on differentiation (De Santis et al., 1997; Ebert et al., 1999).

The interactions of the EGF-CFC proteins in *Xenopus* and Zebrafish have produced good evidence for the receptors that are vital for developmental signaling. In these species, Cripto is required for A/P axis and mesodermal patterning, while Cryptic regulates left–right asymmetry in the heart and other organs. Cripto and Cryptic are represented by one member of the family, Frl-1 in *Xenopus* and Oep in the Zebrafish, *Danio rerio* and they regulate both axis/mesoderm formation and left–right asymmetry. The embryos of these species are readily manipulated to express exogenous mRNA and in some studies, heterologous soluble EGF-CFC proteins have been injected to test their effects on subsequent development. In Zebrafish, strong genetic evidence has indicated that EGF-CFC proteins render cells competent to respond to an instructive signal such as Nodal, or another TGFβ ligand. The receptor for the Oep+Nodal ligands is an Activin-type RIIB that requires an Activin RIB partner to activate the Smad2/Smad3 signaling pathway (Gritsman et al., 1999). For example, recombinant Nodal protein was able to induce Smad2 activation by this pathway in mouse EC (P19)

cells, but only when Cripto was expressed (Kumar et al., 2001).

Receptor reconstitution experiments, have shown that Cripto interacts with ALK4, an Activin Type RIB receptor to permit Nodal binding to the ALK4/Act-IIRB complex, leading to Smad phosphorylation (Yeo and Whitman, 2001). The effect of mutations of single codons in Cripto were tested for their effects as measured by phospho-Smad analysis. Injection of synthetic C-terminus tagged mouse Cripto mRNA into *Xenopus* embryos confirmed the requirement for both the EGF-like and the CFC domains. The Activin receptor ALK4 is able to mediate Nodal signaling, but only in the presence to Cripto; accordingly, recombinant Cripto protein binds directly both Nodal and Alk4 receptor (Reissmann et al., 2001). In *Xenopus* embryo animal caps, the orphan type I serine/threonine kinase receptor ALK7 can also act as a receptor for mouse Nodal and *Xenopus* Nodal-related 1 (Xnr1) in receptor reconstitution experiments, indicating that ALK7 can also interact with ActRIIB to confer responsiveness to Xnr1 and Nodal. Both ALK4 and ALK7 receptors can independently bind Xnr1. In addition, Cripto is implicated in Nodal signaling via ALK7, since its expression enhances the ability of ALK7 and ActRIIB to respond to Nodal ligands and it binds directly Alk7 in co-immunoprecipitation assays (Reissmann et al., 2001). Cripto was found to be required for Nodal signaling to Smad2, but not for Nodal to inhibit Bone Morphogenetic Protein (BMP) signaling (Yeo and Whitman, 2001).

The Zebrafish maternal-zygotic one-eyed pinhead (M*zoep* mutant that lacks EGF-CFC gene expression has defects in anterior–posterior axis, defective trunk formation, as well as L/R asymmetry defects and the presence of a single midline eye. Studies using the mutant animal can be informative by the injection of recombinant protein or mRNA into embryos to determine the degree of rescue of the mutant phenotype. In spite of the species and sequence difference, wild-type mouse Cripto or Xenopus Frl-1 proteins can fully rescue the trunk defects of *oep* mutants and the soluble protein lacking the last 16 amino acids is also active (Gritsman et al., 1999; Minchiotti et al., 2001). Of several mutations in single amino acids in mouse Cripto that were tested, two in the EGF-like domain (G71 and F78) lead to loss of rescue function, defining these residues as essential for Cripto function, at least in this assay. A further four mutations in the EGF-like domain and four more in the CFC-domain gave intermediate rescue in a dose-dependent manner. A structural model that predicts in silico, the molecular shape of Cripto was built (Fig. 2) and shows that the most critical residues are grouped at one side of the molecule. Important residues in the EGF-like (N67, S77, R88, and E91) and CFC domain (H104, L114, L122, and R116) are required, indicating the cooperation of both these motifs in forming an active site (Minchiotti et al., 2001). These data will be useful in testing how Cripto interacts with its putative receptors and whether different receptors are utilized in different tissues.

The question of receptor usage was posed for the effects of Cripto in mammary epithelial cells. Is Nodal, a molecule thought to be restricted to the early embryo, expressed in this tissue? Surprisingly, the answer was affirmative as tested by Bianco et al. (2002). A human brain phage-display library with human recombinant Cripto as bait, was used to detect and identify a receptor in mammary epithelial cells. Phage inserts with identity to the Type I Activin receptor RIB/ALK4, were detected, and shown to bind to and immunoprecipitate with Cripto. No Activin Type II partner for normal Activin receptor activity was found on the surface of mouse mammary cells. However, Nodal was found to be expressed after embryogenesis in the mammary gland and to be required together with ALK4 for Cripto signaling via Smad2 phosphorylation in epithelial cells (Bianco et al., 2002). When recombinant extracellular domains of these Activin receptors were tested in an ELISA binding assay, soluble Cripto bound specifically and with high affinity to the extracellular domain (ECD) of ALK4, but not the ECDs of Activin RIIA or ActivinRIIB. In this in vitro assay, Cripto bound to ALK4 in the absence of any co-receptor. The levels of mRNA expressed in the developing mammary gland measured by RT-PCR, show that the pattern of expression levels of Cripto and Nodal are parallel while ALK4 expression remains unchanged through puberty, pregnancy, and lactation. ActRIIB is also expressed throughout development of the mammary gland with an increase during lactation. Therefore, in the mouse, mammary cells do express the Activin receptor partner to ALK4, even though it does not seem to be required for Cripto binding and signaling by Nodal. Only Nodal, Cripto, and ALK4 are required to generate a signal in a mammary cell line, to activate Smad2. Independent of this signaling pathway, Cripto can also activate the MAPK and the Akt pathways in the same mammary epithelial cells and this does not require Nodal or ALK4. Therefore, the morphogenesis signaling pathway may be generated via Nodal, ALK4, and Smad2, but the proliferative (transforming?) pathway activates MAPK and Akt. This leads to the question of how Cripto finds a receptor without Nodal as a cofactor and of the nature of the receptor. (For a recent review on Activins in organ development, see Ball and Risbridger, 2001.)

CRIPTO RECEPTOR(S)

We hypothesize that the GPI-anchored extracellular form of the Cripto molecule is a crucial characteristic for some of its biological functions based on autocrine effects, ligand recognition, ligand-receptor binding strength and/or efficiency, and possibly also to generate the signals and graded responses by the receptor into the selection of specific signaling pathways. However, the soluble monomer form is also active and must bind to a receptor or a co-receptor at the membrane. The type of Cripto receptor and the affinity of binding are hypothesized to play a large role in the specific signaling pathway used and in the specific response produced in a target cell. There is no evidence that Cripto needs to be activated by dimerization, although this cannot be ruled out once it has bound to a receptor. In general, the more intense the stimulus, the more variable the response may be. For instance, some growth factors including Cripto, can affect cell shape and cell migration by secondary effects on the cytoskeleton, as well as stimulating cell proliferation. This may involve interactions

with the extracellular matrix and these are included in the following models.

There are at least five cellular responses that Cripto can stimulate. They are morphogenesis/differentiation, survival, proliferation, deregulated or transformed growth, and increased motility. The scheme illustrated in Figure 3A offers the simplest combination of molecular components of a small class of proteins that can be assembled at the membrane through the special properties of lipid rafts. Lipid rafts are structures that interrupt the lipid bilayer at the surface of cells by their disordered composition consisting of high levels of cholesterol and sphingolipids. Lipid rafts can form the anchorage for extracellular molecules that have GPI linkages and for intracellular signaling molecules such as c-Src and FRS2, that have myristylated or acylated extensions that enter the lipid raft from inside the cell. The assumption is that once in the raft, they can interact without requiring the protein backbone to be in contact. Model A depicts that Cripto could interact with c-Src, the most common of the non-receptor tyrosine kinases that attach in this way to the membrane. There is good reason to think that c-Src is a partner in this and other schemes, because when Src-like kinases are treated with the inhibitors, PP1 or PP2, downstream activation (i.e., tyrosine transphosphorylation) of ErbB4 and MAPK is blocked in a number of mouse and human mammary epithelial cell lines (Salomon et al., 2000). The data suggest that c-Src is the upstream activator that is directly coupled to Cripto through an ALK-4 and Nodal-independent signaling pathway because ErbB-4 transphosphorylation and MAPK activation are not blocked by a DN-ALK4 in cells that are also null for Nodal expression. Alternatively, in Model B, an unidentified receptor kinase is also inserted into or adjacent to the lipid raft where Cripto can interact without binding directly. Possibly this is how ErbB4 might become phosphorylated. The importance of ErbB4 to signaling in transformed mammary epithelial cells was shown using a ribozyme vector to reduce ErbB4 expression in T47-D human breast cancer cells. MAPK activation by Cripto was severely attenuated in these cells. Whether this is also true for other breast cancer cell lines or other non-transformed mouse or human mammary epithelial cells that also respond to Cripto with respect to MAPK activation is not known.

The signaling pathway utilized by Cripto in the embryo and possibly in the developing mammary gland is probably best represented by Model C in Figure 3. In these tissues, Cripto binds to and requires Nodal, which binds to the Activin Type IB/ALK4 Receptor; probably the p60 kDa protein shown to bind to Cripto (Bianco et al., 1999). In the embryo and mammary gland, the ALK4 receptor partner is ActIIB. The activation of ALK4 leads to the phosphorylation of Smad2 and 3 leading to the activation of Smad4, which then carries the signal to the nucleus for cellular responses by target gene regulation. Model D is a variant of model B, wherein GPI-anchored Cripto, in lipid rafts can interact with myristylated c-Src and with myr-FRS2 that can bind to the FGFR1 when activated. The FGF/FGFR/FRS2 pathway operates in embryos in response to FGF (Ong et al., 2000; Kusakabe et al., 2001) and in the development of the mammary gland. FGFR2 has been shown to play a role in ductal morphogenesis in the virgin mammary gland and in alveolar–lobular development during pregnancy (Jackson et al., 1997) and FGFs and FGFR1 are expressed on breast cancer cells (Yoshimura et al., 1998). Activated FRS2 can bind to Grb2 and to the phosphatase Shp2 to crosstalk with pathways leading to growth and motility. This indirect binding via the FGF signaling pathway is another possible effect of Cripto.

The cytokine receptor gp130 and its partner LIFR are expressed in breast cancer cells (Douglas et al., 1997). LIF, the ligand for this receptor is also expressed in breast cancer cells (Chiu et al., 1996) and has been shown to stimulate the growth of breast cancer cell lines, but with less effect on normal mammary cells (Estrov et al., 1995). It is possible that breast cell growth is, in part, regulated by Cripto interaction with this cytokine system (model E in Fig. 3). Note that the molecular size of gp130 is similar to the size of one of the proteins that is detected after cross-linking to Cripto (Bianco et al., 1999). LIF inhibits the differentiation of ES cells and also induces branching tubulogenesis in the developing kidney (Sariola, 2001), although a similar effect has not been tested in the mammary gland. There is also evidence for a role for LIF and other members of the IL6 family of cytokines in cardiomyocyte growth and function. In ES cell aggregates or EBs differentiating to cardiomyocytes as described earlier, LIF has to be removed for differentiation to start. Since ES cells express Cripto, we speculate that Cripto could bind and replace LIF on the receptor pair, LIFR/gp130 heterodimer depicted in Figure 3E activate the Jak/Stat pathway for differentiation of cardiomyocytes. Consider also that this receptor pair is known to play a role in cardiomyocyte function, for instance, in stress responses leading to cardiomyocyte enlargement and heart failure (Hirota et al., 1999). Another cytokine, cardiotrophin1, also rapidly activates the LIFR/gp130 receptor heterodimer on ES cells and leads to the tyrosine phosphorylation of gp130 in developing cardiomyocytes (Wollert and Chien, 1997). Similarly LIF or IL6 additions to cardiomyocyte cultures cause the cells to stimulate myosin light chain protein (MLC-2) by signaling via the Jak/Stat pathway to increase cardiomyocyte size (Kodama et al., 1997). It is possible, therefore, that Cripto interacts with this receptor system to regulate the development of the cardiomyocyte during embryogenesis. In cancer cells the Stat pathway becomes readily unregulated. Constitutive activation of Stat3 has been detected in a large range of human breast cancer cells and was shown to be maintained by upstream Src and Jak activation and probably generated via activated tyrosine kinase receptors. The application of a dominant negative Stat3 induced apoptosis (Garcia et al., 2001) indicating the importance of the Stat transcription factors in tumorigenesis. Perhaps the activation of the Cripto receptor exacerbates this effect in mammary cancer cells.

Many different cell surface and matrix proteoglycan core proteins are expressed in the mammary gland and in mammary cells in culture. Heparan sulfate proteoglycans at the cell surface modulate the activities of a large number of extracellular ligands such as TGFβ, VEGF, FGF, HGF, and Wnts (Bernfield et al., 1999).

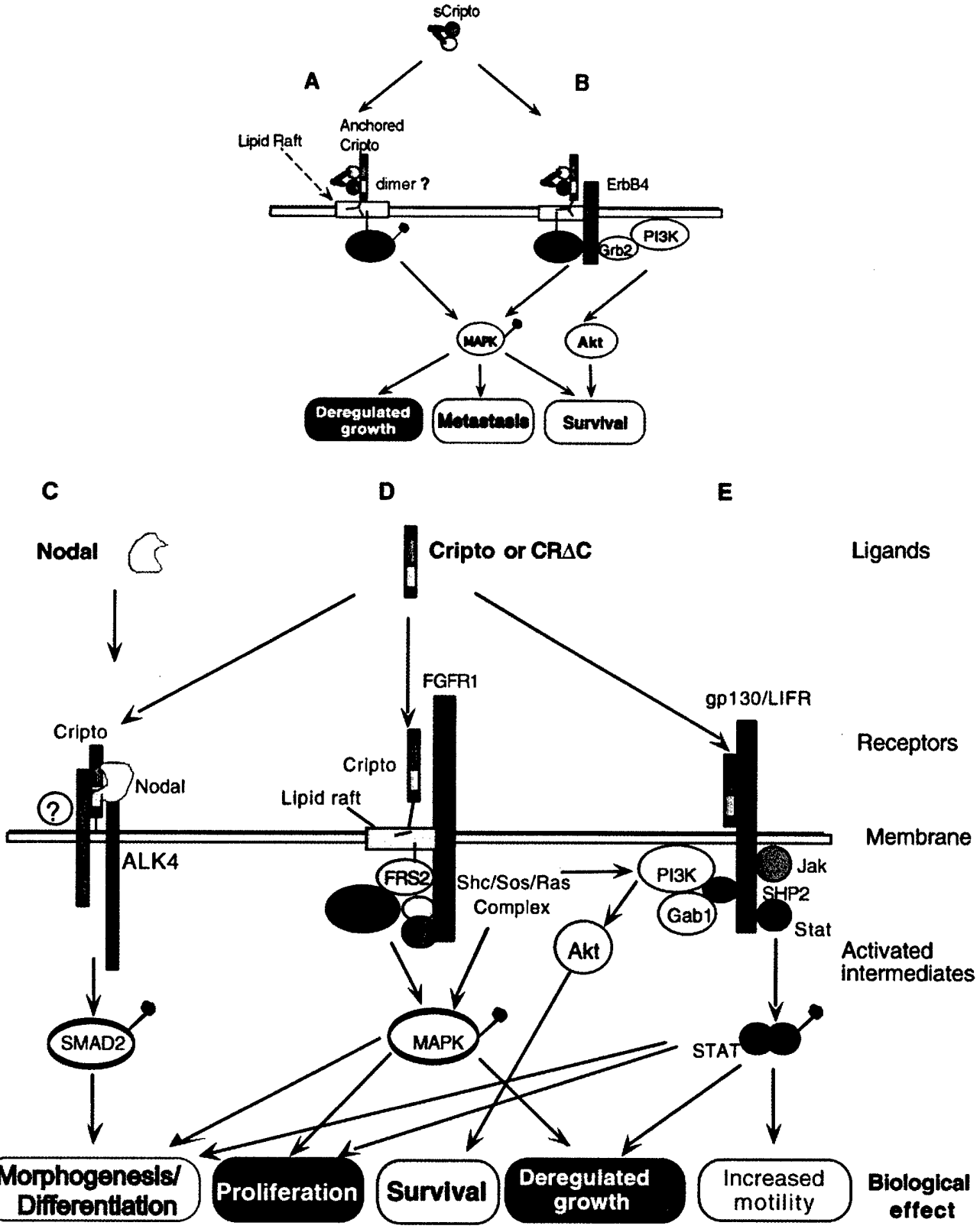

Fig. 3. *(Continued)*

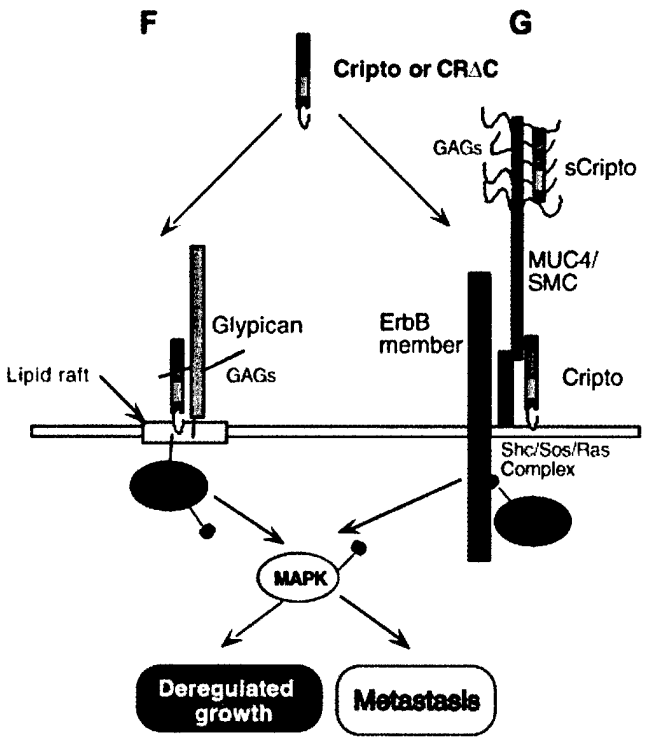

Fig. 3. Putative Cripto receptors and some signaling factors that may operate in the mammary gland. **A**: The simplest mode for Cripto interaction with the intracellular signaling component c-Src, to activate growth, survival, and metastatic pathways. This is possible through the location of the partners in lipid rafts that can bring factors together by their concentration there. **B**: Cripto is known to activate the ErbB4 receptor, but only indirectly. This is known to be important for proliferative responses. **C**: Cripto acts as a cofactor with Nodal to activate the ALK4 (Act-RIB). The involvement of an Act-RIIB does not appear to be necessary as described by Bianco et al. (unpublished communications). **D**: Cripto is known to activate the FGF Receptor-I through the intermediary FRS2, to activate the MAPK pathway. **E**: Cripto could also interact with the gp130/LIFR cytokine receptor complex that is found on ES cells and mammary carcinoma cells, but there is as yet no evidence for this. **F**: Cripto is likely to find another component in lipid rafts, the proteoglycan glypican, whose GAG moieties can bind a number of growth factors. Thus glypican may act as a receptor or co-receptor. **G**: The mucin family of glycoproteins are over-expressed in mammary carcinoma cells and the membrane inserted component of MUC4 could also act as an adapter for crosstalk with the ErbB family.

A molecule of Mr130 kDa is a good candidate for performing a role as a Cripto receptor or co-receptor if it is known to be expressed in a manner that parallels the levels and activities of Cripto. Glypican is a candidate because it is an extracellular proteoglycan of 130 kDa that is GPI inserted into lipid rafts in the membrane (Delehedde et al., 2001) and is known to act as a cofactor in FGF and TGFβ signaling. Glypican is known to bind to some isoforms of VEGF to potentiate binding to the Flk1 receptor and to stimulate angiogenesis (Robinson and Stringer, 2001). Proteoglycans can bind multiple proteins simultaneously and bring them together. Therefore glypican could serve as a cofactor to bind soluble Cripto to promote synergy with other growth factors and their receptors (Fig. 3F) and this could be readily tested. A similar format could operate for the sialomucins (see Fig. 3G for a model). Mucins are a large group of proteins that contain *O*-linked saccharides of which the larger molecules are viscous and generally have a protective function for the cell. Some mucins are membrane inserted and some are soluble. For example, Muc4/Smc is formed from a single polypeptide chain that is proteolytically cleaved into a heterodimer. One subunit, ASGP-2 (sialoglycoprotein) is a membrane inserted protein with two EGF-like domains and is a partner to the larger polypeptide, ASPG-1 of 120–140 kDa, that is heavily decorated with proteoglycan chains (Sherblom and Carraway, 1980). FGF-like proteins such as Cripto can bind to HSPG moieties and potentially generate a signal through the EGF domains in the ASPG-2 chain, which have consensus binding sequences for the ErbB receptors. In this respect, ASGP-2 was shown to co-immunoprecipitate with ErbB2 (Sheng et al., 1992). Interestingly, the expression of Muc4 during mammary development parallels that of Cripto and Muc4, like Cripto, is secreted into the milk. In general Muc4 is over-expressed in cancer cells and inhibits cell–cell interaction, thus contributing to invasiveness and metastatic behavior of cells. A different proteoglycan, DC3/Muc1 is also associated with breast cancer and is able to bind to c-Src after its phosphorylation by the activated EGF receptor (Li et al., 2001). This may also serve to crosstalk with Cripto. (For more details on proteoglycan roles in breast cancer see a recent review Carraway et al., 2001). These suggestions for possible new types of receptors for the Cripto growth factor have some credence and could provide some avenues to explore.

CONCLUSIONS AND POSSIBILITIES FOR CANCER THERAPEUTICS

Cripto as a marker

Cripto could be an important indicator of the initiation of transformation and degree of progression of the tumorigenic process, in carcinoma of the breast, colon, lung, pancreas, stomach, and bladder. Cripto is certainly synthesized at increasing levels with the progression of mammary tumor development in animal models (Kenney et al., 1996; Niemeyer et al., 1999). Cripto has also been shown to cause mammary adenocarcinoma in transgenic mice over-expressing Cripto in mammary tissue.

Cripto activates a number of signaling pathways

Cripto activates a number of signaling pathways of which the most defined is during development. In this case Cripto functions as a cofactor for Nodal, an important morphogen, binding Activin receptor heterodimers and signaling through the Smad transcription factor pathway. Cripto may perform several roles in the mammary gland by stimulating ductal morphogenesis in the virgin animal; by regulating the proliferation of lobular–alveolar epithelial cells during pregnancy; and in the inhibition of the production of milk after lactation and possibly by contributing to apoptosis of the epithelial cells at the end of lactation. High levels of Cripto fall to undetectable levels in the resting gland and only rise again in the event of inappropriate conditions leading to hyperplasia and tumorigenic progression. During the development of the mammary gland, Nodal may be

required with Cripto to interact with the Activin receptors ALK4 or ALK7, to signal via the Smad transcription factors.

Cripto can activate the ErbB4 receptor indirectly

Cripto can activate the ErbB4 receptor indirectly by as yet unknown mechanism(s) and this may be an essential signal during lactation where ErbB4 performs an obligatory role in regulating milk protein expression (Jones et al., 1999), and where c-Src is a required effector in this situation. What is needed now is a search for other receptors that may act through specific mechanisms in specific cell types to mediate Cripto functions.

Other receptors or co-receptors

Receptors that have been found to be over-expressed in tumor cell lines, especially mammary tumor cells and mammary tumors, include ErbB receptors, FGF receptors, the cytokine receptors, proteoglycans glypican and the sialomucins. These components of the normal cell become elevated in breast cancer tissues and could lead to one or all of the putative signaling programs outlined here. In addition, ligands for the ErbB and FGF receptors also become over-expressed to create positive feedback loops. All of these may contribute to increasing progression of growth rates that increase the chances of genetic changes and to inappropriate survival of transformed cells and to the loss of cell adhesion leading to metastases. Each of these avenues is worthy of study.

Attention to some candidate receptors

This review draws attention to some candidate receptors, but more study is needed. Cripto itself or its receptor(s) may be appropriate therapeutic targets in cancer, or more usefully, the prevention of Cripto re-expression or action. In one approach, a ribozyme-based vector was designed that inhibited Cripto translation (Kintner and Hosick, 1998). Likewise, the use of AS oligonucleotides against Cripto have shown activity in inhibiting breast, colon, and ovarian cell growth (Normanno et al., 2001).

Over-expressed growth factors

It should be kept in mind that many other growth factors when over-expressed, are tumorigenic in the mammary gland. Therefore, it is likely that no single growth factor will hold the masterkey to therapy. In this respect a mixture of AS oligonucleotides to Amphiregulin, Cripto and TGFα was shown to inhibit the growth of a human breast carcinoma cell line in vitro, when individually applied at 0.7 μM each (De Luca et al., 1999). The combination of different AS oligos significantly reduced xenograft tumor growth in nude mice treated in vivo, suggesting a possible therapeutic approach (De Luca et al., 2000).

Structure of cripto

Knowledge of the structure of Cripto and its receptors will be a first goal towards intercepting the binding of Cripto and blocking the generation of transforming signals. Since this does not require the agent to enter cells, it is a desirable approach to therapy. Ultimately, only understanding the signal pathway may provide a common therapeutic target that may be a more general focus for intervention. If the hypothesis is correct that Cripto operates through several signaling pathways, each leading to a distinct response, then it will be possible to target tumor cells specifically.

LITERATURE CITED

Abe Y, Odaka M, Inagaki F, Lax I, Schlessinger J, Kohda D. 1998. Disulfide bond structure of human epidermal growth factor receptor. J Biol Chem 273:11150–11157.

Ball EMA, Risbridger GP. 2001. Activins as regulators of branching morphogenesis [review]. Dev Biol 238:1–12.

Bamford RN, Roessler E, Burdine RD, Saplakoglu U, dela Cruz J, Splitt M, Towbin J, Bowers P, Marino B, Schier AF, Shen MM, Muenke M, Casey B. 2000. Loss-of-function mutations in the EGF-CFC gene CFC1 are associated with human left–right laterality defects. Nat Genet 26:365–369.

Bernfield M, Gotte M, Park PW, Reizes O, Fitzgerald ML, Lincecum J, Zako M. 1999. Functions of cell surface heparan sulfate proteoglycans. Annu Rev Biochem 68:729–777.

Bianco C, Kannan S, De Santis M, Seno M, Tang CK, Martinez-Lacaci I, Kim N, Wallace-Jones B, Lippman ME, Ebert AD, Weehselberger C, Salomon DS. 1999. Cripto-1 indirectly stimulates the tyrosine phosphorylation of erb B-4 through a novel receptor. J Biol Chem 274:8624–8629.

Bianco C, Wechselberger C, Ebert A, Khan NI, Sun YP, Salomon DS. 2001. Identification of Cripto-1 in human milk. Breast Cancer Res Treat 66:1–7.

Bianco C, Adkins H, Wechselberger C, Seno M, Normanno N, De Luca A, Sun Y, Khan N, Kenney N, Williams K, Sanicola M, Salomon DS. 2002. Cripto-1 activates Nodal and ALK4 dependent and independent signalling pathways in mammary epithelial cells. (In press).

Brandt R, Normanno N, Gullick WJ, Lin JH, Harkins R, Scheider D, Jones BW, Ciardiello F, Persico MG, Armenante F, Kim N, Salomon DS. 1994. Identification and biological characterization of an epidermal growth factor-related protein: Cripto-1. J Biol Chem 269:17320–17328.

Carraway KL, Price-Schiavi SA, Komatsu M, Jepson S, Perez A, Carraway CA. 2001. Muc4/sialomucin complex in the mammary gland and breast cancer. J Mammary Gland Biol Neoplasia 6:323–337.

Chiu JJ, Sgagias MK, Cowan KH. 1996. Interleukin 6 acts as a paracrine growth factor in human mammary carcinoma cell lines. Clin Cancer Res 2:215–221.

Ciardello F, Dono R, Kim N, Persico MG, Salomon DS. 1991. Expression of *cripto*, a novel gene of the epidermal growth factor gene family, leads to in vitro transformation of a normal mouse mammary epithelium cell line. Cancer Res 51:1051–1054.

Ciccodicola A, Dono R, Obici S, Simeone A, Zollo M, Persico MG. 1989. Molecular characterization of a gene of the 'EGF family' expressed in undifferentiated human NTERA2 teratocarcinoma cells. EMBO J 8:1987–1991.

Colas JF, Schoenwolf GC. 2000. Subtractive hybridization identifies chick-cripto, a novel EGF-CFC ortholog expressed during gastrulation, neurulation and early cardiogenesis. Gene 255:205–217.

De Luca A, Casamassimi A, Selvam MP, Losito S, Ciardiello F, Agrawal S, Salomon DS, Normanno N. 1999. EGF-related peptides are involved in the proliferation and survival of MDA-MB-468 human breast carcinoma cells. Int J Cancer 80:589–594.

De Luca A, Arra C, D'Antonio A, Casamassimi A, Losito S, Ferraro P, Ciardiello F, Salomon DS, Normanno N. 2000. Simultaneous blockage of different EGF-like growth factors results in efficient growth inhibition of human colon carcinoma xenografts. Oncogene 19:5863–5871.

De Santis ML, Kannan S, Smith GH, Seno M, Bianco C, Kim N, Martinez-Lacaci I, Wallace-Jones B, Salomon DS. 1997. Cripto-1 inhibits beta-casein expression in mammary epithelial cells through a p21ras-and phosphatidylinositol 3′-kinase-dependent pathway. Cell Growth Differ 8:1257–1266.

De Santis ML, Martinez-Lacaci I, Bianco C, Seno M, Wallace-Jones B, Kim N, Ebert A, Wechselberger C, Salomon DS. 2000. Cripto-1 induces apoptosis in HC-11 mouse mammary epithelial cells. Cell Death Differ 7:189–196.

Delehedde M, Lyon M, Sergeant N, Rahmoune H, Fernig DG. 2001. Proteoglycans: Pericellular and cell surface multireceptors that integrate external stimuli in the mammary gland. J Mammary Gland Biol Neoplasia 6:253–273.

Ding J, Yang Y, Yan Y-T, Chan A, Desai N, Wynshaw-Boris A, Shen MM. 1998. Cripto is required for correct orientation of the anterior–posterior axis in the mouse embryo. Nature 395:702–707.

Dono R, Montuori N, Rocchi M, De Ponti-Zilli L, Ciccodicola A, Persico MG. 1991. Isolation and characterization of the CRIPTO autosomal gene and its X-linked related sequence. Am J Hum Genet 49:555–565.

Dono R, Scalera L, Pacifico F, Acampora D, Persico MG, Simeone A. 1993. The murine cripto gene: Expression during mesoderm induction and early heart morphogenesis. Development 118:1157–1168.

Douglas AM, Goss GA, Sutherland RL, Hilton DJ, Berndt MC, Nicola NA, Begley CG. 1997. Expression and function of members of the cytokine receptor superfamily on breast cancer cells. Oncogene 14:661–669.

Ebert AD, Wechselberger C, Frank S, Wallace-Jones B, Seno M, Martinez-Lacaci I, Bianco C, De Santis M, Weitzel HK, Salomon DS. 1999. Cripto-1 induces phosphatidylinositol 3′-kinase-dependent phosphorylation of AKT and glycogen synthase kinase 3 beta in human cervical carcinoma cells. Cancer Res 59:4502–4505.

Ebert AD, Wechselberger C, Nees M, Clair T, Schaller G, Martinez-Lacaci I, Wallace-Jones B, Bianco C, Weitzel HK, Salomon DS. 2000. Cripto-1-induced increase in vimentin expression is associated with enhanced migration of human Caski cervical carcinoma cells. Exp Cell Res 257:223–229.

Ertoy D, Ayhan A, Sarac E, Karaagaoglu E, Yasui W, Tahara E. 2000. Clinicopathological implication of cripto expression in early stage invasive cervical carcinomas. Eur J Cancer 36:1002–1007.

Estrov Z, Samal B, Lapushin R, Kellokumpu-Lehtinen P, Sahin AA, Kurzrock R, Talpaz M, Aggarwal BB. 1995. Leukemia inhibitory factor binds to human breast cancer cells and stimulates their proliferation. J Interferon Cytokine Res 15:905–913.

Garcia R, Bowman TL, Niu G, Yu H, Minton S, Muro-Cacho CA, Cox CE, Falcone R, Fairclough R, Parsons S, Laudano A, Gazit A, Levitzki A, Kraker A, Jove R. 2001. Constitutive activation of Stat3 by the Src and JAK tyrosine kinases participates in growth regulation of human breast carcinoma cells. Oncogene 20:2499–2513.

Gritsman K, Zhang J, Cheng S, Heckscher E, Talbot WS, Schier AF. 1999. The EGF-CFC protein one-eyed pinhead is essential for nodal signaling. Cell 97:121–132.

Herrington EE, Ram TG, Salomon DS, Johnson GR, Gullick WJ, Kenney N, Hosick HL. 1997. Expression of epidermal growth factor-related proteins in the aged adult mouse mammary gland and their relationship to tumorigenesis. J Cell Physiol 170:47–56.

Hirota H, Chen J, Betz UAK, Rajewsky K, Gu Y, Ross J, Muller W, Chien KR. 1999. Loss of a gp130 cardiac muscle cell survival pathway is a critical event in the onset of heart failure during biomechanical stress. Cell 97:189–198.

Jackson D, Bresnick J, Rosewell I, Crafton T, Poulsom R, Stamp G, Dickson C. 1997. Fibroblast growth factor receptor signalling has a role in lobuloalveolar development of the mammary gland. J Cell Sci 110:1261–1268.

Johnson SE, Rothstein JL, Knowles BB. 1994. Expression of epidermal growth factor family gene members in early mouse development. Dev Dyn 201:216–226.

Jones FE, Welte T, Fu XY, Stern DF. 1999. ErbB4 signaling in the mammary gland is required for lobuloalveolar development and Stat5 activation during lactation. J Cell Biol 147:77–88.

Kannan S, De Santis M, Lohmeyer M, Riese DJ, Smith GH, Hynes N, Seno M, Brandt R, Bianco C, Persico G, Kenney N, Normanno N, Martinez-Lacaci I, Ciardello F, Stern DF, Gullick WJ, Salomon DS. 1997. Cripto enhances the tyrosine phosphorylation of Shc and activates mitogen-activated protein kinase (MAPK) in mammary epithelial cells. J Biol Chem 272:3330–3335.

Kenney NJ, Huang RP, Johnson GR, Wu JX, Okamura D, Matheny W, Kordon E, Gullick WJ, Plowman G, Smith GH, Salomon DS, Adamson ED. 1995. Detection and location of amphiregulin and Cripto-1 expression in the developing postnatal mouse mammary gland. Mol Reprod Dev 41:277–286.

Kenney NJ, Smith GH, Maroulakou IG, Green JH, Muller WJ, Callahan R, Salomon DS, Dickson RB. 1996. Detection of amphiregulin and Cripto-1 in mammary tumors from transgenic mice. Mol Carcinog 15:44–56.

Kinoshita N, Minshull J, Kirschner MW. 1995. The identification of two novel ligands of the FGF receptor by a yeast screening method and their activity in Xenopus development. Cell 83:621–630.

Kintner RL, Hosick HL. 1998. Reduction of Cripto-1 expression by a hammerhead-shaped RNA molecule results from inhibition of translation rather than mRNA cleavage. Biochem Biophys Res Commun 245:774–779.

Kodama H, Fukuda K, Pan J, Makino S, Baba A, Hori S, Ogawa S. 1997. Leukemia inhibitor factor, a potent cardiac hypertrophic cytokine, activates the JAK/STAT pathway in rat cardiomyocytes. Circ Res 81:656–663.

Kouhara H, Hadari YR, Spivak-Kroizman T, Schilling J, Bar-Sagi D, Lax I, Schlessinger J. 1997. A lipid-anchored Grb2-binding protein that links FGF-receptor activation to the Ras/MAPK signaling pathway. Cell 89:693–702.

Kumar A, Novoselov V, Celeste AJ, Wolfman NM, ten Dijke P, Kuehn MR. 2001. Nodal signaling uses activin and transforming growth factor-beta receptor-regulated Smads. J Biol Chem 276:656–661.

Kusakabe M, Masuyama N, Hanafusa H, Nishida E. 2001. Xenopus FRS2 is involved in early embryogenesis in cooperation with the Src family kinase Laloo. EMBO Rep 2:727–735.

Li Y, Ren J, Yu W, Li Q, Kuwahara H, Yin L, Carraway KL 3rd, Kufe D. 2001. The epidermal growth factor receptor regulates interaction of the human DF3/MUC1 carcinoma antigen with c-Src and beta-catenin. J Biol Chem 276:35239–35242.

Liguori G, Tucci M, Montuori N, Dono R, Lago CT, Pacifico F, Armenante F, Persico MG. 1996. Characterization of the mouse Tdgf1 gene and Tdgf pseudogenes. Mamm Genome 7:344–348.

Lohmeyer M, Harrison PM, Kannan S, DeSantis M, O'Reilly NJ, Sternberg MJ, Salomon DS, Gullick WJ. 1997. Chemical synthesis, structural modeling, and biological activity of the epidermal growth factor-like domain of human cripto. Biochemistry 36:3837–3845.

Medina D, Oborn CJ, Kittrell FS, Ullrich RL. 1986. Properties of mouse mammary epithelial cell lines characterized by in vivo transplantation and in vitro immunocytochemical methods. J Natl Cancer Inst 76:1143–1156.

Minchiotti G, Parisi S, Liguori G, Signore M, Lania G, Adamson ED, Lago CT, Persico GM. 2000. Membrane-anchorage of Cripto protein by glycosylphosphatidylinositol and its distribution during early mouse development. Mech Dev 90:133–142.

Minchiotti G, Manco G, Parisi S, Lago C, Rosa F, Persico G. 2001. Structure-function analysis of the EGF-CFC family member Cripto identifies residues essential for nodal signalling. Development 128:4501–4510.

Niemeyer CC, Persico MG, Adamson ED. 1998. Cripto: Roles in mammary cell growth, survival, differentiation and transformation. Cell Death Differ 5:440–449.

Niemeyer CC, Spencer-Dene B, Wu J-X, Adamson ED. 1999. Preneoplastic mammary tumor markers: Cripto and Amphiregulin are overexpressed in hyperplastic stages of tumor progression in transgenic mice. Int J Cancer 81:588–591.

Normanno N, Ciardiello F, Brandt R, Salomon DS. 1994. Epidermal growth factor-related peptides in the pathogenesis of human breast cancer. Breast Cancer Res Treat 29:11–27.

Normanno N, Kim N, Wen D, Smith K, Harris AL, Plowman G, Colletta G, Ciardiello F, Salomon DS. 1995. Expression of messenger RNA for amphiregulin, heregulin, and cripto-1, three new members of the epidermal growth factor family, in human breast carcinomas. Breast Cancer Res Treat 35:293–297.

Normanno N, Bianco C, De Luca A, Salomon DS. 2001. The role of EGF-related peptides in tumor growth. Front Biosci 6:D685–D707.

Ong SH, Guy GR, Hadari YR, Laks S, Gotoh N, Schlessinger J, Lax I. 2000. FRS2 proteins recruit intracellular signaling pathways by binding to diverse targets on fibroblast growth factor and nerve growth factor receptors. Mol Cell Biol 20:979–989.

Panico L, D'Antonio A, Salvatore G, Mezza E, Tortora G, De Laurentiis M, De Placido S, Giordano T, Merino M, Salomon DS, Mullick WJ, Pettinato G, Schnitt SJ, Bianco AR, Ciardiello F. 1996. Differential immunohistochemical detection of transforming growth factor alpha, amphiregulin and CRIPTO in human normal and malignant breast tissues. Int J Cancer 65:51–56.

Ponting CP, Russell RB. 2000. Identification of distant homologues of fibroblast growth factors suggests a common ancestor for all beta-trefoil proteins. J Mol Biol 302:1041–1047.

Reissmann E, Jornvall H, Blokzijl A, Andersson O, Chang C, Minchiotti G, Persico MG, Ibanez CF, Brivanlou AH. 2001. The orphan receptor ALK7 and the Activin receptor ALK4 mediate signaling by Nodal proteins during vertebrate development. Genes Dev 15:2010–2022.

Robinson CJ, Stringer SE. 2001. The splice variants of vascular endothelial growth factor (VEGF) and their receptors. J Cell Sci 114:853–865.

Saccone S, Rapisarda A, Motta S, Dono R, Persico GM, Della Valle G. 1995. Regional localization of the human EGF-like growth factor

CRIPTO gene (TDGF-1) to chromosome 3p21. Hum Genet 95:229–230.
Salomon DS, Bianco C, De Santis M. 1999. Cripto: A novel epidermal growth factor (EGF)-related peptide in mammary gland development and neoplasia [review]. Bioessays 21(1):61–70.
Salomon DS, Bianco C, Ebert AD, Khan NI, De Santis M, Normanno N, Wechselberger C, Seno M, Williams K, Sanicola M, Foley S, Gullick WJ, Persico G. 2000. The EGF-CFC family: Novel epidermal growth factor-related proteins in development and cancer. Endocr Relat Cancer 7:199–226.
Sariola H. 2001. The neurotrophic factors in non-neuronal tissues. Cell Mol Life Sci 58:1061–1066.
Schier AF. 2001. Axis formation and patterning in zebrafish. Curr Opin Genet Dev 11:393–404.
Schier AF, Shen MM. 2000. Nodal signalling in vertebrate development. Nature 403:385–389.
Schiffer SG, Foley S, Kaffashan A, Hronowski X, Zichittella A, Yeo CY, Miatkowski K, Adkins HB, Damon B, Whitman M, Sanicola M, Williams KP. 2001. Fucosylation of Cripto is required for its ability to facilitate Nodal signaling. J Biol Chem 276:37769–37778.
Shen MM, Schier AF. 2000. The EGF-CFC gene family in vertebrate development. Trends Genet 16:303–309.
Shen MM, Wang H, Leder P. 1997. A differential display strategy identifies Cryptic, a novel EGF-related gene expressed in the axial and lateral mesoderm during mouse gastrulation. Development 124:429–442.
Sheng Z, Wu K, Carraway KL, Fregien N. 1992. Molecular cloning of the transmembrane component of the 13762 mammary adenocarcinoma sialomucin complex. A new member of the epidermal growth factor superfamily. J Biol Chem 267:16341–16346.
Sherblom AP, Carraway KL. 1980. A complex of two cell surface glycoproteins from ascites mammary adenocarcinoma cells. J Biol Chem 255:12051–12059.
Wechselberger C, Ebert AD, Bianco C, Khan NI, Sun Y, Wallace-Jones B, Montesano R, Salomon DS. 2001. Cripto-1 enhances migration and branching morphogenesis of mouse mammary epithelial cells. Exp Cell Res 266:95–105.
Wollert KC, Chien KR. 1997. Cardiotrophin-1 and the role of gp130-dependent signaling pathways in cardiac growth and development [review] [98 refs]. J Mol Med 75(7):492–501.
Xu C, Liguori G, Adamson ED, Persico MG. 1998. Cardiac differentiation is blocked in embryonic stem cells lacking Cripto-1. Dev Biol 196:237–247.
Xu C, Liguori G, Persico MG, Adamson ED. 1999. Abrogation of the Cripto gene in mouse leads to failure of post-gastrulation morphogensis and lack of differentiation of cardiomyocytes. Development 126:483–494.
Yeo C, Whitman M. 2001. Nodal signals to Smads through Cripto-dependent and Cripto-independent mechanisms. Mol Cell 7:949–957.
Yoshimura N, Sano H, Hashiramoto A, Yamada R, Nakajima H, Kondo M, Oka T. 1998. The expression and localization of fibroblast growth factor-1 (FGF-1) and FGF receptor-1 (FGFR-1) in human breast cancer. Clin Immunol Immunopathol 89:28–34.
Zhang J, Talbot WS, Schier AF. 1998. Positional cloning identifies zebrafish one-eyed pinhead as a permissive EGF-related ligand required during gastrulation. Cell 92:241–251.

Article

Nodal-dependent Cripto signaling promotes cardiomyogenesis and redirects the neural fate of embryonic stem cells

Silvia Parisi,[1] Daniela D'Andrea,[1] Carmine T. Lago,[1] Eileen D. Adamson,[2] M. Graziella Persico,[1] and Gabriella Minchiotti[1]

[1]Institute of Genetics and Biophysics, "Adriano Buzzati-Traverso," Consiglio Nazionale delle Ricerche, 80131 Naples, Italy
[2]Cancer Research Center, The Burnham Institute, La Jolla, CA 92037

The molecular mechanisms controlling inductive events leading to the specification and terminal differentiation of cardiomyocytes are still largely unknown. We have investigated the role of Cripto, an EGF-CFC factor, in the earliest stages of cardiomyogenesis. We find that both the timing of initiation and the duration of Cripto signaling are crucial for priming differentiation of embryonic stem (ES) cells into cardiomyocytes, indicating that Cripto acts early to determine the cardiac fate. Furthermore, we show that failure to activate Cripto signaling in this early window of time results in a direct conversion of ES cells into a neural fate. Moreover, the induction of Cripto activates the Smad2 pathway, and overexpression of activated forms of type I receptor ActRIB compensates for the lack of Cripto signaling in promoting cardiomyogenesis. Finally, we show that Nodal antagonists inhibit Cripto-regulated cardiomyocyte induction and differentiation in ES cells. All together our findings provide evidence for a novel role of the Nodal/Cripto/Alk4 pathway in this process.

Introduction

Specification of vertebrate cardiac mesoderm is the first developmental step leading to heart formation occurring concurrently with gastrulation (Fishman and Chien, 1997). The formation of a vertebrate heart from an amorphous field of precursor cells takes place through multiple developmental steps, such as determination of the cardiac field in the mesoderm, differentiation of cardiac precursor cells into cardiomyocytes, and heart morphogenesis (Olson and Srivastava, 1996). No other early differentiation event is more vital for survival; it must occur in a short time to provide a working circulation system for the rapidly growing embryo (Rosenthal and Xavier-Neto, 2000). Precursor cells, destined for the heart, originate in the lateral epiblast and migrate through the primitive streak to emerge as cardiogenic mesoderm already specified as distinct cardiac lineages. Bilateral fields of cardiogenic mesoderm continue to migrate rostrally and eventually join at their anterior boundaries to form the cardiac crescent, where they commit to cardiac fate (Rosenthal and Xavier-Neto, 2000). The understanding of early cardiogenesis is of particular interest as cardiomyocyte loss in mammals is largely irreversible and frequently underlies the diminished cardiac function associated with heart diseases (Gepstein, 2002). Recently, some of the secreted factors required for cardiogenesis have been identified (McFadden and Olson, 2002). Members of the bone morphogenetic protein (BMP), Wnt, and EGF-CFC families have been implicated in vertebrate myocardial development. Zebrafish with mutations in the BMP2 homologue gene *swirl* and one-eyed pinhead (the zebrafish member of the vertebrate EGF-CFC family) exhibit severe defects in myocardial differentiation and reduced expression of two early markers of the myocardial precursors Nkx2.5 and GATA5 (Reiter et al., 2001). Results obtained in *Xenopus* and chick indicate that BMP signals from the endoderm induce cardiomyocyte fate, whereas Wnt-mediated signals from the underlying neural tube and notochord suppress cardiomyocyte specification (Schultheiss et al., 1997; Marvin et al., 2001; Tzahor and Lassar, 2001). It has been hypothesized that cardiac muscle cell specification is likely to depend on the location and

Address correspondence to Gabriella Minchiotti, Institute of Genetics and Biophysics, "A. Buzzati-Traverso," CNR Via Pietro Castellino 111, 80131 Naples, Italy. Tel.: 39-081-6132354. Fax: 39-081-6132595. email: minchiot@iigb.na.cnr.it

Key words: Cripto; cardiomyocytes; neurons; differentiation; Nodal signaling

Abbreviations used in this paper: BMP, bone morphogenetic protein; ca, constitutively activated; Cerberus-S, Cerberus-Short; EB, embryoid body; ES, embryonic stem; HPRT, hypoxanthine phosphoribosyltransferase; MHC, myosin heavy chain; MLC, myosin light chain; wt, wild type.

The Journal of Cell Biology, Volume 163, Number 2, October 27, 2003 303–314
http://www.jcb.org/cgi/doi/10.1083/jcb.200303010

duration of signals governing more general developmental decisions in the early embryo (Rosenthal and Xavier-Neto, 2000). In this scenario, the mouse *cripto* gene, the founding member of the EGF-CFC family, appeared to have a crucial role. In mouse embryos, the *cripto* expression profile is associated with the developing heart structures and is detected first in the precardiac mesoderm (Dono et al., 1993). Later on, at 8.5 dpc, *cripto* expression is found in the ventriculus, before being specifically restricted, at 9.5 dpc, to the truncus arteriosus of the developing heart (Dono et al., 1993). Notably, mouse *cripto* mutants exhibit defects in myocardial development, as evidenced by the absence of expression of terminal myocardial differentiation genes such as α-myosin heavy chain (αMHC) and myosin light chain 2v (MLC2v) (Ding et al., 1998; Xu et al., 1999). Accordingly, by using embryoid bodies (EBs) derived from Cripto$^{-/-}$ ES cells, it has been shown that *cripto* is essential for cardiomyocyte induction and differentiation (Xu et al., 1998). However, how *cripto* functions to regulate cardiogenesis is still unknown. To study this process, we took advantage of embryonic stem (ES) cells, which have been widely used as a model system of cardiogenesis, proven to be a powerful tool to study early events of cardiac induction (Doetschman et al., 1993; Monzen et al., 2001, 2002; Boheler et al., 2002). To create a system in which we could manipulate Cripto activity, we developed an assay in which recombinant Cripto protein restored cardiomyocyte differentiation in Cripto$^{-/-}$ ES cells. This approach allowed us to define the dynamics of Cripto signaling required for differentiation of cardiac precursor cells. We showed that Cripto is required in a precise moment during differentiation, after which it fails to specify the cardiac lineage. Moreover, we found that the absence of Cripto signaling in this early acting window of time resulted in a direct conversion of Cripto$^{-/-}$ EB–derived cells into a neural fate. This observation suggests that Cripto inhibits mammalian neuralization and supports the hypothesis that a default model for neural specification is operating in ES cells. Furthermore, we show that Cripto protein activates the Smad2 pathway during cardiomyocyte induction and, moreover, that overexpression of an activated form of type I receptor ActRIB restored the ability of Cripto$^{-/-}$ ES cells to differentiate into cardiomyocytes. Taken together, our results indicate that Cripto participates in heart development, regulating early events that lead to cardiac specification, and highlight a novel role for the Nodal/Cripto/Alk4 pathway in cardiomyogenesis.

Results

Secreted Cripto retains its ability to rescue cardiomyocyte differentiation

Previous data on cultured ES cells lacking *cripto* have revealed an essential role of *cripto* for contractile cardiomyocyte formation. Cripto$^{-/-}$ ES cells selectively lose the ability to form beating cardiomyocytes, a process that can be rescued by expression of Cripto (Xu et al., 1998). As Cripto is a GPI-anchored membrane protein, we first determined if a secreted form of Cripto could restore cardiomyocyte differentiation in Cripto$^{-/-}$ ES cells (Fig. 1). To this end, we overexpressed a secreted derivative of Cripto, which lacks the hydrophobic COOH terminus region required for membrane anchorage (Minchiotti et al., 2000), in Cripto$^{-/-}$ ES cells and compared its activity to that of wild-type (wt) Cripto (Fig. 2 A). A pooled population of cells selected for resistance to puromycin were examined for the number of EBs containing beating areas, from day 8 to 12 of the in vitro differentiation assay. Spontaneous rhythmic contractile myocytes were observed in Cripto$^{-/-}$ ES cells expressing either the membrane-anchored or the secreted Cripto protein (Fig. 2 B). Moreover, similar results were obtained by expressing a secreted Cripto protein that lacks the NH_2 terminus region (EGF-CFC; Fig. 2, A and B), thus indicating that not only membrane anchorage is dispensable for activity, but that the EGF-CFC domain alone is sufficient for Cripto activity in the cardiogenic induction. Previous data have shown that a refolded synthetic Cripto peptide containing the EGF-like domain had mitogenic and branching activity for mammary cell lines (Salomon et al., 1999). We thus went on to define whether the Cripto EGF-like domain alone was able to induce cardiogenesis similar to the EGF-CFC peptide. Two *cripto* cDNA deletion derivatives encoding either the EGF-like domain retaining the NH_2 terminus region (EGF long) or just the EGF domain (EGF short; Fig. 2 A) were generated. No beating areas were observed in EBs derived from Cripto$^{-/-}$ ES cells expressing either EGF long or EGF short peptide (Fig. 2 B), thus indicating that both EGF and CFC domains of Cripto are essential for cardiogenic induction. Western blot analysis showed that the EGF long and EGF short peptides were produced and secreted as efficiently as EGF-CFC (Fig. 2 C and not depicted), thus demonstrating that their inability to rescue the mutant phe-

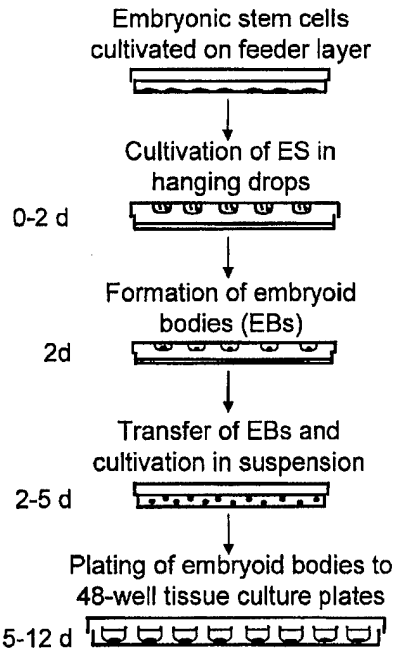

Figure 1. **Schematic representation of the experimental protocol used for ES cell differentiation into cardiomyocytes (adapted from Maltsev et al., 1993).**

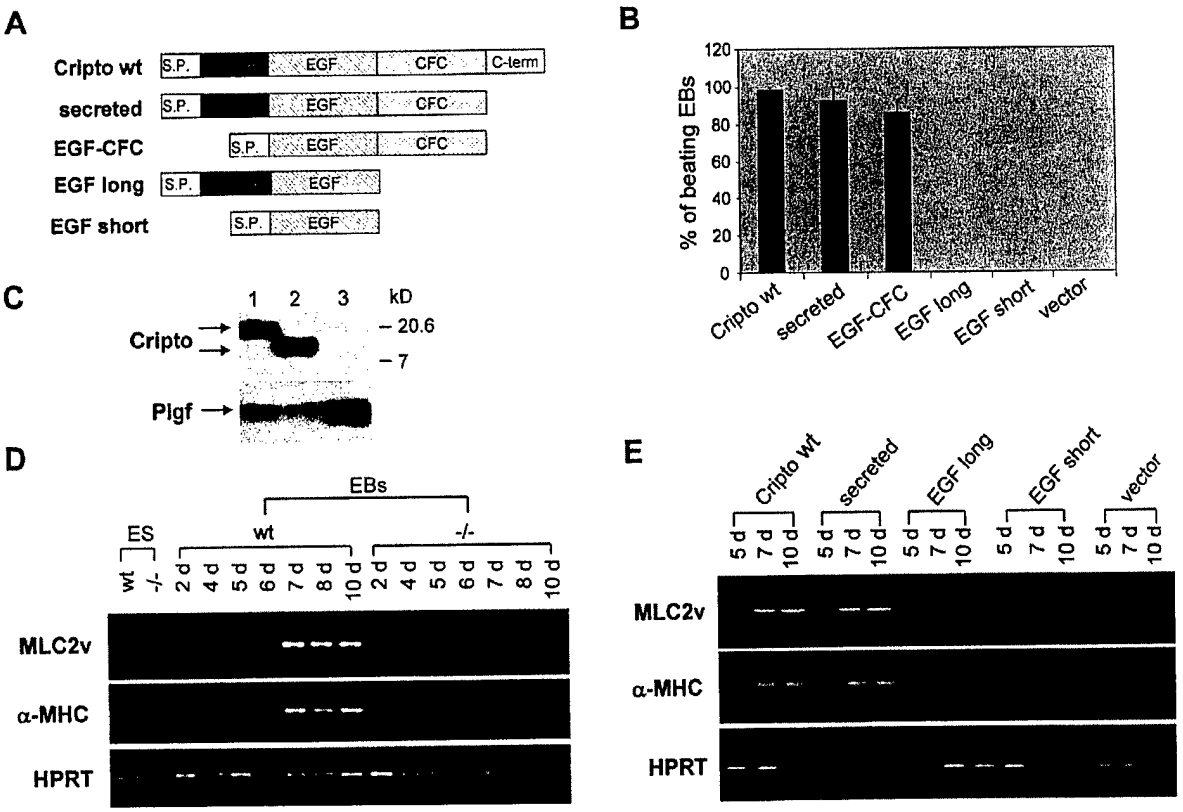

Figure 2. **Functional dissection of Cripto.** (A) Schematic representation of *cripto* cDNA derivatives. S.P., signal peptide. (B) Determination of minimal domains required for Cripto activity in cardiomyocyte differentiation. Either wt or deleted *cripto* mutant derivatives were transfected into Cripto$^{-/-}$ ES cells; empty vector was used as control. The percentage of EBs with rhythmically contracting areas detectable by light microscopy was scored on day 8 to 12. Data are representative of at least two independent experiments. (C) Western blot analysis of conditioned media from 293EBNA cells transfected with *cripto* cDNA deletion derivatives. Cells were cotransfected with *Plgf* expression vector as an internal control (see Materials and methods). Lane 1, EGF-CFC; lane 2, EGF long; lane 3, vector. The molecular mass of protein standards is indicated (kD). (D) Expression of cardiac-specific genes MLC2v and αMHC during in vitro differentiation of either wt or Cripto$^{-/-}$ ES cells. RT-PCR was performed on RNA extracted from either undifferentiated ES cells or EBs throughout a differentiation period of 10 d (days 2–10). HPRT gene expression was analyzed as an internal control. (E) RNA expression levels of MLC2v and cardiac αMHC genes during in vitro differentiation of Cripto$^{-/-}$ ES cells overexpressing either wt or *cripto* deletion mutants. RNA was harvested at days 5, 7, and 10 of the differentiation protocol and subjected to RT-PCR. Empty vector was used as a negative control. HPRT gene expression was analyzed as an internal control. The results are representative of two independent differentiation programs.

notype was not due to a difference in protein expression level. To support the morphological data observed, we examined the expression levels of the cardiac-specific αMHC and MLC2v, two major contractile proteins of cardiomyocytes. As expected, expression of both the αMHC and MLC2v genes was induced in wt ES cells but not in Cripto$^{-/-}$ cells from day 7 of in vitro differentiation (Fig. 2 D). Importantly, the expression pattern of αMHC and MLC2v genes in wt ES cells was reproduced in Cripto$^{-/-}$ cells expressing either wt Cripto or the secreted derivative, but not in cells expressing either EGF long or EGF short peptides (Fig. 2 E).

Timing and duration of Cripto activity in cardiomyocyte differentiation

To gain further insight into the functional role of Cripto in cardiogenic induction and differentiation, we first examined the timing of Cripto expression during ES cell differentiation. Western blot analysis performed with anti-Cripto antibodies on lysates from both wt and Cripto$^{-/-}$ ES cells revealed that Cripto was detectable as early as day 0 and peaked in expression by day 4 in wt EBs (Fig. 3). Importantly, the transient nature of Cripto accumulation suggested that its activity might be required at a defined step in cardiomyocyte differentiation. The time window of Cripto action could not be adequately investigated by means of transfection assays. Therefore, to directly address this issue, a recombinant soluble Cripto protein was used in which the hydrophobic COOH terminus was replaced by a 6xHis epitope (Cripto-His; Minchiotti et al., 2001). Based on our observation that secreted Cripto protein is able to promote cardiogenesis when expressed in the Cripto$^{-/-}$ ES cells (Fig. 2 B), experiments were performed where Cripto signaling was reconstituted by addition of recombinant secreted Cripto protein directly to the cells (Fig. 4). Addition of Cripto during the 0–2-d interval effectively restored the dif-

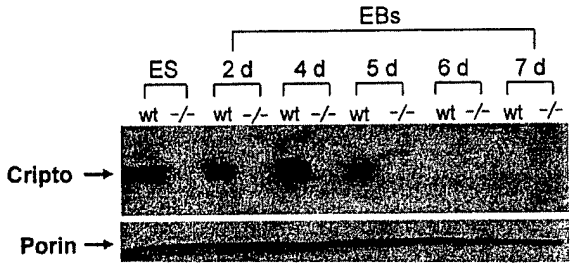

Figure 3. **Cripto expression profile during the in vitro differentiation of ES cells.** Total lysates of either undifferentiated ES cells or EBs at different days of differentiation (2–7 d), derived from either RI (wt) or DE7 (Cripto$^{-/-}$) ES cells, were collected in lysis buffer and analyzed by Western blot using a polyclonal anti-Cripto antiserum (Minchiotti et al., 2000). Data were normalized to the expression level of Porin.

ferentiation ability of Cripto$^{-/-}$ ES cells. Addition at later time points resulted in dramatically reduced cardiomyocyte differentiation (Fig. 4 A). Comparable results were obtained with two independent Cripto$^{-/-}$ ES clones (DE7 and DE14; Xu et al., 1998), thus excluding any phenotype difference due to clonal variation (Fig. 4 A). All together, these data indicated that stimulation in trans with soluble Cripto protein was fully efficient in promoting cardiomyocyte induction and differentiation and, more interestingly, defined exactly when Cripto activity was required to promote specification of the cardiac lineage. Furthermore, to define the optimal concentration of Cripto required to promote cardiogenesis, increasing amounts of purified recombinant Cripto protein were added directly to the culture medium of 2-d-old Cripto$^{-/-}$ EBs from either DE7 or DE14 cell lines for 24 h (Fig. 4 B). Increasing amounts of recombinant Cripto resulted in enhanced differentiation efficiency (Fig. 4 B), thus indicating that Cripto-mediated cardiogenic induction was dose dependent.

Having shown that the timing and dose of Cripto signaling activation were crucial to promote cardiomyocyte induction and differentiation, we thus went on to define whether the duration of Cripto signaling was crucial for its biological response. 2-d-old EBs from DE7 or DE14 Cripto$^{-/-}$ ES cells were treated with 10 μg/ml of recombinant Cripto for various lengths of time, washed to remove unbound Cripto, and then cultured for the remaining days. An effective Cripto response required a minimum induction of 24 h, while shorter inductions showed markedly reduced activity (Fig. 4 C). Taken together, our data demonstrated that the amount, timing, and duration of Cripto signaling were all crucial factors to achieve cardiogenic induction and differentiation.

Direct conversion of Cripto$^{-/-}$ EB–derived cells into a neural fate

Our observation that initiation of Cripto signaling in an early acting window of time is crucial for priming differentiation of ES cells to cardiac fate prompted us to gain further insight into the functional role of Cripto at an early phase of ES cell differentiation. Interestingly, when Cripto$^{-/-}$ EBs were plated onto an adhesive substrate, a population of cells with a neuron-like morphology was observed that produced a network surrounding the aggregates. This characteristic morphology was never observed either in wt EBs or in Cripto$^{-/-}$ EBs treated with effective doses of Cripto protein. To confirm that those cells were indeed neurons, immunofluorescence analysis was performed on both wt and Cripto$^{-/-}$ EBs, by using antibodies that recognize the neuron-specific form of class βIII tubu-

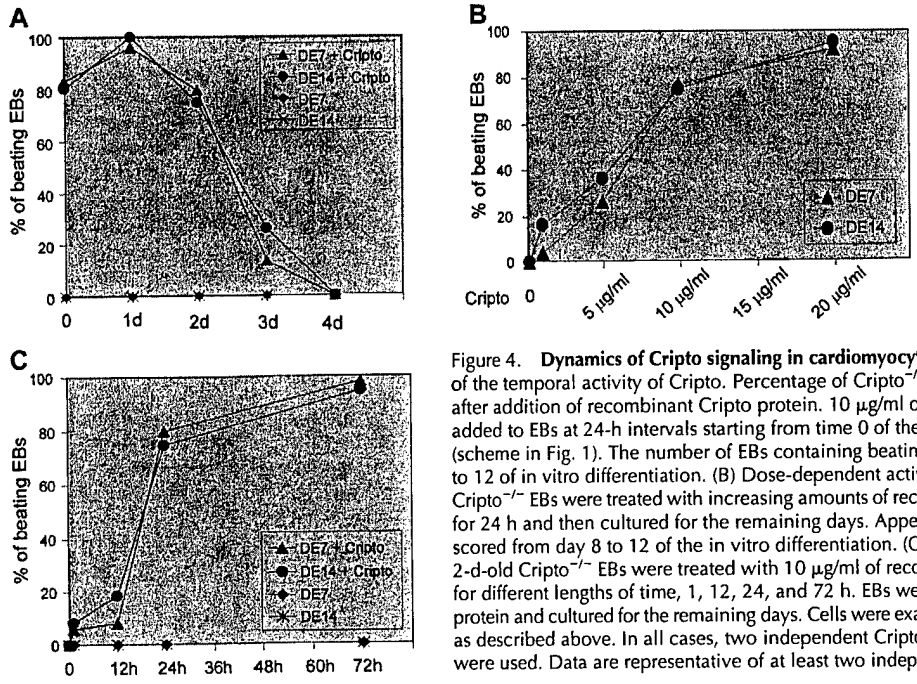

Figure 4. **Dynamics of Cripto signaling in cardiomyocyte differentiation.** (A) Definition of the temporal activity of Cripto. Percentage of Cripto$^{-/-}$ EBs containing beating areas after addition of recombinant Cripto protein. 10 μg/ml of soluble Cripto protein was added to EBs at 24-h intervals starting from time 0 of the in vitro differentiation assay (scheme in Fig. 1). The number of EBs containing beating areas was scored from day 8 to 12 of in vitro differentiation. (B) Dose-dependent activity of Cripto protein. 2-d-old Cripto$^{-/-}$ EBs were treated with increasing amounts of recombinant soluble Cripto protein for 24 h and then cultured for the remaining days. Appearance of beating areas was scored from day 8 to 12 of the in vitro differentiation. (C) Duration of Cripto signaling. 2-d-old Cripto$^{-/-}$ EBs were treated with 10 μg/ml of recombinant soluble Cripto protein for different lengths of time, 1, 12, 24, and 72 h. EBs were then washed to remove the protein and cultured for the remaining days. Cells were examined for cardiac differentiation as described above. In all cases, two independent Cripto$^{-/-}$ ES clones (DE7 and DE14) were used. Data are representative of at least two independent experiments.

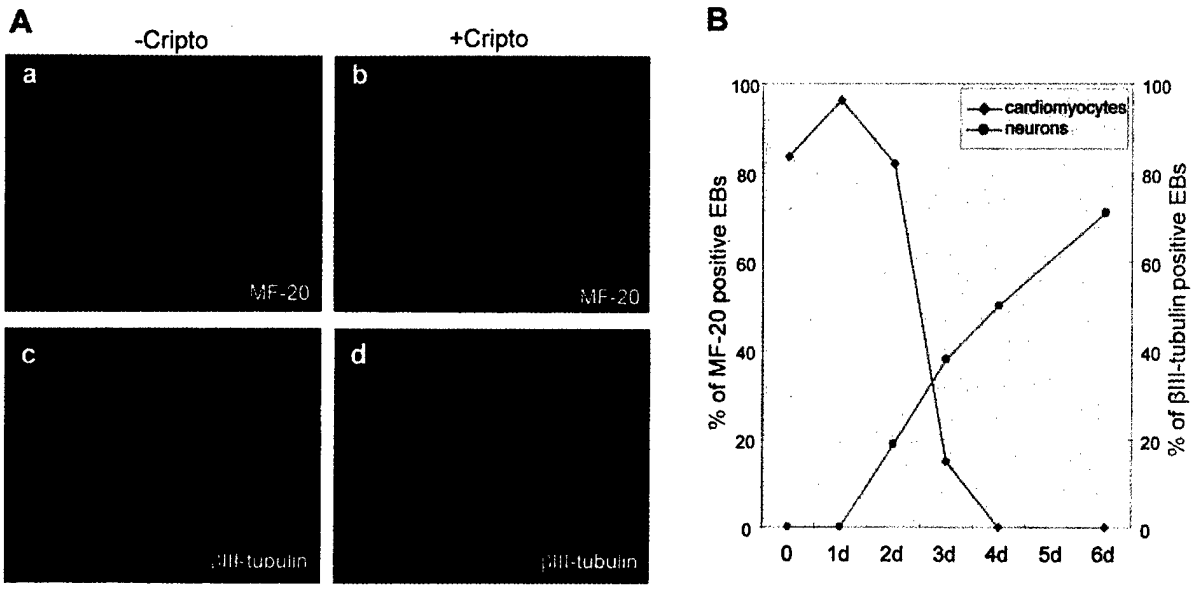

Figure 5. **Cripto promotes cardiomyocyte differentiation and inhibits neural differentiation of ES cells according to the timing of exposure.** (A) Cardiomyocyte versus neuronal differentiation of Cripto$^{-/-}$ EBs as revealed by indirect immunofluorescence. 2-d-old Cripto$^{-/-}$ EBs, derived from DE7 cell line, were either left untreated (a and c) or treated for 24 h with 10 μg/ml of recombinant Cripto protein (b and d). On day 12 of in vitro differentiation, expression of either sarcomeric myosin or βIII-tubulin was revealed by immunofluorescence using anti–MF-20 (red, a and b) or βIII-tubulin (green, c and d) antibodies, respectively. Data are representative of at least two independent experiments. Comparable results were obtained with Cripto$^{-/-}$ DE14 ES cell line. (B) Cardiomyocyte versus neuronal differentiation of Cripto$^{-/-}$ EB–derived cells depends on the timing of exposure to Cripto. Percentage of Cripto$^{-/-}$ EBs stained for βIII-tubulin (red plot) or MF-20 (blue plot) after addition of recombinant Cripto protein at different time points. 10 μg/ml of recombinant Cripto protein was added to EBs at 24-h intervals starting from time 0 of the in vitro differentiation assay. On day 12 of in vitro differentiation, EBs were stained for either βIII-tubulin or MF-20 antibodies. Data are representative of two independent experiments.

lin. These antibodies stained clusters of cells in Cripto$^{-/-}$ EBs, revealing the presence of a dense network of neurons (Fig. 5 A). Neurons were detected in 71% of Cripto$^{-/-}$ EBs, whereas βIII-tubulin–positive cells were never detected in both wt EBs and rescued Cripto$^{-/-}$ EBs that, on the contrary, showed extensive areas of MF-20–positive cardiomyocytes (Fig. 5 A). To gain insight into this issue, we used our controlled differentiation assay to modulate Cripto signaling and to eventually score EB-derived cells for either cardiomyocyte or neuron differentiation, by using morphological criteria as well as immunofluorescence analysis. Addition of Cripto protein during the 0–2-d interval rescued, as expected, the cardiac phenotype of Cripto$^{-/-}$ ES cells (Fig. 5 B), but also resulted in a dramatic inhibition of neural differentiation (Fig. 5 B). Conversely, addition of recombinant Cripto at later time points (i.e., 3–6-d interval) resulted in progressive impairment of cardiac differentiation (see previous paragraph and Fig. 5 B) and, at the same time, increased competence of the EB-derived cells to acquire a neural phenotype, resulting in close to 70% of Cripto$^{-/-}$ EBs that show extensive areas of βIII-tubulin–positive cells. All together our results support the hypothesis that Cripto signaling represses neural differentiation in ES cells and, moreover, show that the restricted time window of Cripto signaling required to achieve proper terminal cardiac differentiation of Cripto$^{-/-}$ ES cells correlates with the competence window for those cells to become committed to a neuronal phenotype.

Cripto activates a Smad2 pathway associated with cardiomyocyte differentiation

Findings in mice, *Xenopus*, and zebrafish point to a strong functional link between the EGF-CFC proteins and TGFβ ligand Nodal (Shen and Schier, 2000; Adamson et al., 2002). Accordingly, recent studies have shown that Cripto can associate with type I receptor ActRIB (Alk4) and can form a complex together with Nodal and type II receptor ActRIIB (Reissmann et al., 2001; Yeo and Whitman, 2001; Bianco et al., 2002; Yan et al., 2002). Activation of Smad proteins by phosphorylation is a universal signal transduction event following activation of Alk receptors. To ask whether Cripto activates the Smad2 pathway during cardiomyocyte induction and differentiation, 2-d-old Cripto$^{-/-}$ EBs were starved in low serum for 3 h and then stimulated with recombinant soluble Cripto protein for 30, 60, or 120 min. Western blot analysis revealed that phosphorylation of Smad2 significantly increased after treatment with recombinant Cripto (Fig. 6). Smad2 phosphorylation was detectable already after 30-min treatment, persisting at comparable levels even after prolonged exposure to Cripto protein. An anti-Smad2/3 antibody applied to the same blot was used to normalize for total amount of protein (Fig. 6). In vitro studies on mammary cell lines have suggested that Cripto is involved in the Ras/Raf/MEK/MAPK pathway (Salomon et al., 1999). When we looked for activation of the MAP kinase ERK by using an anti–phospho-ERK antibody, recombinant Cripto was unable to activate MAP kinase (unpub-

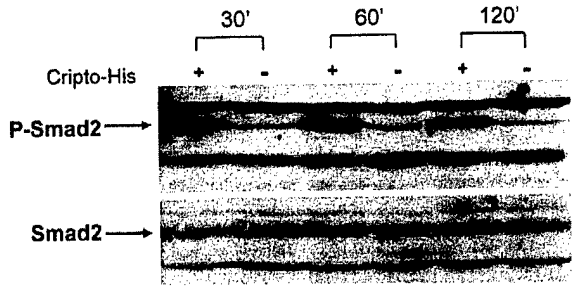

Figure 6. **Activation of Smad2 in Cripto$^{-/-}$ cell aggregates treated with recombinant Cripto protein.** 2-d-old Cripto$^{-/-}$ EBs were serum starved for 3 h and then treated with 10 μg/ml of recombinant Cripto protein for 30', 60', or 120' or left untreated, as indicated. Smad2 activation was detected by Western blot analysis using anti–phospho-Smad2 antibody. Levels of total Smad2 were also compared.

lished data); thus indicating that the Smad2 pathway was selectively activated during cardiomyocyte induction and differentiation induced by Cripto.

To our knowledge, no data are available on the expression profile of all components of the Alk4/ActRIIB/Nodal complex during the differentiation of ES cells; thus, we first measured by RT-PCR the expression of Nodal, Alk4, and ActRIIB in EBs derived from both wt and Cripto$^{-/-}$ ES cells. Nodal, Alk4, and ActRIIB were expressed in all analyzed stages (Fig. 7 A). If Cripto signaling in cardiomyocyte differentiation acts via the Alk4 receptor, overexpression of a constitutively active type I receptor would be expected to compensate for the lack of Cripto signaling in promoting cardiomyocyte differentiation. We overexpressed in Cripto$^{-/-}$ ES cells the wt or constitutively activated form (ca) of either human HA-tagged Alk4 or its zebrafish counterpart Taram-A (Renucci et al., 1996). Type I receptor serine/threonine kinases can be activated in a ligand- and type II receptor–independent manner by replacing an acidic residue for a specific threonine within the juxtamembrane region of the intracellular domain, a segment known to be involved in kinase regulation (Wieser et al., 1995). Overexpression of either Alk4 ca or

Table I. **Percentage of beating EBs from Cripto$^{-/-}$ ES cells transfected with either wt or ca form of human Alk4 or zebrafish Taram-A receptors**

Cells	Construct	EBs scored	% of beating EBs
DE7	None	70	0
DE7	Cripto wt	50	96.6
DE7	Alk4 wt	76	0
DE7	Alk4 ca	50	16.0
DE7	Taram-A wt	55	0
DE7	Taram-A ca	64	45.0
DE7	Empty vector	56	0
DE14	None	80	0
DE14	Cripto wt	54	94.4
DE14	Taram-A wt	50	1.9
DE14	Taram-A ca	51	62.2
DE14	Empty vector	60	0

Data are representative of at least two independent experiments. DE7 and DE14 are two independent Cripto$^{-/-}$ clones.

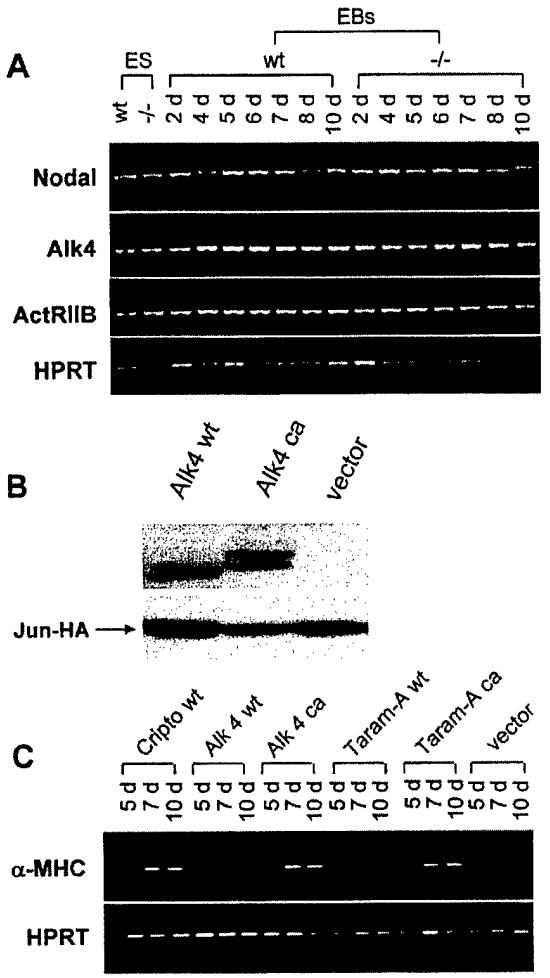

Figure 7. **Expression profile of Nodal, Alk4, and ActRIIB during cardiomyocyte differentiation and their effects on cardiac induction.** (A) RNA expression levels of Nodal, Alk4, and ActRIIB genes during in vitro differentiation of ES cells. RT-PCR analysis was performed on RNA extracted from either undifferentiated ES or EBs (either wt or Cripto$^{-/-}$) throughout a differentiation period of 10 d (days 2–10). HPRT gene was used as an internal control. (B) Western blot analysis of total lysates from 293EBNA cells transfected with either wt or ca form of HA-tagged human Alk4. Cells were cotransfected with Jun-HA expression vector as an internal control. A monoclonal anti-HA antibody was used to detect protein levels. (C) RNA expression profile of the αMHC gene during differentiation of Cripto$^{-/-}$ ES cells (days 5, 7, and 10) overexpressing wt and activated forms of either Alk4 or Taram-A. HPRT gene was used as an internal control.

Taram-A ca partially restored the ability of Cripto$^{-/-}$ ES cells to differentiate into cardiomyocytes (Table I). On the contrary, overexpression of the wt receptors, either Taram-A or Alk4, had no significant activity despite their similar expression levels (Fig. 7 B). Furthermore, addition of recombinant Cripto to Alk4 ca–expressing cells restores cardiomyocyte differentiation close to controls (Table II). In accordance with the morphological data, expression of the αMHC gene was only detected in Cripto$^{-/-}$ ES cells expressing the activated form of the receptors (Fig. 7 C). Altogether, our results pro-

Table II. **Percentage of beating EBs from transfected Cripto$^{-/-}$ ES cells**

Construct	Protein	EBs scored	% of beating EBs
Alk4 ca	None	50	16.0
Alk4 ca	Cripto[a]	87	87.3
Empty vector	None	49	0
Empty vector	Cripto[a]	60	96.6

[a]2-d-old EBs were treated with 10 μg/ml of recombinant Cripto for 3 d.

vide an intriguing link between Alk4/Smad pathway activation by Cripto and cardiomyocyte development.

Analysis of Cripto mutants identifies key residues both in the EGF and in the CFC domain

We showed above that the EGF-CFC domain is sufficient to promote cardiogenic induction when overexpressed in Cripto$^{-/-}$ ES cells, whereas the EGF domain alone is unable to rescue the biological activity. To determine the contribution of the EGF and CFC domains, single amino acid substitutions were introduced into the *cripto* cDNA (Fig. 8 A), and the activity of the corresponding mutant proteins was compared with the wt in the cardiomyocyte assay. Although each mutant was expressed at levels comparable to wt Cripto (Fig. 8 B), three of them were completely inactive or showed a strongly reduced activity in our assay (Table III). Similar results were obtained with two independent Cripto$^{-/-}$ ES clones (Table III). To support the observed morphological data, the expression of the αMHC and the MLC2v genes was examined by RT-PCR on total RNA prepared from EBs derived from Cripto$^{-/-}$ ES cells overexpressing Cripto mutant derivatives (Fig. 8 C). Expression of αMHC and MLC2v genes was either absent or reduced in cells overexpressing G71N, F78A, or W107G *cripto* mutants, whereas it was restored in Cripto$^{-/-}$ cells transfected with wt *cripto*. Together these data show that critical amino acid residues are located in both EGF and CFC domains, thus indicating the requirement of both domains for Cripto activity in cardiogenic induction.

Table III. **Percentage of beating EBs from Cripto$^{-/-}$ ES cells transfected with either wt or Cripto mutant derivatives**

Cells	Construct	EBs scored	% of beating EBs
DE7	None	97	0
DE7	Cripto wt	56	98.2
DE7	N63I	54	91.5
DE7	G71N	54	0
DE7	T72A	62	90.3
DE7	S77A	60	95.0
DE7	F78A	47	42.5
DE7	F78W	60	95.0
DE7	H104A	56	89.3
DE7	W107G	57	7.6
DE7	R116G	49	80.0
DE7	L122N	103	92.0
DE7	Empty vector	65	0
DE14	None	85	0
DE14	Cripto wt	54	94.4
DE14	G71N	49	0
DE14	F78A	45	66.0
DE14	W107G	57	30.5
DE14	Empty vector	71	0

Data are representative of at least two independent experiments. DE7 and DE14 are two independent Cripto$^{-/-}$ clones.

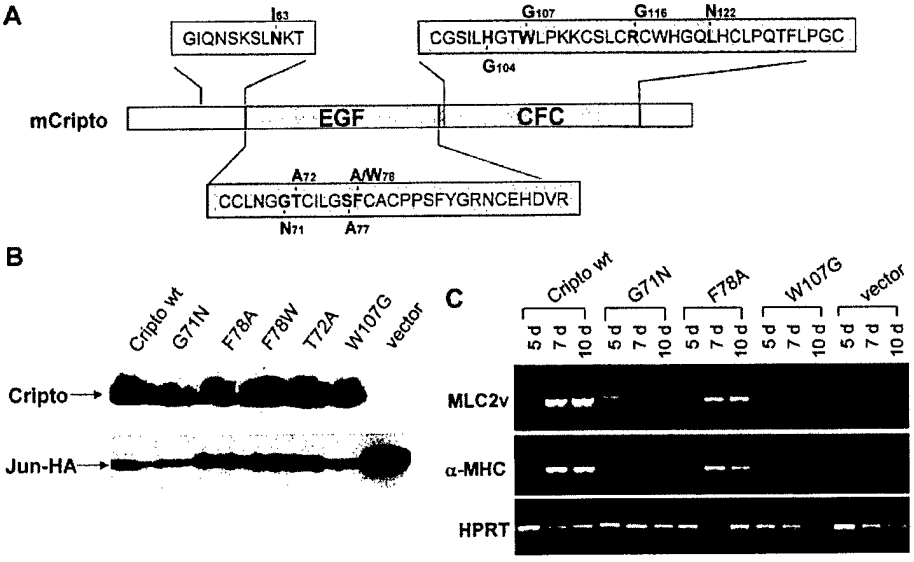

Figure 8. **Identification of Cripto key residues required for cardiac induction and differentiation.** (A) Schematic representation of wt and mutant Cripto derivatives. (B) Western blot analysis of total lysates from 293EBNA cells transfected with either wt or mutant *cripto* derivatives. Jun-HA expression vector was cotransfected as an internal control. Either polyclonal anti-Cripto or monoclonal anti-HA antibodies were used to detect protein levels. (C) RNA expression levels of the cardiac αMHC and MLC2v genes during in vitro differentiation of Cripto$^{-/-}$ ES cells (days 5, 7, and 10) overexpressing either wt or mutant *cripto* derivatives. Expression level of HPRT gene was analyzed as an internal control.

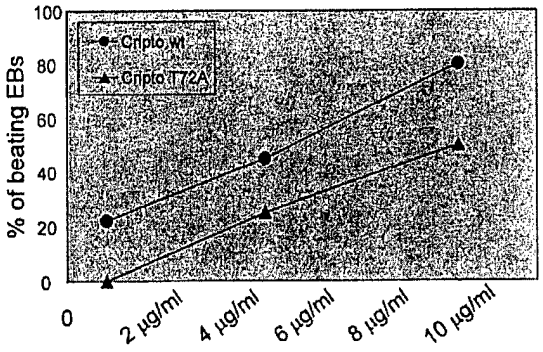

Figure 9. **Modulation of Cripto activity by O-fucosylation.** Dose-dependent activity of T72A mutant Cripto compared with wt Cripto as assayed in cardiomyocyte differentiation assay. 2-d-old Cripto$^{-/-}$ EBs were treated with increasing amounts of either recombinant soluble T72A mutant or wt Cripto protein for 24 h and then cultured for the remaining days. Appearance of beating areas was scored from day 8 to 12 of the in vitro differentiation. Data are representative of two independent experiments.

Recent reports have shown that Cripto is modified by the addition of sugar residues. N-linked glycosylation was shown to affect Cripto biological activity in the zebrafish assay (Minchiotti et al., 2001). More recently, an O-linked fucosylation of Cripto has been reported to be required for Cripto signaling activity in cotransfection assay in mammalian cells (Schiffer et al., 2001; Yan et al., 2002). To assess if posttranslational modifications were required for Cripto activity in cardiogenic induction, two alanine substitutions were generated, corresponding to either the N-glycosylation site (N63I) or the O-linked fucosylation site (T72A). The activities of the corresponding mutant proteins were tested in the differentiation assay and compared with wt Cripto. Based on the percentage of EBs containing beating areas, both mutant proteins had comparable ability in promoting cardiomyocyte differentiation, compared with wt Cripto (Table III), thus suggesting that addition of sugar residues was not strictly required for Cripto activity in ES cells.

However, a role of these modifications in the modulation of Cripto signaling might be masked in our assay due to overexpression of the proteins. To overcome this limitation, we purified a recombinant Cripto T72A mutant protein from conditioned medium of transfected 293 cells, and its activity was compared with the wt Cripto. When used in the cardiomyocyte differentiation assay, the Cripto T72A mutant protein resulted in close to a 30% reduction in the numbers of Cripto$^{-/-}$ EBs displaying beating cardiomyocytes, compared with the wt Cripto (Fig. 9). A similar reduction was observed when using Cripto T72A in the Smad2 phosphorylation assay, indicating that doses higher than those used for wt Cripto were required to achieve equivalent induction (unpublished data).

Nodal antagonists inhibit Cripto activity in cardiomyogenesis

To gain direct evidence that Nodal signaling is indeed required to support Cripto-regulated cardiac induction and differentiation in ES cells, we sought to determine whether

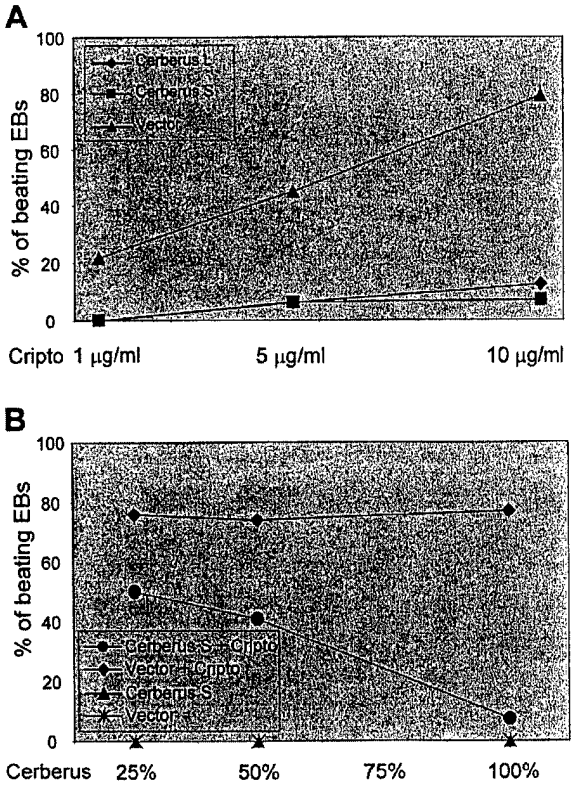

Figure 10. **Exposure to Cerberus inhibits Cripto activity in cardiomyocyte differentiation assay.** (A) Cerberus inhibits Cripto-dependent cardiomyocyte differentiation of Cripto$^{-/-}$ EBs. 2-d-old Cripto$^{-/-}$ EBs were cultured for 24 h in the presence of 100% (vol/vol) of media supernatant from 293T cells transiently expressing either Cerberus, Cerberus-S, or empty vector as control, in the presence of increasing amounts of recombinant Cripto protein. The number of Cripto$^{-/-}$ EBs containing beating areas was scored from day 8 to 12 of in vitro differentiation. Data are representative of two independent experiments. (B) Inhibition of Cripto by Cerberus-S is dose dependent. 2-d-old Cripto$^{-/-}$ EBs were cultured for 24 h with 10 μg/ml of soluble Cripto protein in the presence of increasing amounts (vol/vol) of media from 293T cells transiently expressing Cerberus-S. Cells were examined for cardiac differentiation as described above. Data are representative of two independent experiments.

inhibition of Nodal signaling might interfere with Cripto ability to promote cardiomyogenesis. To directly address this point, 2-d-old Cripto$^{-/-}$ EBs were treated with increasing amounts of recombinant Cripto (1–10 μg/ml) in a media containing the supernatant collected from a transiently transfected 293T cell line producing Cerberus protein. This multifunctional antagonist inhibits Nodal as well as BMP and Wnt signaling. However, a truncated form of Cerberus, named Cerberus-Short (Cerberus-S), is a specific Nodal antagonist (Piccolo et al., 1999). The presence of either Cerberus or Cerberus-S supernatant resulted in a significant inhibition of Cripto ability to prime cardiomyocyte differentiation compared with control supernatant (Fig. 10 A). Furthermore, we treated Cripto$^{-/-}$ EBs with 10 μg/ml of recombinant Cripto in the presence of increasing amounts of Cerberus-S–containing medium,

Table IV. **Percentage of beating EBs from Cripto$^{-/-}$ ES cells transfected with Nodal antagonists**

Construct	Protein	EBs scored	% of beating EBs
Empty vector	None	40	0
Empty vector	Cripto[a]	58	85
Cerberus	None	34	0
Cerberus	Cripto[a]	49	10.3
Cerberus-S	None	36	0
Cerberus-S	Cripto[a]	40	8.3

[a]2-d-old EBs were treated with 10 μg/ml of recombinant Cripto for 3 d.

thus being able to show that inhibition of Cripto activity by Cerberus-S was indeed dose dependent (Fig. 10 B). Finally, as an additional control, we used Cripto$^{-/-}$ ES cells transfected with either Cerberus or Cerberus-S expression vectors, before treatment of the derived EBs with recombinant Cripto. In accord with the results obtained with conditioned media, expression of either Cerberus or Cerberus-S resulted in a significant inhibition of Cripto activity (Table IV). Together, these results show that Cerberus and Cerberus-S can act as effective antagonists of Cripto signaling in ES cell differentiation and provide evidence for a functional role of the Nodal pathway in Cripto-mediated specification of the cardiac lineage.

Discussion

Role of secreted Cripto as a priming factor for cardiomyogenesis

Cripto is a GPI-anchored protein; however, recent data in zebrafish have shown that Cripto protein could be provided in a soluble form to enable proper Nodal signal propagation (Minchiotti et al., 2001). Moreover, previous data on chimeric mouse embryos established from a combination of wt and Cripto$^{-/-}$ ES cells suggested that Cripto acts nonautonomously during development (Xu et al., 1998). Due to the absence of analysis of cellular genetic markers, and because only late-stage chimeric embryos were analyzed, the cell autonomous or nonautonomous activity of Cripto is an issue that still remains unsolved (Rosa, 2002). Expression of different deletion mutant derivatives of *cripto* cDNAs in Cripto$^{-/-}$ ES cells led us to demonstrate that secreted Cripto could efficiently induce cardiogenesis and, moreover, that expression of the EGF-CFC domain was sufficient to restore the ability of Cripto$^{-/-}$ ES cells to differentiate into cardiomyocytes. Furthermore, we showed that the Cripto EGF domain is required, but not sufficient, for cardiomyogenesis. In contrast, it was previously demonstrated that a refolded synthetic human Cripto peptide comprising only the EGF-like domain displayed high affinity binding and mitogenic activity on mammary cell lines (Salomon et al., 1999). Considering the high percentage of amino acid identity in the EGF domain between human and mouse Cripto (Dono et al., 1993), this observation strengthened the hypothesis that there may be divergent Cripto signaling pathways, depending both on different Cripto domains and on specific cell types, that remain to be explored in the future.

Dose and temporal regulation of Cripto signaling in the commitment of ES cells to cardiac fate

EB differentiation is currently considered a powerful model system, reproducing many aspects of in vivo tissue formation during the crucial, but less accessible, stages of mammalian embryogenesis, thus providing access to early cell populations that develop in a normal fashion (Keller, 1995). The timing of initiation of Cripto signaling and the strength and duration of the signal are interdependent variables that have not yet been resolved experimentally, mainly due to the complexity of in vivo analysis. Western blot analysis performed on total lysates, prepared at different times of ES cell in vitro differentiation, showed a regulated accumulation of Cripto protein whose expression was restricted to the very beginning of the differentiation program.

We then used soluble Cripto protein on Cripto$^{-/-}$ ES cells to modulate Cripto signaling and measured its effect on cardiomyocyte differentiation. Kinetic experiments performed by adding recombinant Cripto protein directly to the culture medium of Cripto$^{-/-}$ ES cells demonstrated that stimulation in trans with a soluble Cripto peptide was capable of promoting cardiac induction and, strikingly, revealed an early acting window of time in which the initiation of Cripto signaling is crucial for priming differentiation of ES cells to cardiac fate. Having defined the timing of Cripto signaling, we next examined two more variables, dose and duration of signaling. Either different amounts of Cripto protein for a defined length of time or a high dose of Cripto peptide for various lengths of time was used on Cripto$^{-/-}$ EBs. Both protein dose and signaling duration were crucial parameters. Worth noticing, our results show that transient presence of Cripto is inadequate and that sustained Cripto signaling is strictly required to promote cardiogenesis. We thus propose that Cripto activity at a given time, strength of the signal, and length of the time of exposure are critical parameters for the correct specification and differentiation of the cardiac lineage.

Neural cell fate is established from Cripto$^{-/-}$ EB–derived cells in the absence of retinoic acid

Several studies demonstrated that neural differentiation from ES cells relies upon an aggregation step followed by exposure to specific inducing factors, such as retinoic acid (Bain et al., 1995, 1996; Okabe et al., 1996). Our present findings indicate that in the absence of retinoic acid, Cripto$^{-/-}$ EB–derived cells spontaneously differentiate into neurons. Furthermore, we show that the timing of Cripto signaling required for priming differentiation of cardiac cells resembles the competence window of EB-derived cells to acquire a neural character. All together, our results indicate that Cripto signaling is strictly required in an early acting window to negatively regulate neural differentiation and, at the same time, to permit differentiation of ES cells to cardiac fate.

Recent studies have investigated the mechanisms underlying neural specification in uncommitted ES cells (Tropepe et al., 2001). However, the role of the pathways that have been implicated in neural generation in the context of stem cells is still under investigation (Munoz-Sanjuan and Brivanlou, 2002). Although a better understanding of the molecu-

lar events that mediate the acquisition of neural fates of ES cells in the absence of Cripto signaling is required, our controlled differentiation paradigm could represent an attractive system to further investigate this issue.

Cripto signaling pathway in cardiomyogenesis

Both genetic and biochemical data indicate a role for Cripto and, more generally, for the EGF-CFC factors in Nodal signaling (Gritsman et al., 1999; Reissmann et al., 2001; Schiffer et al., 2001; Yan et al., 2002). More recently, findings in *Xenopus* and zebrafish have also shown that the TGFβ Vg1/GDF1-like signals depend on EGF-CFC proteins (Cheng et al., 2003).

We observed a significant increase in Smad2 phosphorylation consequent to treatment of Cripto$^{-/-}$ ES cells with recombinant Cripto protein for different lengths of time. This suggests that Cripto signaling acts through the Smad2 pathway to promote cardiac induction and reveals a potential role of Nodal signaling in cardiogenesis. Acute stimulation by Cripto, although competent in activating Smad2, is insufficient to achieve proper terminal cardiac differentiation, again highlighting the importance of signal duration for cardiomyogenesis.

Activation of Alk4/Tar-A signaling and cardiac induction

One critical function of Cripto during development is to render Activin type I receptor competent for activation by Nodal and to potentiate Nodal-triggered Alk7 signaling activity (Gritsman et al., 1999; Reissmann et al., 2001; Yeo and Whitman, 2001; Yan et al., 2002). Here we show that activated forms of either Alk4 or zebrafish Taram-A partially compensate for the lack of Cripto in the cardiomyocyte differentiation assay, suggesting that, indeed, this receptor family is involved in Cripto-mediated cardiomyogenesis. The incomplete rescue could be due to different reasons. As overexpression experiments do not allow the modulation of receptor signaling both in terms of timing and signal strength, we measured the effect of constitutive, but not transient (acute), activation of Alk4-mediated signaling. Cripto may also interact either with other Alk or TGFβ receptor family members or still unknown molecules to promote cardiomyocyte induction and differentiation in ES cells.

Mutational dissection of Cripto

The mutational dissection of Cripto enabled us to define that both the EGF and the CFC domains are crucial for Cripto activity in cardiogenesis. Remarkably, the biological activities of the Cripto mutants in cardiogenic induction correlate well with their effects on Alk4/Nodal signaling. First, the two amino acids located in the EGF domain whose mutation significantly reduces or completely abolishes Cripto activity, namely G71 and F78, also appeared to be strictly required to rescue cell competence to respond to Nodal signaling in the zebrafish assay (Minchiotti et al., 2001). Interestingly, the impaired activity of mutant Cripto protein was dependent on the amino acids chosen for the substitution. In fact, while substitution of phenylalanine to alanine (F78A) significantly reduced protein activity, a tryptophan in the same position (F78W) preserved Cripto ability to promote cardiogenesis. Worth noting, F78 is fully exposed in the 3D model of Cripto and has been hypothesized to be involved in protein binding (Lohmeyer et al., 1997; Minchiotti et al., 2001). Second, receptor reconstitution experiments in *Xenopus* have indicated that the EGF domain of Cripto is crucial for Nodal binding to the Alk4/ActRIIB receptor complex (Yeo and Whitman, 2001), while the CFC domain was required for Cripto to interact with the Alk4 receptor. Specifically, either double or triple mutations in the CFC domain, including the amino acid W107, have been reported to impair Alk4-dependent Cripto activity (Yeo and Whitman, 2001; Yan et al., 2002). Here, we show that the single amino acid substitution of residue W107 in the CFC domain severely impairs the ability of Cripto to promote cardiac induction in Cripto$^{-/-}$ ES cells. Finally, several reports have described the modification of Cripto by the addition of sugar residues, including a rare case of fucosylation, suggesting that the activity of Cripto may be controlled by the extent of its glycosylation or fucosylation (for review see Rosa, 2002). Here we show that an alanine substitution in the site of O-fucosylation (T72A; Yan et al., 2002) generates a Cripto mutant protein that is still competent to promote cardiomyocyte differentiation, although showing a reduced activity compared with the wt. Although T72A modification of Cripto has been previously shown to be completely inactive in facilitating Nodal signaling in *Xenopus* (Schiffer et al., 2001) and in coculture assay (Yan et al., 2002), recent data showed that mutant embryos lacking *O*-fucosyltransferase do not resemble the *cripto* knockout phenotype, thus suggesting a less stringent requirement for *O*-fucose on Cripto activity in vivo than in reporter assay (Shi and Stanley, 2003).

Nodal signaling is required for Cripto-regulated cardiomyogenesis

Results reported herein suggested that Nodal signaling was required for Cripto-regulated cardiac induction and differentiation. To obtain more direct evidence to support this hypothesis, we performed loss-of-function experiments by using Nodal antagonists in our controlled differentiation assay. To this end, either Cerberus or Cerberus-S proteins were used, either by transfecting Cripto$^{-/-}$ ES cells with corresponding expression vectors or by using conditioned media containing the recombinant proteins. In both cases, the presence of either Cerberus or Cerberus-S results in a strong inhibition of Cripto activity in the differentiation assay, thus supporting the idea that Nodal is indeed required to mediate Cripto-dependent cardiomyocyte induction and differentiation of ES cells.

Understanding the early events of lineage segregation during differentiation of mammalian cells is crucial for the prospects of controlling stem cell differentiation for biomedical application. Although ES cells represent a viable source of donor cells for transplantation and gene delivery, the successful use of ES-derived donor cells would require the generation of essentially pure cultures of specific cell types (Boheler et al., 2002). In this respect, our results open new insights into the understanding of the molecular mechanisms by which *cripto* regulates cardiogenesis, and will hopefully contribute to the characterization of the molecular signals that control both cardiac and neuronal differentiation of stem cells as the first step in the ongoing efforts to employ these cells in regenerative medicine.

Materials and methods

Plasmids and mutants

The pallino βA vector was derived from the pallino vector (provided by S. Chiocca, European Institute of Oncology, Milan, Italy) by replacing the CMV promoter with the chicken β-actin promoter (pCXN2 vector; Niwa et al., 1991). Restriction sites were blunt ended using Klenow polymerase. All the *cripto* mutant derivatives were obtained as previously described (Minchiotti et al., 2001). The Cripto-His here renamed "secreted Cripto" and the EGF-CFC derivatives have been previously described (Minchiotti et al., 2001). The *cripto* EGF long (nucleotide −5 to +288 of *cripto* cDNA; Dono et al., 1993), *cripto* EGF short (nucleotide −5 to +75 fused to +157/+288 of *cripto* cDNA), wt and activated (ca) Alk4, wt and activated (ca) Taram-A, Cerberus, and Cerberus-S cDNAs were all subcloned into pallino βA vector.

Cell cultures and ES differentiation

Human embryonic kidney 293 and 293EBNA cells and undifferentiated ES cells were cultured as previously described (Xu et al., 1999; Minchiotti et al., 2001). For in vitro differentiation, ES cells were cultivated in EBs essentially as previously described (Wobus et al., 1991; Maltsev et al., 1993; Fig. 1). The EBs were plated separately onto gelatin-coated 48-well plates for morphological analysis or onto 100-mm tissue culture plates for RT-PCR and Western blot.

Cell transfections and proteins

Undifferentiated ES cells (10^7/ml) were electroporated with linearized DNA (30 μg) at 400 V, 250 μF. 1 wk after selection with 2 μg/ml puromycin, resistant clones were pooled, expanded, and subjected to the differentiation assay. Transfection of 293EBNA cells was performed as previously described (Minchiotti et al., 2000).

Recombinant secreted Cripto proteins were obtained and purified as previously described (Minchiotti et al., 2001). Conditioned media containing either Cerberus or Cerberus-S were obtained from 293T cells as previously described (Piccolo et al., 1999).

Western blotting

Either undifferentiated ES cells or EBs were lysed either in a buffer containing 10 mM Tris/Cl, pH 8, 140 mM NaCl, 2 mM EDTA, pH 8, 1% NP-40 or dissolved in Laemmli lysis buffer (Laemmli, 1970) and analyzed by Western blot using the Trans-Blot Semi-dry System (Bio-Rad Laboratories). The anti-HA (12CA5) antibody (ROCHE), anti-Porin 31HL antibody (Calbiochem), anti-Smad2/3, and anti–phospho-Smad2 (Ser465/467) (Upstate Biotechnology) were used according to the manufacturer's instructions.

RNA preparation and RT-PCR

Total RNA from either undifferentiated ES cells or EBs was extracted with TRIzol kit (Life Technologies) according to the manufacturer's instructions and reverse transcribed to cDNA with SuperScript II reverse transcriptase (Life Technologies) and random hexamers (as primers). cDNA samples synthesized from 100 ng of total RNA were subjected to PCR amplification with specific primers. The primers and the PCR conditions used were as follows: Nodal, 5′-TTCCTTCTCAGGTCACGTTTGC-3′ (forward) and 5′-GGTGGGGTTGGTATCGTTTCA-3′ (reverse), annealing temperature 58°C, cycles 35, producing a 518-bp fragment; ALK-4, 5′-AAGGATCCAGGCTCTGCTGTGTGCC-3′ (forward) and 5′-ACGGATCCATGTCCAACCTCTGGCGG-3′ (reverse), annealing temperature 60°C, cycles 30, 411-bp fragment; ActRIIB, 5′-ATGTGCCGTGGTGTCGTGGT-3′ (forward) and 5′-GACCTCCTGATCAGGGATAC-3′ (reverse), annealing temperature 58°C, cycles 30, 54-bp fragment; MLC2v, 5′-GCCAAGAAGCGGATAGAAGGCGGG-3′ (forward) and 5′-CTGTGGTTCAGGGCTCAGTCCTTC-3′ (reverse), annealing temperature 70°C, cycles 33, 490-bp fragment; cardiac αMHC, 5′-GGAAGAGTGAGCGGCGCATCAAGG-3′ (forward) and 5′-CTGCTGGAGAGGTTATTCCTCG-3′ (reverse), annealing temperature 65°C, cycles 30, 301-bp fragment. A set of primers for hypoxanthine phosphoribosyltransferase (HPRT), 5′-CCTGCTGGATTACATTAAAGCACTG-3′ (forward) and 5′-CCTGAAGTACTCATTATAGTCAAGG-3′ (reverse), annealing temperature 58°C, cycles 25, 369-bp fragment, was used as a control.

Immunofluorescence of EBs

Adherent EBs were fixed either in methanol/acetone (7:3; MF-20 antibody) or in 4% paraformaldehyde in PBS (β-tubulin isotype III). EBs were treated with 0.1% Triton X-100 (Sigma-Aldrich), 10% normal goat serum (Dako-Cytomation) in PBS and incubated with primary antibodies in 10% NGS, 1× PBS at the following working dilutions: anti–neurofilament-M (1:400; Chemicon International), anti–β-tubulin isotype III (1:400; Sigma-Aldrich), and anti–sarcomeric myosin (MF-20, 1:50; monoclonal supernatant obtained from the Developmental Studies Hybridoma Bank, University of Iowa). After washing, EBs were incubated with secondary antibodies, either fluorescein (Boehringer) or rhodamine conjugated (Jackson ImmunoResearch Laboratories), in 10% NGS, 1× PBS. After PBS wash, EBs were counterstained with DAPI and mounted in Vecta Shield medium (Vector Laboratories). Labeling was visualized by epifluorescent illumination using an Axioskop 2 microscope, and images were acquired on an Axiocam ARC camera (Carl Zeiss MicroImaging, Inc.).

We thank Mrs. M. Terracciano and Salvatore Ponticelli for technical assistance, Miss M. D'Agostino for correcting and typing the manuscript, and Frederic Rosa, Daniel Constam, and Stefano Piccolo for their gifts of plasmids. We are grateful to Scott Frank for his thoughtful comments on the manuscript and Drs. Frederic Rosa, Umberto di Porzio, and Mark Mercola for their valuable comments and helpful suggestions. S. Parisi wishes to thank F. Volpicelli for helpful advice and for providing reagents.

This work was supported by grants from the Department of Defense Breast Cancer Research Program, U.S. Army Medical Research and Materiel Command (to E.D. Adamson), the Associazione Italiana Ricerca sul Cancro, and BioGeM s.c.a.r.l. (to M.G. Persico). D. D'Andrea was supported by a fellowship from the Fondazione Italiana Ricerca sul Cancro.

Submitted: 3 March 2003
Accepted: 10 September 2003

References

Adamson, E.D., G. Minchiotti, and D.S. Salomon. 2002. Cripto: a tumor growth factor and more. *J. Cell. Physiol.* 190:267–278.

Bain, G., D. Kitchens, M. Yao, J.E. Huettner, and D.I. Gottlieb. 1995. Embryonic stem cells express neuronal properties in vitro. *Dev. Biol.* 168:342–357.

Bain, G., W.J. Ray, M. Yao, and D.I. Gottlieb. 1996. Retinoic acid promotes neural and represses mesodermal gene expression in mouse embryonic stem cells in culture. *Biochem. Biophys. Res. Commun.* 223:691–694.

Bianco, C., H.B. Adkins, C. Wechselberger, M. Seno, N. Normanno, A. De Luca, Y. Sun, N. Khan, N. Kenney, A. Ebert, et al. 2002. Cripto-1 activates nodal- and ALK4-dependent and -independent signaling pathways in mammary epithelial cells. *Mol. Cell. Biol.* 22:2586–2597.

Boheler, K.R., J. Czyz, D. Tweedie, H.T. Yang, S.V. Anisimov, and A.M. Wobus. 2002. Differentiation of pluripotent embryonic stem cells into cardiomyocytes. *Circ. Res.* 91:189–201.

Cheng, S.K., F. Olale, J.T. Bennett, A.H. Brivanlou, and A.F. Schier. 2003. EGF-CFC proteins are essential coreceptors for the TGF-beta signals Vg1 and GDF1. *Genes Dev.* 17:31–36.

Ding, J., L. Yang, Y.T. Yan, A. Chen, N. Desai, A. Wynshaw-Boris, and M.M. Shen. 1998. Cripto is required for correct orientation of the anterior-posterior axis in the mouse embryo. *Nature.* 395:702–707.

Doetschman, T., M. Shull, A. Kier, and J.D. Coffin. 1993. Embryonic stem cell model systems for vascular morphogenesis and cardiac disorders. *Hypertension.* 22:618–629.

Dono, R., L. Scalera, F. Pacifico, D. Acampora, M.G. Persico, and A. Simeone. 1993. The murine *cripto* gene: expression during mesoderm induction and early heart morphogenesis. *Development.* 118:1157–1168.

Fishman, M.C., and K.R. Chien. 1997. Fashioning the vertebrate heart: earliest embryonic decisions. *Development.* 124:2099–2117.

Gepstein, L. 2002. Derivation and potential applications of human embryonic stem cells. *Circ. Res.* 91:866–876.

Gritsman, K., J. Zhang, S. Cheng, E. Heckscher, W.S. Talbot, and A.F. Schier. 1999. The EGF-CFC protein one-eyed pinhead is essential for nodal signaling. *Cell.* 97:121–132.

Keller, G.M. 1995. In vitro differentiation of embryonic stem cells. *Curr. Opin. Cell Biol.* 7:862–869.

Laemmli, U.K. 1970. Cleavage of structural proteins during the assembly of the head of bacteriophage T4. *Nature.* 227:680–685.

Lohmeyer, M., P.M. Harrison, S. Kannan, M. DeSantis, N.J. O'Reilly, M.J. Sternberg, D.S. Salomon, and W.J. Gullick. 1997. Chemical synthesis, structural modeling, and biological activity of the epidermal growth factor-like domain of human cripto. *Biochemistry.* 36:3837–3845.

Maltsev, V.A., J. Rohwedel, J. Hescheler, and A.M. Wobus. 1993. Embryonic stem cells differentiate in vitro into cardiomyocytes representing sinusnodal, atrial and ventricular cell types. *Mech. Dev.* 44:41–50.

Marvin, M.J., G. Di Rocco, A. Gardiner, S.M. Bush, and A.B. Lassar. 2001. Inhi-

bition of Wnt activity induces heart formation from posterior mesoderm. *Genes Dev.* 15:316–327.

McFadden, D.G., and E.N. Olson. 2002. Heart development: learning from mistakes. *Curr. Opin. Genet. Dev.* 12:328–335.

Minchiotti, G., S. Parisi, G. Liguori, M. Signore, G. Lania, E.D. Adamson, C.T. Lago, and M.G. Persico. 2000. Membrane-anchorage of Cripto protein by glycosylphosphatidylinositol and its distribution during early mouse development. *Mech. Dev.* 90:133–142.

Minchiotti, G., G. Manco, S. Parisi, C.T. Lago, F. Rosa, and M.G. Persico. 2001. Structure-function analysis of the EGF-CFC family member Cripto identifies residues essential for nodal signalling. *Development.* 128:4501–4510.

Monzen, K., Y. Hiroi, S. Kudoh, H. Akazawa, T. Oka, E. Takimoto, D. Hayashi, T. Hosoda, M. Kawabata, K. Miyazono, et al. 2001. Smads, TAK1, and their common target ATF-2 play a critical role in cardiomyocyte differentiation. *J. Cell Biol.* 153:687–698.

Monzen, K., R. Nagai, and I. Komuro. 2002. A role for bone morphogenetic protein signaling in cardiomyocyte differentiation. *Trends Cardiovasc. Med.* 12: 263–269.

Munoz-Sanjuan, I., and A.H. Brivanlou. 2002. Neural induction, the default model and embryonic stem cells. *Nat. Rev. Neurosci.* 3:271–280.

Niwa, H., K. Yamamura, and J. Miyazaki. 1991. Efficient selection for high-expression transfectants with a novel eukaryotic vector. *Gene.* 108:193–199.

Okabe, S., K. Forsberg-Nilsson, A.C. Spiro, M. Segal, and R.D. McKay. 1996. Development of neuronal precursor cells and functional postmitotic neurons from embryonic stem cells in vitro. *Mech. Dev.* 59:89–102.

Olson, E.N., and D. Srivastava. 1996. Molecular pathways controlling heart development. *Science.* 272:671–676.

Piccolo, S., E. Agius, L. Leyns, S. Bhattacharyya, H. Grunz, T. Bouwmeester, and E.M. De Robertis. 1999. The head inducer Cerberus is a multifunctional antagonist of Nodal, BMP and Wnt signals. *Nature.* 397:707–710.

Reissmann, E., H. Jornvall, A. Blokzijl, O. Andersson, C. Chang, G. Minchiotti, M.G. Persico, C.F. Ibanez, and A.H. Brivanlou. 2001. The orphan receptor ALK7 and the Activin receptor ALK4 mediate signaling by Nodal proteins during vertebrate development. *Genes Dev.* 15:2010–2022.

Reiter, J.F., H. Verkade, and D.Y. Stainier. 2001. Bmp2b and Oep promote early myocardial differentiation through their regulation of gata5. *Dev. Biol.* 234: 330–338.

Renucci, A., V. Lemarchandel, and F. Rosa. 1996. An activated form of type I serine/threonine kinase receptor TARAM-A reveals a specific signalling pathway involved in fish head organiser formation. *Development.* 122:3735–3743.

Rosa, F.M. 2002. Cripto, a multifunctional partner in signaling: molecular forms and activities. *Sci. STKE.* 2002:PE47.

Rosenthal, N., and J. Xavier-Neto. 2000. From the bottom of the heart: anteroposterior decisions in cardiac muscle differentiation. *Curr. Opin. Cell Biol.* 12: 742–746.

Salomon, D.S., C. Bianco, and M. De Santis. 1999. Cripto: a novel epidermal growth factor (EGF)-related peptide in mammary gland development and neoplasia. *Bioessays.* 21:61–70.

Schiffer, S.G., S. Foley, A. Kaffashan, X. Hronowski, A.E. Zichittella, C.Y. Yeo, K. Miatkowski, H.B. Adkins, B. Damon, M. Whitman, et al. 2001. Fucosylation of Cripto is required for its ability to facilitate nodal signaling. *J. Biol. Chem.* 276:37769–37778.

Schultheiss, T.M., J.B. Burch, and A.B. Lassar. 1997. A role for bone morphogenetic proteins in the induction of cardiac myogenesis. *Genes Dev.* 11:451–462.

Shen, M.M., and A.F. Schier. 2000. The EGF-CFC gene family in vertebrate development. *Trends Genet.* 16:303–309.

Shi, S., and P. Stanley. 2003. Protein O-fucosyltransferase 1 is an essential component of Notch signaling pathways. *Proc. Natl. Acad. Sci. USA.* 100: 5234–5239.

Tropepe, V., S. Hitoshi, C. Sirard, T.W. Mak, J. Rossant, and D. van der Kooy. 2001. Direct neural fate specification from embryonic stem cells: a primitive mammalian neural stem cell stage acquired through a default mechanism. *Neuron.* 30:65–78.

Tzahor, E., and A.B. Lassar. 2001. Wnt signals from the neural tube block ectopic cardiogenesis. *Genes Dev.* 15:255–260.

Wieser, R., J.L. Wrana, and J. Massague. 1995. GS domain mutations that constitutively activate T beta R-I, the downstream signaling component in the TGF-beta receptor complex. *EMBO J.* 14:2199–2208.

Wobus, A.M., G. Wallukat, and J. Hescheler. 1991. Pluripotent mouse embryonic stem cells are able to differentiate into cardiomyocytes expressing chronotropic responses to adrenergic and cholinergic agents and Ca^{2+} channel blockers. *Differentiation.* 48:173–182.

Xu, C., G. Liguori, E.D. Adamson, and M.G. Persico. 1998. Specific arrest of cardiogenesis in cultured embryonic stem cells lacking Cripto-1. *Dev. Biol.* 196: 237–247.

Xu, C., G. Liguori, M.G. Persico, and E.D. Adamson. 1999. Abrogation of the Cripto gene in mouse leads to failure of postgastrulation morphogenesis and lack of differentiation of cardiomyocytes. *Development.* 126:483–494.

Yan, Y.T., J.J. Liu, Y. Luo, C. E, R.S. Haltiwanger, C. Abate-Shen, and M.M. Shen. 2002. Dual roles of Cripto as a ligand and coreceptor in the nodal signaling pathway. *Mol. Cell. Biol.* 22:4439–4449.

Yeo, C., and M. Whitman. 2001. Nodal signals to Smads through Cripto-dependent and Cripto-independent mechanisms. *Mol. Cell.* 7:949–957.

ACADEMIC PRESS

Available online at www.sciencedirect.com
SCIENCE DIRECT®

DEVELOPMENTAL BIOLOGY

Developmental Biology 264 (2003) 537–549

www.elsevier.com/locate/ydbio

Anterior neural plate regionalization in *cripto* null mutant mouse embryos in the absence of node and primitive streak

Giovanna L. Liguori,[a,*] Diego Echevarría,[b] Raffaele Improta,[a] Massimo Signore,[a,1] Eileen Adamson,[c] Salvador Martínez,[b] and M. Graziella Persico[a]

[a] *Institute of Genetics and Biophysics "A. Buzzati-Traverso", CNR, Via Guglielmo Marconi 12, 80125 Naples, Italy*
[b] *Instituto de Neurociencias UMH-CSIC, University Miguel Hernandez, Campus de San Juan, 03550 Alicante, Spain*
[c] *The Burnham Institute, La Jolla Cancer Research Center, 10901, N. Torrey Pines Road, La Jolla, CA 92037, USA*

Received for publication 17 March 2003, revised 12 August 2003, accepted 18 August 2003

Abstract

The relation between the role of the organizer at the gastrula stage and the activity of earlier signals in the specification, maintenance, and regionalization of the developing brain anlage is still controversial. Mouse embryos homozygous for null mutation in the *cripto* gene die at about 9.0 days postcoitum (d.p.c.) and fail to gastrulate and to form the node (the primary organizer). Here, we study the presence and the distribution of anterior neural plate molecular domains in *cripto* null mutants. We demonstrate that, in $cripto^{-/-}$ embryos, the main prosencephalic and mesencephalic regions are present and that they assume the correct topological organization. The identity of the anterior neural domains is maintained in mutant embryos at 8.5 d.p.c., as well as in mutant explants dissected at 8.5 d.p.c. and cultured in vitro for 24 h. Our data imply the existence of a stable neural regionalization of anterior character inside the $cripto^{-/-}$ embryos, despite the failure in both the gastrulation process and node formation. These results suggest that, in mouse embryos, the specification of the anterior neural identities can be maintained without an absolute requirement for the embryonic mesoderm and the node.

Keywords: Node; AVE; cripto; Anterior neural plate; Regionalization; Maintenance

Introduction

Classical embryological experiments have identified the existence of a specific population of cells in the gastrulae of the amphibian (dorsal blastopore lip), the zebrafish (dorsal embryonic shield), the bird (Hensen's node), and the mouse (node) that act to organize the body plan (reviewed by Lemaire and Kodjabachian, 1996). The organizer has been defined as a specialized region of the vertebrate embryo, that can act as an independent unit controlled by self-sustaining signals, and that is able to recruit surrounding ectoderm cells to become neural, giving them a complete anterior–posterior (A/P) pattern. Heterotopic transplantation experiments have highlighted that the mouse node is able to induce a secondary axis but, unlike the Xenopus organizer, the mouse node is not sufficient to induce duplication of the most anterior structures (Beddington, 1994). These findings indicate that the murine node might not possess all the properties for a complete A/P regionalization of the neural axis.

Evidence that signals from outside the classical organizer could be required for induction of the anterior neural plate (ANP) was first produced in mouse by physical ablation of the anterior visceral endoderm (AVE) (Thomas and Beddington, 1996) and confirmed by the comparative analysis of *Lim1*, *nodal*, and *Otx2* knock-out and chimeric embryos (Acampora et al., 1995; Conlon et al., 1994; Rhinn et al., 1998; Shawlot and Behringer, 1995; Shawlot et al., 1999; Varlet et al., 1997). Collectively, the results of these experiments indicate that the mouse node does not initiate the

* Corresponding author. Fax: +0039-081-6132-352.
E-mail address: liguori@iigb.na.cnr.it (G.L. Liguori).
[1] Present address: MRC Centre for Developmental Neurobiology, New Hunt's House, King's College London, Guy's Campus, London Bridge, London, SE1 1UL, UK.

0012-1606/$ – see front matter © 2003 Elsevier Inc. All rights reserved.
doi:10.1016/j.ydbio.2003.08.023

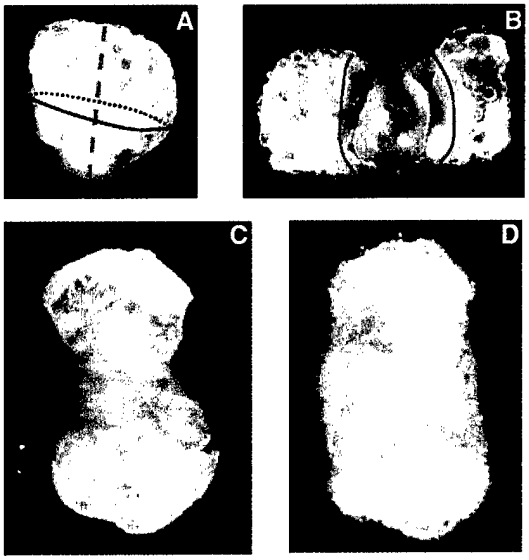

Fig. 1. In vitro cultured *cripto*$^{-/-}$ explant. (A) *cripto*$^{-/-}$ embryo at 8.5 d.p.c. The red line indicates the boundary between embryonic and extraembryonic regions, while the green dotted line indicates the axis along which the embryo is cut to open. (B) Ventral view of the opened embryo. The embryonic region is in the middle, while the extraembryonic region is at the periphery of both sides of the embryo. (C) *cripto*$^{-/-}$ explant at 0 h of in vitro culture on steady membrane filters. (D) *cripto*$^{-/-}$ explant after 24 h of in vitro culture, showing the preserved morphology of the tissue in the explant.

anterior pattern, and that a head organizer activity might reside in the AVE (reviewed by Beddington and Robertson, 1998, 1999). A two-step model for mouse anterior neural development proposes that initial specification of anterior neural identity requires the AVE, while the subsequent maintenance and refinement of the previously induced identities involve signals emitted by the node and its derivatives (Shawlot et al., 1999; Thomas and Beddington, 1996). Recent studies supporting this model also point to a role of node derivatives in maintaining and stabilizing the anterior neural specification. Camus and coworkers (2000) have demonstrated that, in the mouse embryo, the removal of the rostral segment of the anterior midline, containing the prechordal mesoderm, causes head truncation accompanied by the loss of several forebrain markers. Moreover, the analysis of *HNF3β/Foxa2* conditional mutants has shown that, in the absence of the axial mesendoderm, specification of the ANP occurs, but is labile (Hallonet et al., 2002). However, results have also been produced that do not fit with the above model. Anterior neural induction does not occur in *Wnt3*$^{-/-}$ embryos, which lack the primitive streak and the node, despite apparently normal AVE development (Liu et al., 1999). Furthermore, heterotopic transplantation experiments show that the AVE alone fails to induce ectopic neural tissue (Tam and Steiner, 1999). Both findings argue against a role of the AVE as the embryonic head organizer. On the other hand, *HNF3β* null mutants lack the node and the axial mesendoderm, but, surprisingly, the patterning along A/P axis is only slightly affected (Ang and Rossant, 1994; Klingensmith et al., 1999; Weinstein et al., 1994).

To summarize the above, the specific role of the AVE and the node during anterior neural development remains a contentious issue. Our work intends to contribute to the debate, by analyzing in detail the anterior neural patterning in *cripto*$^{-/-}$ embryos. *cripto* null mutants represent the only mouse mutant model to combine the lack of primitive streak and node and the distal mislocalization of a still functional AVE (Beddington, 1998; Ding et al., 1998), thus providing a powerful tool to gain insight into the specification, regionalization, and stabilization of the ANP in the mouse embryo. *cripto* is the founding member of the family of EGF-CFC genes which code for extracellular factors that, in conjunction with nodal, a ligand of the transforming growth factor beta (Tgf-β) family, are involved in the molecular control of several early decisions during vertebrate embryonic development (Minchiotti et al., 2002; Reissmann et al., 2001; Shen and Schier, 2000; Yan et al., 2002). The mouse *cripto* gene is expressed in the whole epiblast before gastrulation and, successively, in the forming mesoderm and in the developing heart (Ding et al., 1998; Dono et al., 1993; Minchiotti et al., 2000). Targeted inactivation of *cripto* causes early embryonic lethality, at approximately 9.0 days postcoitum (d.p.c.), affecting the definition of A/P polarity, embryonic mesoderm formation, and cardiac development (Ding et al., 1998; Xu et al., 1999). Here, we determine the expression pattern of diagnostic anterior neural markers in both *cripto*$^{-/-}$ embryos and in vitro cultured explants, focusing our attention on the definition and the maintenance of the spatial relationships among the different expression domains. Our analysis elucidates the molecular identity of *cripto*$^{-/-}$ anterior neuroectoderm and indicates that the correct specification and location of the presumptive anterior neural territories may occur and be maintained even in the absence of the node and its derivatives.

Materials and methods

Production of mutant embryos

The analysis of *cripto* inactivation was performed in a mixed genetic background composed of 25% 129SvJ, 25% Black Swiss, and 50% C57B16. Mutant homozygotes were obtained by crossing heterozygous mice. Noon of the day on which the vaginal plug was detected was considered as 0.5 d.p.c. in the timing of the embryo collection. For the genotyping of pups and embryos, DNA was extracted from the tail tips and yolk sac, respectively, and then analyzed by means of PCR as previously described (Xu et al., 1999).

Embryo dissection and explant culture

Timed pregnant *cripto*$^{-/-}$ mice were killed by cervical dislocation, and embryos at 8.5 d.p.c. were dissected from

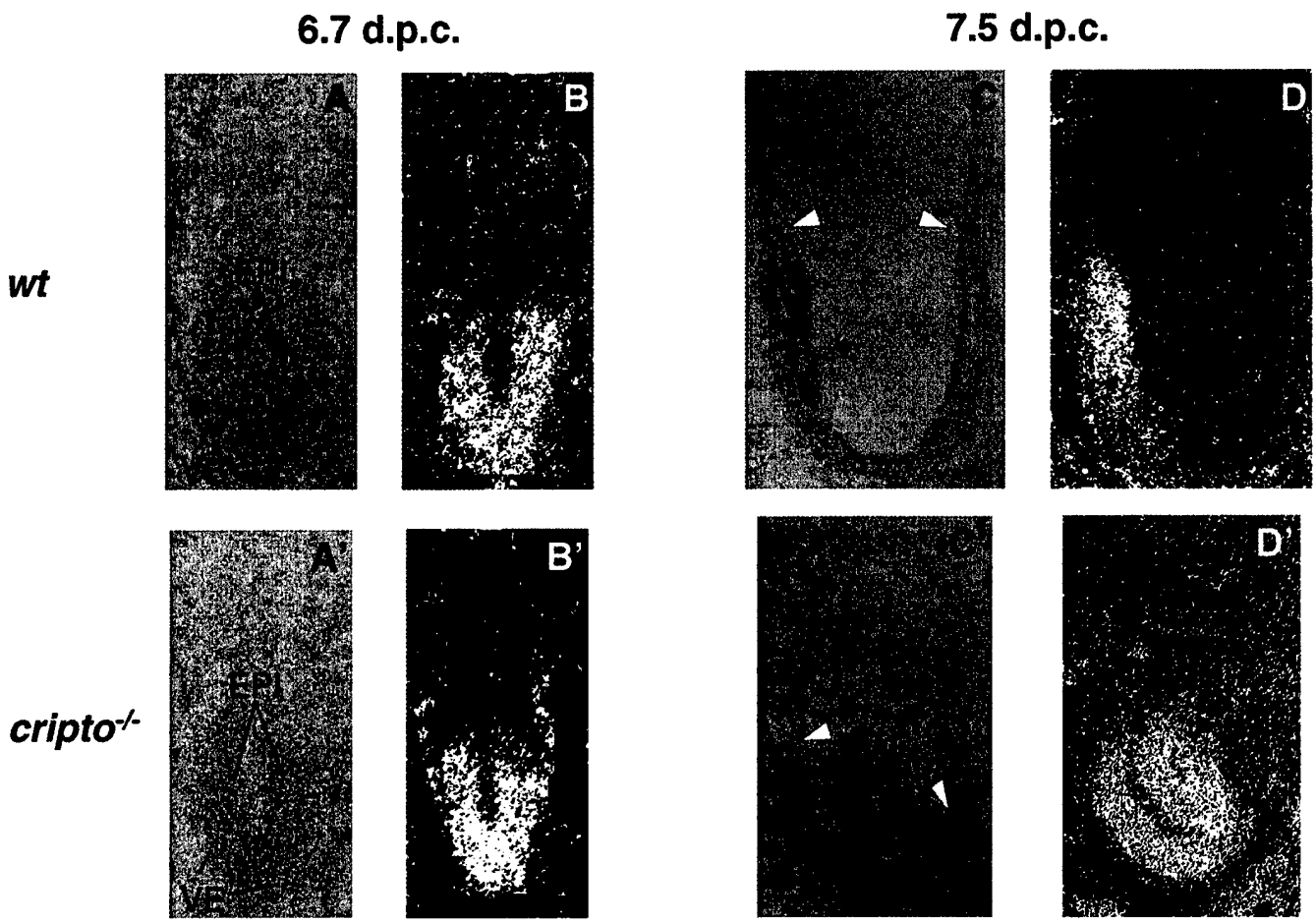

Fig. 2. Comparison of *Otx2* gene expression in wt and *cripto*$^{-/-}$ embryos at both 6.7 and 7.5 d.p.c. (A, A′, C, C′) Bright-field and (B, B′, D, D′) dark-field images of in situ hybridizations on sagittal sections of wt (upper panel) and *cripto*$^{-/-}$ (lower panel) embryos. *Otx2* expression in the epiblast (EPI) and embryonic visceral endoderm (VE) of 6.7-d.p.c. wt (A, B) and *cripto*$^{-/-}$ (A′, B′) embryos. (C, D) *Otx2* expression in the anterior embryonic region of 7.5-d.p.c. wt embryo and (C′, D′) in almost all the embryonic region of *cripto* null mutant at 7.5 d.p.c. Arrowheads label the extension of neural plate (empty arrowheads) and the caudal limit of *Otx2* expression (red arrowheads).

decidual tissue in chilled Hank's medium (Gibco-Life Technologies). For explant in vitro culture, wt embryos were opened and treated as previously described (Echevarria et al., 2001). The *cripto*$^{-/-}$ embryos showed a sac shape in which it was only possible to recognize an embryonic (lower) and an extraembryonic (upper) region (Fig. 1A). These embryos were first cut apically so as to remove the most external part of the extraembryonic region, and then opened longitudinally along two opposite axes, starting from the extraembryonic and moving toward the embryonic region (Fig. 1A). The result was a symmetric bow-tie-shaped explant in which the embryonic region was in the center and the extraembryonic at the periphery of both sides of the explant (Fig. 1B, C, and D). Both wt and mutant explants were cultured in vitro for 24–30 h as previously described (Echevarria et al., 2001). Both embryos and in vitro cultured explants were fixed for a time varying from 3 h to overnight in 4% paraformaldehyde in PBS at 4°C, washed in PBT (0.1% Tween 20 in PBS), dehydrated through ascending methanol, and stored at −20°C.

In situ hybridization on sections

RNA probes were synthesized from linearized plasmid in the presence of ^{35}S-CTP (Amersham) (Simeone, 1999). In situ hybridization (ISH) experiments on sections were performed as previously described (Simeone, 1999). Autoradiography was performed by using Kodak NTB2 emulsion, with exposure times from 15 to 20 days. After developing, sections were counterstained with hematoxylin and then mounted in DEPEX. Serially labeled sections were examined and photographed in both dark- and bright-fields, using a Zeiss compound microscope/Polaroid camera with Kodak Elite II film.

Whole-mount in situ hybridization (WISH)

RNA antisense probes were synthesized from linearized plasmid in the presence of Digoxigenin-UTP (Boehringer Manheim) or Fluorescein-UTP (Boehringer Manheim). Embryos were hybridized at 68°C in 50% formamide, 5× SSC,

Table 1
Summary of the whole-mount in situ hybridization experiments on wt and *cripto*$^{-/-}$ samples at 8.5 d.p.c.

Gene	N.embr*	N.expl*	Ant. Pros.		Dienc.		Mes.		Isthmus		Ant. Rhomb	
			wt	−/−	wt	−/−	wt	−/−	wt	−/−	wt	−/−
Sox2	4/4		+	+	+	+	+	+	+	+	+	+
Otx2	12/14	4/4	+	+	+	+	+	+				
Bf1	4/4		+	+								
Six3	3/3	4/4	+	+	+	+						
Nkx2.1	3/3		+	+								
Nkx2.2	3/3		+	+								
Pax6	3/3		+	+	+	+						
Irx3	4/4	3/3			+	+	+	+	+	+	+	+
Wnt1	4/4	3/3					+	+	+	+		
Fgf8	8/10	4/5	+	−					+	+		
Pax2	3/3		+	+			+	+	+	+	+	+
Gbx2	8/10	4/5							+	+	+	+
Shh	0/3		+	−	+	−	+	−	+	−	+	−

* indicates the number of positive samples (embryos in the second lane and explants in the third lane) out of the number of total samples analyzed. For each marker, the positive embryos show always comparable expression.

pH 5, 0.1% Tween 20, 50 μg/ml heparin, 50 μg/ml tRNA, 50 μg/ml salmon sperm DNA, using a probe concentration of 100–500 ng/ml. Embryos were washed three times for 1 h each wash at 68°C in 50% formamide, 4× SSC, pH 5, 1% SDS, and then three times for 1 h each at 68°C in 50% formamide, 2× SSC, pH 5. Hybridization was detected with alkaline-phosphatase-coupled anti-Digoxigenin antibodies (Boehringer Manheim), followed by a reaction with nitroblue tetrazolium chloride (NBT) and 5-Bromo-4-chloro-3-indolyl phosphate, 4-toluidine salt (BCIP) (Boehringer Manheim), developing a blue color and thereafter, for the double WISH, with alkaline-phosphatase-coupled anti-fluorescein antibodies (Boehringer Manheim), followed by a reaction with 2-(4 Iodophenyl)-3-(4nitrophenyl)-5-phenyltetrazolium chloride (INT) and BCIP (Boehringer Manheim), developing a red color. Stained embryos were examined and photographed by using a Leica MZ12 dissection microscope. All the images were processed in AdobePhotoshop 5.0 (Adobe System Inc., Mountain View, CA). The following probes were used: *Bf1* (Hatini et al., 1994), *Fgf8* (Crossley and Martin, 1995), *Irx3* (Bosse et al., 1997), *Gbx2* (Wassarman et al., 1997), *Nkx2.1* (Pabst et al., 2000), *Nkx2.2* (Shimamura et al., 1995), *Otx2* (Simeone et al., 1992), *Pax2* (Rowitch and McMahon, 1995), *Pax6* (Walther and Gruss, 1991), *Shh* (Echelard et al., 1993), *Six3* (Oliver et al., 1995), *Sox2* (Collignon et al., 1996), and *Wnt1* (Joyner, 1996).

Results

cripto$^{-/-}$ *embryos essentially consist of anterior neuroectoderm*

We first analyzed the expression profile of the anterior neural marker *Otx2* during the development of *cripto*$^{-/-}$ mutants, using ISH on both sections and whole embryos (Figs. 2, 3A and A′). At 6.7 d.p.c., wt and mutant embryos showed comparable *Otx2* expression in the whole embryonic ectoderm (Fig. 2A, B, A′, and B′), while at 7.5 d.p.c., *Otx2* transcripts were restricted to the anterior side of wt embryos (Fig. 2C and D), but persisted in almost the entire embryonic region of *cripto*$^{-/-}$ mutants (Fig. 2C′ and D′; Ding et al., 1998). At 8.5 d.p.c., the *Otx2* expression, which at this stage identifies forebrain and midbrain regions, was maintained throughout the *cripto*$^{-/-}$ embryos (Fig. 3A and A′; Table 1). To verify if the *Otx2* expression, observed in 8.5 d.p.c. *cripto*$^{-/-}$ embryos, actually reflected a neural phenotype rather than the presence of undifferentiated ectoderm (as in the wt embryo at the onset of gastrulation), we also examined the expression of the pan-neural marker *Sox2*. We found *Sox2* transcripts in almost all the embryonic cells of *cripto*$^{-/-}$ mutants (Fig. 3B′; Table 1). The comparison between *Otx2* and *Sox2* transcripts distribution indicated that the two expression domains were almost completely overlapping and that most *Otx2*-expressing cells also expressed *Sox2*, demonstrating their neural character. Thus, we conclude that, at 8.5 d.p.c., *cripto*$^{-/-}$ embryos principally consist of neuroectodermal cells, most of which express the anterior marker *Otx2*. The widespread *Otx2* expression suggests the presence of putative forebrain and midbrain territories.

cripto$^{-/-}$ *embryos express forebrain markers*

To determine the identity of the neural tissue present in *cripto*$^{-/-}$ embryos, we analyzed the expression at 8.5 d.p.c. of specific diagnostic markers (Table 1). We first investigated the pattern of the forebrain genes *Bf1* (which identifies most of the telencephalon; data not shown), *Six3*, and *Nkx2.1* (which both mark the hypothalamus and optic stalk primordium; Fig. 4A and B) (Hatini et al., 1994; Oliver et

al., 1995; Shimamura et al., 1995). All the genes were expressed at the distal tip of *cripto* mutant embryos (Fig. 4A′ and B′; data not shown). We also investigated the expression of the *Nkx2.2* (Fig. 4C) and *Pax6* (Fig. 4D) genes, which are expressed more widely along the A/P neural axis of wt embryos (Shimamura et al., 1995; Walther and Gruss, 1991). *Nkx2.2* is expressed in a medial rostral region of the forebrain and, moreover, in the basal plate of almost the entire central nervous system (CNS) (Fig. 4C). *Pax6* expression identifies the prosencephalon (the optotelencephalic region and the diencephalic area), the hindbrain, and the spinal cord (Fig. 4D). In the *cripto* null mutants, we detected *Nkx2.2* expression at the distal embryonic tip (Fig. 4C′) and *Pax6* expression in a thick band close to the distal tip of the embryo (Fig. 4D′). Ding and coworkers (1998) have clearly shown that posterior neuroectoderm is absent in *cripto*$^{-/-}$ embryos. Therefore, the expression of the latter two genes that we detected in *cripto* null mutants might only be assigned to forebrain domains.

These data show that *cripto*$^{-/-}$ embryos, despite the extremely severe morphological phenotype, express all the forebrain genes examined and suggest the presence of all the forebrain territories that these markers identify. More interestingly, these genes were expressed in an ordered manner and always showed the same spatial distribution.

cripto$^{-/-}$ *embryos express midbrain and isthmic markers*

Based on the above results, we went on to analyze the expression of midbrain and isthmic genes (Fig. 5; Table 1). All the genes examined were also expressed in more posterior domains along the axis of the wt embryo. However, we only considered the expression domains inside the ANP, because the other structures are absent in *cripto*$^{-/-}$ embryos (Ding et al., 1998; Xu et al., 1999). Our analysis showed *Irx3* expression, which marks caudal diencephalon, mesencephalon, and rhombencephalon (Fig. 5A; Bosse et al., 1997), in a large proximal region of *cripto* null mutant embryos (Fig. 5A′). We also detected *Wnt1* transcripts, which identify at this stage the dorsal midbrain and isthmus (Fig. 5B; Wurst and Bally-Cuif, 2001), and *Fgf8* transcripts, which mark the isthmus and the anterior neural ridge (ANR) (Fig. 5C; Crossley and Martin, 1995), in a circumferential ring of proximal cells in *cripto*$^{-/-}$ embryos (Fig. 5B′ and C′). No *Fgf8* expression was detected at the distal embryonic tip of *cripto*$^{-/-}$ mutants (Fig. 5C′), suggesting the absence of the ANR primordium (Fig. 5C). Instead, *Pax2* expression was found in two different domains in *cripto*$^{-/-}$ embryos: one small domain at the very distal tip of the embryos, probably indicating the optic stalk primordium, and a second domain located approximately at the boundary between the embryonic and extraembryonic regions, which coincides with the mid–hindbrain expression in wt embryos (Fig. 5D and D′). Finally, the *Gbx2* expression, which defines the isthmus and anterior hindbrain (Fig. 5E; Wassarman et al., 1997), was restricted to the most proximal side of the mutant embryos (Fig. 5E′). We did not find in the embryonic region of *cripto* null mutants any *Shh* expression (data not shown), which marks the prosencephalic and the mesencephalic basal plate of wt embryos (Echelard et al., 1993).

In conclusion, all the telencephalic, diencephalic, mesencephalic, and isthmic territories investigated are specified in the *cripto*$^{-/-}$ embryos, with the exception of the ANR. Moreover, neural markers that in wt embryos define the more rostral regions, are positioned more distally in *cripto*$^{-/-}$ mutants, while markers expressed in the more posterior regions of wt embryos are located more proximally in the mutants. Collectively, these data indicate the presence of a complex neural regionalization of anterior character inside the *cripto*$^{-/-}$ embryos at 8.5 d.p.c.

In vitro cultured cripto$^{-/-}$ *explants maintain the anterior neural regionalization*

cripto$^{-/-}$ embryos die in utero, at about 9.0 d.p.c. (Xu et al., 1999), preventing us from addressing the question if and how anterior neural expression might be further maintained. To investigate whether neural signals acting in *cripto*$^{-/-}$ embryos might specify a stable regionalization inside the anterior neuroectoderm, we made use of embryo culture. It has been shown that, under the opportune conditions, the in vitro development of anterior neural tube dissected at early embryonic stages can mimic development in utero (Echevarria et al., 2001). Furthermore, it has been proposed that in vitro embryo culture can prolong the survival time of the brain anlage in early lethal mutations (Echevarria et al., 2001).

We dissected *cripto*$^{-/-}$ mutants as well as anterior neural tube from control embryos at 8.5 d.p.c. and cultured them in vitro for 24–30 h (Figs. 1 and 6). During this period, neither wt nor *cripto*$^{-/-}$ explants showed appreciable tissue degeneration, and both explants maintained their morphological structure (Figs. 1 and 6). *cripto*$^{-/-}$ explants were heterogeneous in size and shape, as the embryos from which they were derived (Figs. 1 and 6). However, in the bow-tie-shaped *cripto*$^{-/-}$ explants, the distal embryonic region was distinguishable in the center, whereas the extraembryonic one was at both sides. The reciprocal extension of embryonic and extraembryonic regions was variable (Figs. 1 and 6).

We used the explants to investigate the expression profile of most of the genes analyzed in 8.5-d.p.c. embryos (Fig. 6; Table 1). The expression of the more anterior genes, such as *Six3* and *Otx2*, was detected in the middle region of the explants approximately (Fig. 6A and B), corresponding to the distal part of the 8.5-d.p.c. *cripto* null mutants (Figs. 3A′ and 4A′). In perfect agreement, the expression of the more posterior markers, such as *Wnt1*, *Fgf8*, and *Gbx2*, observed at 8.5 d.p.c. in the proximal region of the *cripto*$^{-/-}$ embryos (Fig. 5B′, C′, and E′) was located in the corresponding more external part of the explants (Fig. 6D, E, and F). In

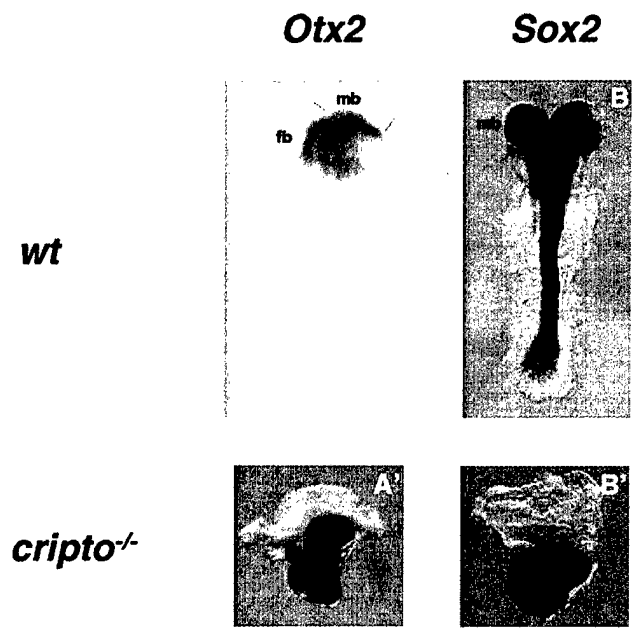

Fig. 3. Comparison between *Otx2* and *Sox2* expression in *cripto*$^{-/-}$ and wt embryos at 8.5 d.p.c, by means of whole-mount in situ hybridization. (B) A dorsal view, whereas all the other pictures are lateral views. (A) *Otx2* expression in the forebrain and midbrain of wt embryo and (A′) in almost all the *cripto*$^{-/-}$ embryonic region. (B) Pan-neural *Sox2* expression in wt embryo. (B′) *Sox2* expression throughout the whole *cripto*$^{-/-}$ embryonic region. Abbreviations: fb, forebrain; mb, midbrain. Black lines indicate the boundaries between the different anterior neural regions.

conclusion, *cripto*$^{-/-}$ explants expressed all the diagnostic markers analyzed in the same topological order identified in 8.5-d.p.c. embryos. These results indicate that *cripto*$^{-/-}$ embryos maintain anterior neural patterning, even after 24 h of in vitro culture.

Topological relationships among the different anterior neural domains are conserved in cripto$^{-/-}$ *embryos*

One fundamental point to be raised is the definition of the spatial relationships among the different anterior neural gene expression patterns in *cripto*$^{-/-}$ embryos. For this purpose, we performed double WISH experiments using the following pairs of genes, *Otx2/Gbx2* (Fig. 7A, A′, D, and D′), *Fgf8/Wnt1* (Fig. 7B and B′), and *Six3/Irx3* (Fig. 7C, C′, E, and E′) on both wt and mutant 8.5-d.p.c. embryos as well as on explants cultured in vitro for 24 h.

In wt embryos, *Otx2* and *Gbx2* expression domains were demonstrated to be juxtaposed (Fig. 7A and D), showing mutual repressing activity (Broccoli et al., 1999; Garda et al., 2001; Millet et al., 1999). The boundary between the two expression domains was shown to define the formation of the isthmic organizer and the source of the Fgf8 signal (Fig. 7B; Garda et al., 2001; Li and Joyner, 2001; Martinez-Barbera et al., 2001). The region rostral to the isthmus, the caudal midbrain, in which *Gbx2* was absent, also expressed *Wnt1* (Fig. 7B; Millet et al., 1999). The double *Otx2/Gbx2* WISH showed that adjacent relation was maintained between these two expression domains in all the *cripto* mutant

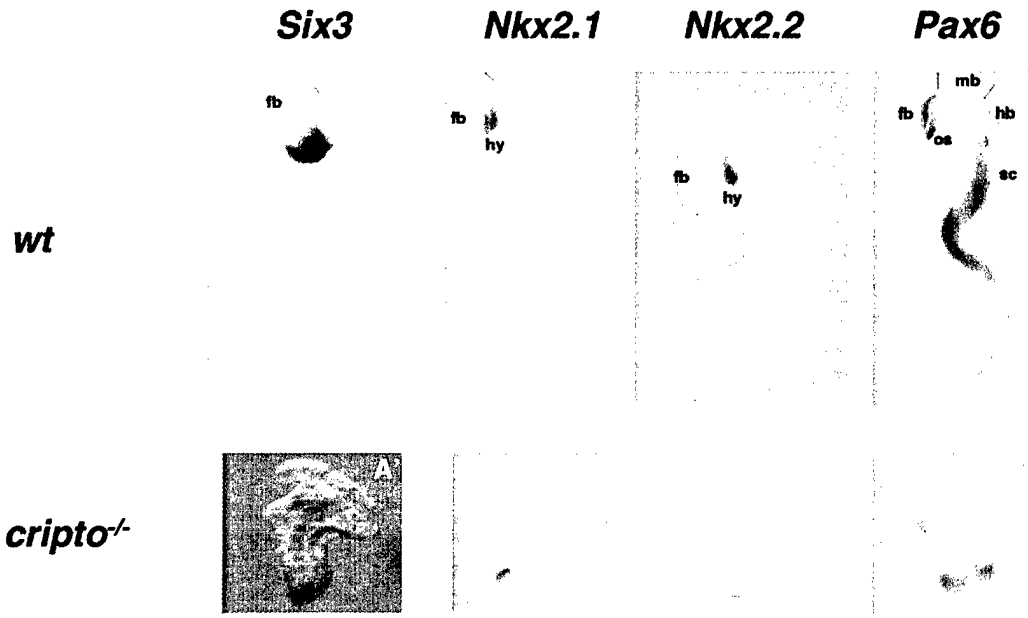

Fig. 4. Forebrain markers are expressed in *cripto*$^{-/-}$ embryos. Whole-mount in situ hybridization analysis of wt and *cripto*$^{-/-}$ embryos at 8.5–9.0 d.p.c. All the pictures are lateral views. (A) *Six3* expression in the forebrain of wt embryo and (A′) at the distal tip of *cripto*$^{-/-}$ embryo. (B) *Nkx2.1* expression in the ventral forebrain of control embryo and (B′) at the distal tip of *cripto*$^{-/-}$ embryo. (C) *Nkx2.2* expression in the medial anterior neural plate and along the hindbrain and spinal cord of wt embryo and (C′) distally in *cripto*$^{-/-}$ embryo. (D) *Pax6* expression identifying the forebrain, hindbrain and spinal cord of wt embryo and (D′) a sharp band close to the distal tip of *cripto*$^{-/-}$ embryo. Abbreviations: fb, forebrain; hb, hindbrain; hy, hypothalamus; os, optic stalk; sc, spinal cord. Black lines indicate the boundaries between the different anterior neural regions.

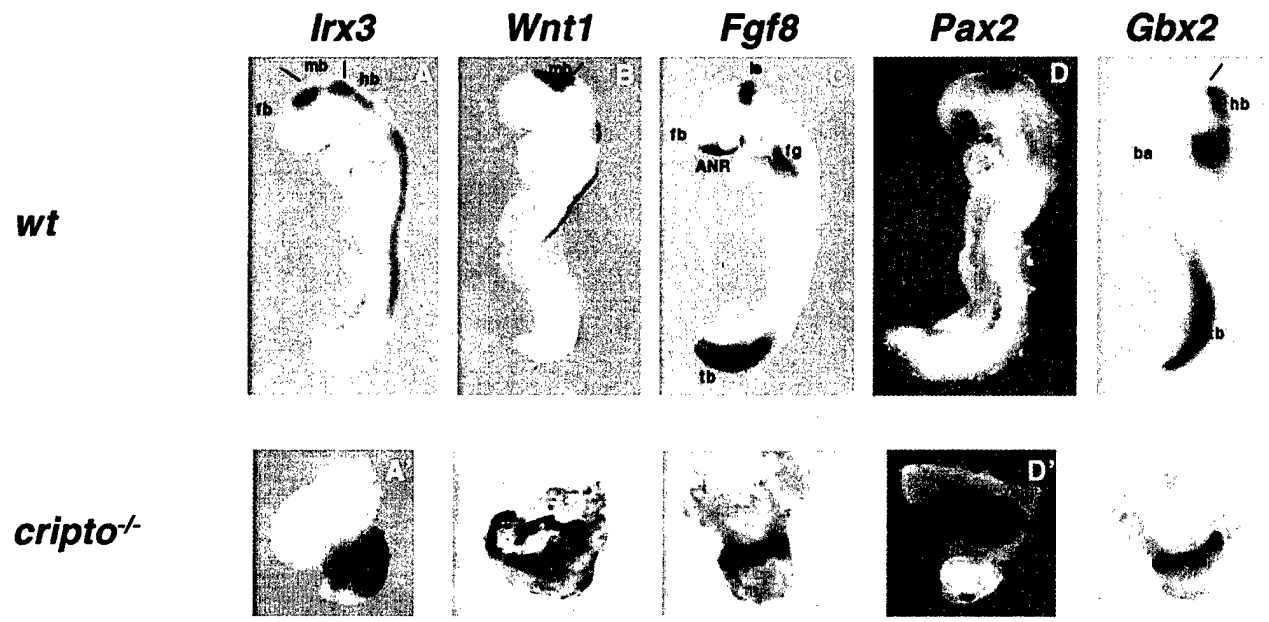

Fig. 5. *cripto*$^{-/-}$ embryos express midbrain and isthmic markers. Whole-mount in situ hybridization analysis of 8.5- to 9.0-d.p.c. wt and *cripto*$^{-/-}$ embryos. All the pictures are lateral views. (A) *Irx3* expression in the caudal diencephalon, midbrain, hindbrain, and spinal cord of wt embryo and (A′) in the intermediate region of *cripto*$^{-/-}$ mutant. (B) *Wnt1* expression in the dorsal midbrain, isthmus, and spinal cord of wt embryo and (B′) in a transverse ring in the proximal *cripto*$^{-/-}$ embryonic region. (C) *Fgf8* expression in the ANR, isthmic primordium, foregut, and tail bud of wt embryo. (C′) Proximal ring of *Fgf8* expression in *cripto*$^{-/-}$ embryo. (D) *Pax2* expression in the optic stalk and midbrain–hindbrain boundary of control embryo and (D′) in both the distal tip and the boundary between embryonic and extraembryonic regions of *cripto* mutant. (E) *Gbx2* expression in the isthmus, anterior hindbrain, branchial arches, and tail bud of wt embryo and (E′) in a proximal ring inside *cripto*$^{-/-}$ embryo. Abbreviations: ANR, anterior neural ridge; ba, branchial arches; fb, forebrain; fg, foregut; hb, hindbrain; Is, isthmus; mb, midbrain; os, optic stalk; sc, spinal cord; tb, tail bud. Boundaries between anterior neural regions are indicated by black lines.

embryos (a total of three) and explants (a total of three) analyzed (Fig. 7A′ and D′). Similarly, the *Wnt1* and *Fgf8* genes, which at this stage define two adjacent narrow stripes corresponding to the isthmic organizer (Fig. 7B), were expressed with a similar pattern in the proximal regions of *cripto* mutant embryos (four out of five) (Fig. 7B′). Moreover, we examined the relative expression of the *Six3* and *Irx3* genes, which define the first one the anterior forebrain and the second one the caudal diencephalon and the mesencephalon. The nested domains of the *Six3* and *Irx3* expressions were also conserved in all the *cripto*$^{-/-}$ embryos (a total of three) and explants (a total of three) analyzed (Fig. 7C, C′, E, and E′).

We can thus conclude that the relative position of the different anterior neural territories is conserved in both *cripto* null mutant embryos and explants. All our data show that a precise A/P polarity is detectable inside the neuroectoderm present in *cripto*$^{-/-}$ mutants, even if rotated at about 90° anticlockwise in relation to the wt and, thus, oriented along the embryonic proximodistal (P/D) axis (Fig. 8). The spatial distribution of the different markers in consecutive ring-like domains, along the P/D axis of *cripto*$^{-/-}$ embryos, corresponding to concentric domains in the explants indicates that neural plate regionalization in cripto mutant embryos develops with a radial distribution rather than with an A/P bilateral symmetry (Fig. 8).

Discussion

Different phases can be distinguished during early brain development, these being the initial induction of the ANP, the successive maintenance of its cephalic character, and the progressive refinement and embellishment of the previously induced identities. Our aim was to investigate the role of the mouse node and AVE in the maintenance of the ANP identities, taking advantage of the peculiar phenotypic characteristics of *cripto*$^{-/-}$ mutants (absence of the node and distal mislocalization of the AVE).

cripto$^{-/-}$ *embryos maintain a regionalized anterior neural plate*

During embryogenesis, *Otx2* gene expression is mainly restricted to forebrain and midbrain regions (Simeone et al., 1992). The *Otx2* gene is also widely expressed in the ectoderm layer of 7.5-d.p.c. *cripto*$^{-/-}$ embryos (Ding et al., 1998), thus suggesting, but not actually proving, that anterior neuroectoderm specification occurs in *cripto* mutants. In fact, since *Otx2* is also expressed in the whole epiblast of wt pregastrula embryo, the *Otx2* transcripts detected in 7.5-d.p.c. *cripto*$^{-/-}$ embryos might simply indicate the persistence of an undifferentiated ectoderm due to the failure of gastrulation. Here, we report that *Otx2* in the embryonic

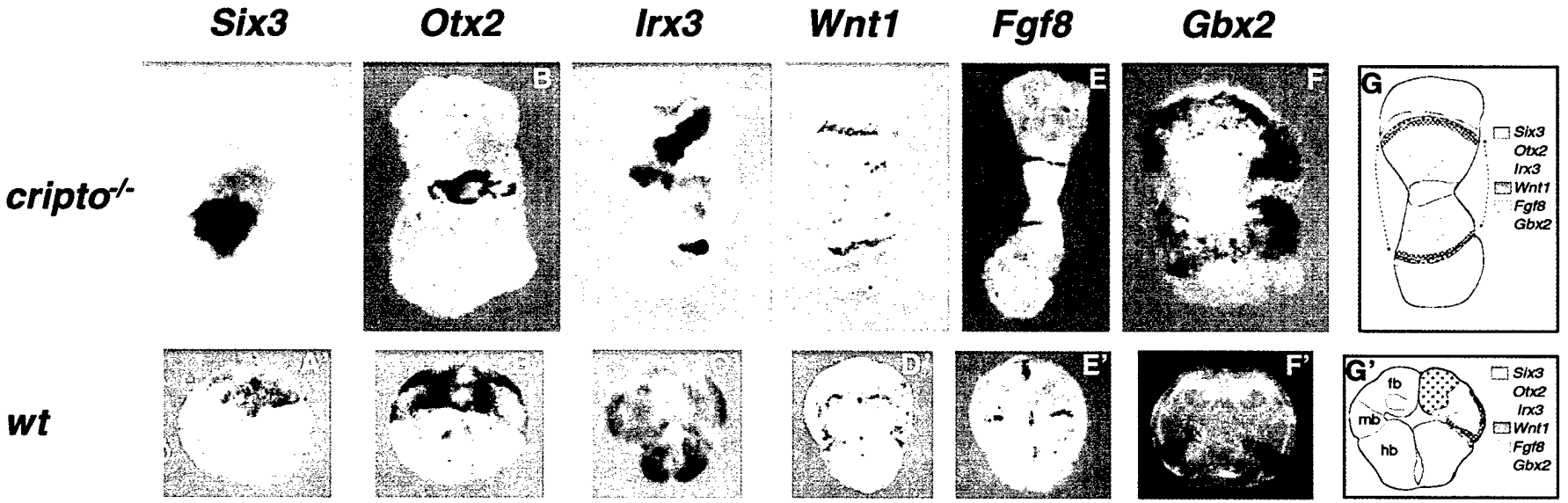

Fig. 6. *cripto*$^{-/-}$ explants maintain anterior neural regionalization. Whole-mount in situ hybridization analysis of 8.5- to 9-d.p.c. *cripto*$^{-/-}$ and wt anterior neural tube explants, after 24 h of in vitro culture. (A) *Six3* expression in the central region of *cripto*$^{-/-}$ explant and (A′) in the anterior forebrain of wt anterior neural tube explant. (B) *Otx2* expression in the middle of *cripto*$^{-/-}$ explant and (B′) in the forebrain and midbrain of wt explant. (C) *Irx3* expression in the medial region of *cripto*$^{-/-}$ explant and (C′) in the caudal diencephalon, mesencephalon, and anterior hindbrain of wt explant. (D) *Wnt1* expression at the boundary between the embryonic and extraembryonic region of *cripto*$^{-/-}$ explant and (D′) in the dorsal midbrain and at the midbrain–hindbrain boundary of wt explant. (E) *Fgf8* expression at the boundary between the embryonic and extraembryonic region of *cripto* null mutant explant and (E′) in the ANR and the isthmic primordium of wt explant. (F) *Gbx2* expression at the extremities of the embryonic region of *cripto*$^{-/-}$ explant and (F′) in the isthmus and anterior hindbrain of wt neural tube explant. (G) Schematic representation of the expression pattern observed in *cripto*$^{-/-}$ and (G′) control explants.

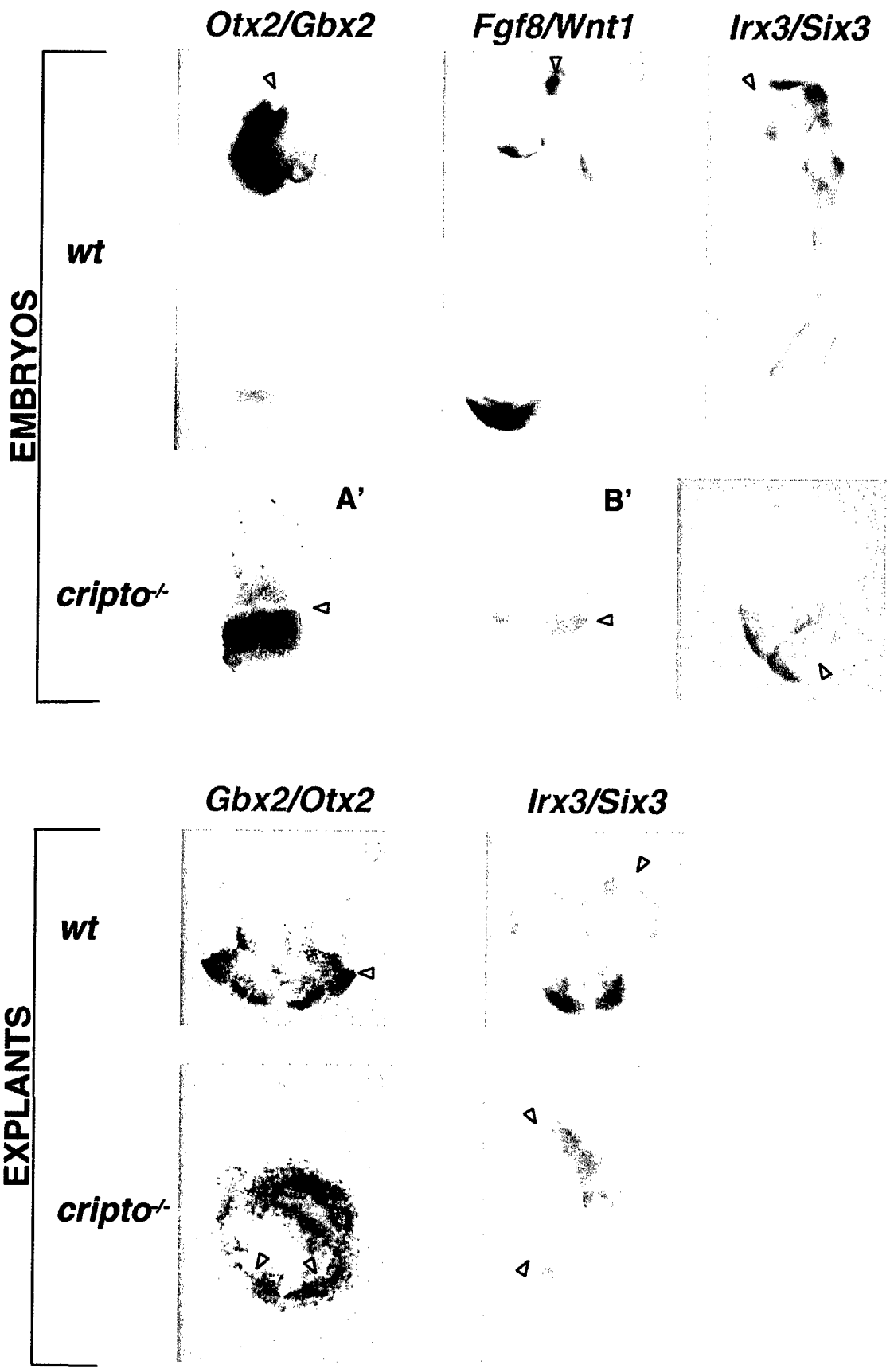

Fig. 7. Topological conservation of the anterior neural domains in *cripto*$^{-/-}$ embryos and explants. *Otx2* and *Gbx2* expression domains are close to each other in correspondence of the wt isthmus (A, D) and are still adjacent in *cripto*$^{-/-}$ embryo (A′) and explant (D′). *Fgf8* and *Wnt1* expression, identifying two adjacent narrow stripes in the isthmic region of the wt embryo (B) and showing a similar pattern in *cripto*$^{-/-}$ mutant (B′). *Six3* and *Irx3* expression domains in wt embryo (C) and explant (E), identifying the first the ventral forebrain and the second the caudal diencephalon, the mesencephalon, and the anterior hindbrain. Conservation of the topological relationships between *Six3* and *Irx3* expression domains in *cripto*$^{-/-}$ embryo (C′) and explant (E′). Arrowheads label the limit between the expression patterns.

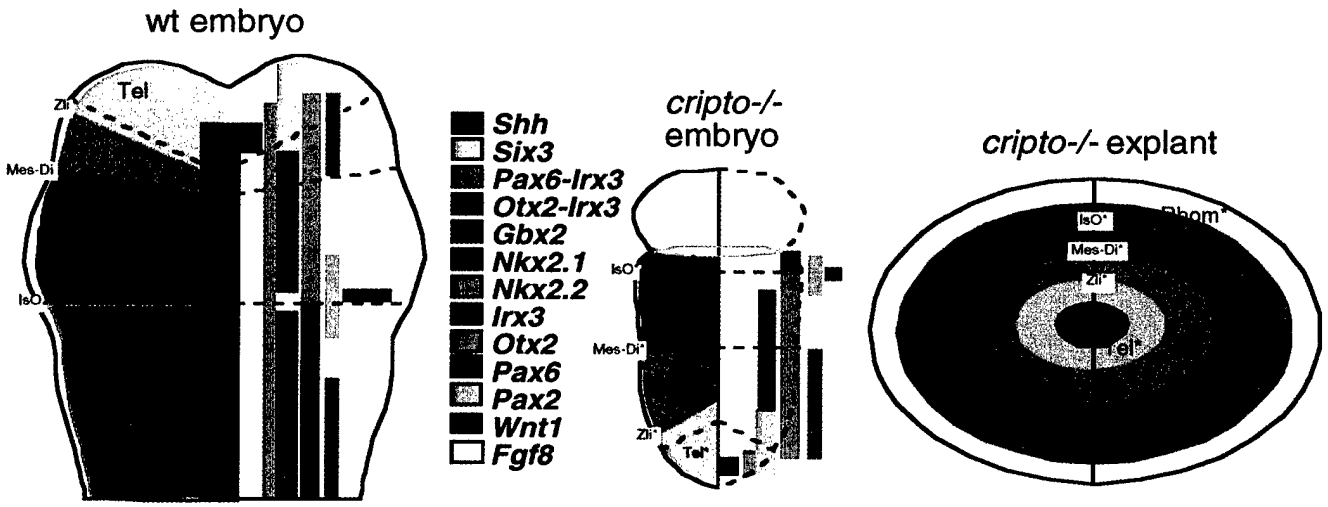

Fig. 8. Schematic comparison of the expression domains of diagnostic anterior neural markers in wt and *cripto*$^{-/-}$ embryos. The topological relationship among the different domains is conserved in *cripto*$^{-/-}$ embryo, denoting that an A/P axis is recognizable inside the mutant neuroectoderm, but still oriented along the embryonic P/D axis. The result is a distribution of the different expression domains as consecutive rings along the P/D axis of *cripto*$^{-/-}$ embryo and, thus, as concentric circles in *cripto*$^{-/-}$ explant, with the anterior neural region in the center of mutant explants and the more posterior domains in progressive external rings. Abbreviations: Di, diencephalon; IsO, isthmic organizer; Mes, mesencephalon; Rhom, rhombencephalon; Tel, telencephalon; ZLI, zona limithans intrathalamica. The asterisks refer to regions in the *cripto*$^{-/-}$ embryos.

ectoderm of *cripto*$^{-/-}$ mutants shows a similar expression of the pan-neural marker *Sox2*, thus demonstrating neural identity. Furthermore, we used both single and double WISHs to reveal a coordinated spatiotemporal expression of all the diagnostic markers analyzed within the neural tissue of *cripto*$^{-/-}$ embryos, identifying forebrain, midbrain, and anterior hindbrain territories. Mutually repressive interactions that occur in wt embryos between the *Otx2* and *Gbx2* or between the *Six3* and *Irx3* genes appear also conserved in *cripto*$^{-/-}$ mutants, since sharp boundaries of these expression patterns are clearly equivalent to the boundaries observed in control embryos. Several papers have demonstrated that the development of delimited edges between different domains is based on the onset of such molecular repressive interactions (Garda et al., 2001; Kobayashi et al., 2002). Finally, *Wnt1* and *Fgf8* expression in *cripto*$^{-/-}$ embryos, as in wt embryos, is located at the deduced boundary between *Otx2* and *Gbx2* expression domains. We conclude that topological relationships among the different anterior gene expression domains, and the relative neural territories, are surprisingly normal in *cripto* mutant embryos, in spite of their extreme degeneration and the absence of both the node and primitive streak.

However, in *cripto*$^{-/-}$ embryos, the anterior neural markers are expressed distally, while more posterior neural genes are expressed proximally (Fig. 8), thus indicating that the A/P axis of the anterior neuroectoderm in *cripto*$^{-/-}$ mutants is oriented along the embryonic P/D axis. In addition, the specification and maintenance of anterior neural identities at the distal tip of *cripto*$^{-/-}$ embryos suggest that the head organizing activity is located distally in these mutants. There might, of course, be additional proximal influence from the boundary between the neural ectoderm and the extraembryonic tissues.

We used in vitro embryo culture to investigate the nature (labile or stable) of the anterior regionalization observed in *cripto*$^{-/-}$ mutants. Both wt neural tube and *cripto*$^{-/-}$ explants preserve tissue integrity and morphology during the time of in vitro culture and both show normal reciprocal localization of the expression domains of several regional markers. Therefore, *cripto*$^{-/-}$ explants, even after 24 h of in vitro culture, maintain anterior neural patterning.

Anterior neuroectoderm of cripto null mutants develops domains that can be characterized as the isthmic organizer and as the ZLI but not as the ANR

The refinement of anterior neural patterning is due to secondary organizers, located at discrete transverse domains of the developing neural primordium and secreting morphogenetic signals that refine the identity of the neighbouring neuroepithelial cells (Echevarría et al., unpublished observations; Martínez and Simeone, 1999). The most studied secondary organizer is the isthmic organizer (Martínez et al., 1991), which is located at the midbrain–hindbrain boundary. In this region, *Fgf8* gene is expressed in correspondence with the contact area between the *Otx2* and *Gbx2* expression domains (Garda et al., 2001). Fgf8 protein has been demonstrated as being the effector molecule for the morphogenetic activities of the isthmus, controlling midbrain and anterior hindbrain regionalization (Crossley et al., 1996; Martínez et al., 1999). There is evidence for an additional secondary organizer, the ANR, which has been implicated in the prosencephalon regionalization. The ANR

also expresses and acts through Fgf8 (Shimamura and Rubenstein, 1997). Moreover, a third neuroepithelial region, the zona limitans intrathalamica (ZLI), situated in the middle of the diencephalic alar plate and related to the alar *Shh* expression (Rubenstein et al., 1994, 1998), has recently been proposed as an organizing center (Echevarria et al., unpublished observations). In the mouse, the ZLI presumptive domain has been identified in the neural plate by *Fgf8* inductive experiments, even earlier than the onset of *Shh* expression (Shimamura and Rubenstein, 1997). From a recent work by the Shimamura group, it can be deduced that, at least in the chick embryo, the ZLI is specified in the contacting domains of *Six3* and *Irx3* expression (Kobayashi et al., 2002).

Our data demonstrate that *cripto* null mutants develop the molecular pattern that characterizes the isthmic organizer (Martínez, 2001; Wassarman et al., 1997; Wurst and Bally-Cuif, 2001). In fact, *cripto*$^{-/-}$ embryos express *Fgf8* in a sharp band at the boundary between *Otx2* (forebrain and midbrain) and *Gbx2* (anterior hindbrain) domains, caudally to the *Wnt1* expression. On the other hand, *cripto* null mutants do not show any additional *Fgf8* expression, suggesting the absence of the ANR, which in control embryos arises at the junction between the most rostral part of the neural plate and the non-neural ectoderm. We hypothesize that the absence of the ANR in *cripto*$^{-/-}$ embryos might be due to the failure in the differentiation of non-neural ectoderm at the distal embryonic tip, which has been shown to express the pan-neural marker *Sox2*. Finally, although *cripto*$^{-/-}$ embryos fail to express *Shh* (Ding et al., 1998; and data not shown), they maintain the normal close and sharp-bounded expression domains of *Six3* and *Irx3* genes, suggesting that the ZLI presumptive domain might normally develop in *cripto*$^{-/-}$ mutants. The absence of *Shh* expression in *cripto*$^{-/-}$ embryos could be due to the lack of unknown additional mechanisms, including time.

The node and its derivatives might be dispensable for the maintenance of a regionalized anterior neural plate

There has been a long-standing controversy on the different roles to attribute to the node (and its derivatives) and the AVE in the ANP development. In fact, most of the genes that have been implicated in the formation of the ANP, such as *Lim1, Hesx1, Otx2,* and *nodal,* are expressed in both AVE and node derivatives (reviewed in Beddington and Robertson, 1998, 1999). *cripto* expression has been located in the forming mesoderm and primitive streak but has never been detected in the VE. The intrinsic value of *cripto* null mutants is, therefore, that, unlike the other null mutants that lack the node and/or its derivatives, *cripto*$^{-/-}$ embryos present a presumably normal VE. *cripto*$^{-/-}$ embryos, thus, provide an appropriate mouse mutant model to investigate whether and to which extent the AVE can mediate both the ANP regionalization and maintenance of anterior neural identity. Our molecular analysis of *cripto*$^{-/-}$ phenotype shows for the first time that *cripto* mutant embryos express diencephalic- and isthmic-specific markers. Interestingly, we have observed that all the genetic expression domains appeared in a topologically ordered manner, just as we can detect in the neural tube of control embryos. This *cripto*$^{-/-}$ anterior neural patterning is conserved after 24 h of in vitro culture. We propose that the persistence of ANP regionalization in the absence of the node and its derivatives may be the result of AVE morphogenetic activity. Since the AVE has been shown to fail to move anteriorwards, rather it persists at the distal tip of *cripto*$^{-/-}$ embryos (Ding et al., 1998), we therefore speculate that the signals emitted by the AVE provide neuroectodermal cells with the positional information necessary for the ANP regionalization. Therefore, even from its ectopic distal location, the AVE might induce a concentric regionalization in the mutant "neural sac." However, we cannot exclude the possibility of an organizer activity in the proximal epiblast or at the boundary between the epiblast and the extraembryonic regions (see Foley et al., 2000; Streit et al., 2000), despite the absence of both morphological and molecular evidence of primitive streak and node (Ding et al., 1998; and our unpublished results). Thus, a proximal organizer might cooperate with the AVE to develop the proximodistal regionalization pattern of the ANP in *cripto* mutants.

We draw attention to two further aspects of our work. First, the detection of the radial symmetry in *cripto* mutants, which fail to gastrulate, let us speculate that the phenomenon of gastrulation might be an evolutionary requirement for A/P axis and bilateral symmetry development in a previously radially organized embryo. Second, the presence of the *Bf1, Six3, Pax6, Nkx2.1,* and *Nkx2.2* transcripts in the distal region of *cripto* mutants indicates that expression of anterior neural markers does not strictly require ANR or *Shh* expression in the ZLI. Since previous analysis on gene-inducing abilities of the ANR and of *Shh* has instead shown their involvement in the control of *Bf1* and of *Nkx2.1* and *Nkx2.2* expression, respectively (Barth and Wilson, 1995; Pabst et al., 2000; Pera and Kessel, 1997; Shimamura and Rubenstein, 1997), our data point to the existence of additional and still unknown mechanisms that regulate gene expression patterns inside the developing CNS.

Acknowledgments

We are grateful to the late Dr. R. Beddington and to Drs. A. Simeone, J. Rossant, and Y. Saga for the generous gift of the probes and for their critical and helpful discussions. We are also grateful to Dr. G. Minchiotti and Prof. J. McGhee for their highly useful and much appreciated suggestions. We thank Mrs. M. Terracciano and Mrs. F. Almagro for technical assistance and Miss M. D'Agostino for correcting and typing the manuscript. This work was supported by grants from the BioGem S.C.A.R.1. Associazione Italiana Ricerca sul Cancro (AIRC) and CNR, PS Murst (to G.P.),

and by EU grants QLG2-CT-1999-00793, QLRT-1999-31556, 1999-31625, 2000-02310, and Spanish MCT grant DGI BFI2002-02979, DIGESIC-MEC PM98-0056, FEDER-1FD97-2090, and also from the Generalitat Valenciana CTDIA/2002/91 (to S.M. and D.E.). BioGem s.c a r.l. provides R.I. salary. G.L. has been awarded an EMBO short term fellowship. This text has been proofread by Helen Warburton, (H & A), Valencia, Spain.

References

Acampora, D., Mazan, S., Lallemand, Y., Avantaggiato, V., Maury, M., Simeone, A., Brûlet, P., 1995. Forebrain and midbrain regions are deleted in Otx2$^{-/-}$ mutants due to a defective anterior neuroectoderm specification during gastrulation. Development 121, 3279–3290.

Ang, S.L., Rossant, J., 1994. HNF-3 beta is essential for node and notochord formation in mouse development. Cell 78, 561–574.

Barth, K.A., Wilson, S.W., 1995. Expression of zebrafish nk2.2 is influenced by sonic hedgehog/vertebrate hedgehog-1 and demarcates a zone of neuronal differentiation in the embryonic forebrain. Development 121, 1755–1768.

Beddington, R.S.P., 1994. Induction of a second neural axis by the mouse node. Development 120, 613–620.

Beddington, R.S.P., 1998. Cripto-analysis of embryonic codes. Nature 395, 641–643.

Beddington, R.S.P., Robertson, E.J., 1998. Anterior patterning in the mouse. Trends Genet. 14, 277–284.

Beddington, R.S.P., Robertson, E.J., 1999. Axis development and early asymmetry in mammals. Cell 96, 195–209.

Bosse, A., Zulch, A., Becker, M.B., Torres, M., Gomez-Skarmeta, J.L., Modolell, J., Gruss, P., 1997. Identification of the vertebrate Iroquois homeobox gene family with overlapping expression during early development of the nervous system. Mech. Dev. 69, 169–181.

Broccoli, V., Boncinelli, E., Wurst, W., 1999. The caudal limit of Otx2 expression positions the isthmic organizer. Nature 401, 164–168.

Camus, A., Davidson, B.P., Billiards, S., Khoo, P., Rivera-Perez, J.A., Wakamiya, M., Behringer, R.R., Tam, P.P., 2000. The morphogenetic role of midline mesendoderm and ectoderm in the development of the forebrain and the midbrain of the mouse embryo. Development 127, 1799–1813.

Collignon, J., Sockanathan, S., Hacker, A., Cohen-Tannoudji, M., Norris, D., Rastan, S., Stevanovic, M., Goodfellow, P.N., Lovell-Badge, R., 1996. A comparison of the properties of Sox-3 with Sry and two related genes, Sox-1 and Sox-2. Development 122, 509–520.

Conlon, F.L., Lyons, K.M., Takaesu, N., Barth, K.S., Kispert, A., Herrmann, B., Robertson, E.J., 1994. A primary requirement for nodal in the formation and maintenance of the primitive streak in the mouse. Development 120, 1919–1928.

Crossley, P.H., Martin, G.R., 1995. The mouse Fgf8 gene encodes a family of polypeptides and is expressed in regions that direct outgrowth and patterning in the developing embryo. Development 121, 439–451.

Crossley, P.H., Martínez, S., Martin, G.R., 1996. Midbrain development induced by FGF8 in the chick embryo. Nature 380, 66–68.

Ding, J., Yang, L., Yan, Y.T., Chen, A., Desai, N., Wynshaw-Boris, A., Shen, M.M., 1998. Cripto is required for correct orientation of the anterior–posterior axis in the mouse embryo. Nature 395, 702–707.

Dono, R., Scalera, L., Pacifico, F., Acampora, D., Persico, M.G., Simeone, A., 1993. The murine Cripto gene: expression during mesoderm induction and early heart morphogenesis. Development 118, 1157–1168.

Echelard, Y., Epstein, D.J., St-Jacques, B., Shen, L., Mohler, J., McMahon, J.A., McMahon, A.P., 1993. Sonic hedgehog, a member of a family of putative signaling molecules, is implicated in the regulation of CNS polarity. Cell 75, 1417–1430.

Echevarria, D., Vieira, C., Martínez, S., 2001. Mammalian neural tube grafting experiments: an in vitro system for mouse experimental embryology. Int. J. Dev. Biol. 45, 895–902.

Foley, A.C., Skromne, I., Stern, C.D., 2000. Reconciling different models of forebrain induction and patterning: a dual role for the hypoblast. Development 127, 3839–3854.

Garda, A., Echevarria, D., Martínez, S., 2001. Neuroepithelial co-expression of Gbx2 and Otx2 precedes Fgf8 expression in the isthmic organizer. Mech. Dev. 101, 111–118.

Hatini, V., Tao, W., Lai, E., 1994. Expression of winged helix genes, BF-1 and BF-2, define adjacent domains within the developing forebrain and retina. J. Neurobiol. 25, 1293–1309.

Hallonet, M., Kaestner, K.H., Martin-Parras, L., Sasaki, H., Betz, U.A., Ang, S.L., 2002. Maintenance of the specification of the anterior definitive endoderm and forebrain depends on the axial mesendoderm: a study using HNF3beta/Foxa2 conditional mutants. Dev. Biol. 243, 20–33.

Joyner, A.L., 1996. Engrailed, Wnt and Pax genes regulate midbrain-hindbrain development. Trends Genet. 12, 15–20.

Klingensmith, J., Ang, S.L., Bachiller, D., Rossant, J., 1999. Neural induction and patterning in the mouse in the absence of the node and its derivatives. Dev. Biol. 216, 535–549.

Kobayashi, D., Kobayashi, M., Matsumoto, K., Ogura, T., Nakafuku, M., Shimamura, K., 2002. Early subdivisions in the neural plate define distinct competence for inductive signals. Development 129, 83–93.

Lemaire, P., Kodjabachian, L., 1996. The vertebrate organizer: structure and molecules. Trends Genet. 12, 525–531.

Li, J.Y., Joyner, A.L., 2001. Otx2 and Gbx2 are required for refinement and not induction of mid-hindbrain gene expression. Development 128, 4979–4991.

Liu, P., Wakamiya, M., Shea, M.J., Albrecht, U., Behringer, R.R., Bradley, A., 1999. Requirement for Wnt3 in vertebrate axis formation. Nat. Genet. 22, 361–365.

Martínez, S., 2001. The isthmic organizer and brain regionalization. Int. J. Dev. Biol. Special Issue 45, 367–371.

Martínez, S., Simeone, A., 1999. Specification and patterning of the rostral neural tube, in: di Porzio, U., Pernas-Alonso, R., Perrone-Capano, C. (Eds.) *Development of Dopaminergic Neurons,* R.G. Landers Company, TX.

Martínez, S., Crossley, P.H., Cobos, I., Rubenstein, J.L.R., Martin, G.R., 1999. FGF-8 induces an isthmic organizer and isthmocerebellar development in the caudal forebrain via a repressive effect on Otx2 expression. Development 126, 1189–1200.

Martínez, S., Wassef, M., Alvarado-Mallart, R.M., 1991. Induction of a mesencephalic phenotype in the 2-day-old chick prosencephalon is preceded by the early expression of the homeobox gene En. Neuron 6, 971–981.

Martinez-Barbera, J.P., Signore, M., Boyl, P.P., Puelles, E., Acampora, D., Gogoi, R., Schubert, F., Lumsden, A., Simeone, A., 2001. Regionalisation of anterior neuroectoderm and its competence in responding to forebrain and midbrain inducing activities depend on mutual antagonism between OTX2 and GBX2. Development 128, 4789–4800.

Millet, S., Campbell, K., Epstein, D.J., Losos, K., Harris, E., Joyner, A.L., 1999. A role for Gbx2 in repression of Otx2 and positioning the mid/hindbrain organizer. Nature 401, 161–164.

Minchiotti, G., Parisi, S., Liguori, G., Signore, M., Lania, G., Adamson, E.D., Lago, C.T., Persico, M.G., 2000. Membrane-anchorage of Cripto protein by glycosylphosphatidylinositol and its distribution during early mouse development. Mech. Dev. 90, 133–142.

Minchiotti, G., Parisi, S., Liguori, G.L., D'Andrea, D., Persico, M.G., 2002. Role of the EGF-CFC gene cripto in cell differentiation and embryo development. Gene 287, 33–37.

Oliver, G., Mailhos, A., Wehr, R., Copeland, N.G., Jenkins, N.A., Gruss, P., 1995. Six3, a murine homologue of the sine oculis gene, demarcates the most anterior border of the developing neural plate and is expressed during eye development. Development 121, 4045–4055.

Pabst, O., Herbrand, H., Takuma, N., Arnold, H.H., 2000. NKX2 gene expression in neuroectoderm but not in mesendodermally derived structures depends on sonic hedgehog in mouse embryos. Dev. Genes Evol. 210, 47–50.

Pera, E.M., Kessel, M., 1997. Patterning of the chick forebrain anlage by the prechordal plate. Development 124, 4153–4162.

Reissmann, E., Jornvall, H., Blokzijl, A., Andersson, O., Chang, C., Minchiotti, G., Persico, M.G., Ibanez, C.F., Brivanlou, A.H., 2001. The orphan receptor ALK7 and the Activin receptor ALK4 mediate signaling by Nodal proteins during vertebrate development. Genes Dev. 15, 2010–2022.

Rhinn, M., Dierich, A., Shawlot, W., Behringer, R.R., Le Meur, M., Ang, S.L., 1998. Sequential roles for Otx2 in visceral endoderm and neuroectoderm for forebrain and midbrain induction and specification. Development 125, 845–856.

Rowitch, D.H., McMahon, A.P., 1995. Pax2 expression in the murine neural plate precedes and encompasses the expression domain of Wnt8 and En1. Mech. Dev. 52, 3–8.

Rubenstein, J.L.R., Martínez, S., Shimamura, K., Puelles, L., 1994. The embryonic vertebrate forebrain: the prosomeric model. Science 266, 578–580.

Rubenstein, J.L.R., Shimamura, K., Martínez, S., Puelles, L., 1998. Regionalization of the prosencephalic neural plate. Annu. Rev. Neurosci. 21, 445–477.

Shawlot, W., Behringer, R.R., 1995. Requirement for Lim1 in head-organizer function. Nature 374, 425–430.

Shawlot, W., Wakamiya, M., Kwan, K.M., Kania, A., Jessell, T.M., Behringer, R.R., 1999. Lim1 is required in both primitive streak-derived tissues and visceral endoderm for head formation in the mouse. Development 126, 4925–4932.

Shen, M.M., Schier, A.F., 2000. The EGF-CFC gene family in vertebrate development. Trends Genet. 16, 303–309.

Shimamura, K., Rubenstein, J.L., 1997. Inductive interactions direct early regionalization of the mouse forebrain. Development 124, 2709–2718.

Shimamura, K., Hartigan, D.J., Martínez, S., Puelles, L., Rubenstein, J.L., 1995. Longitudinal organization of the anterior neural plate and neural tube. Development 121, 3923–3933.

Simeone, A., 1999. Detection of mRNA in tissue sections with radiolabelled riboprobes, in Wilkinson, D.G. (Ed.), In Situ Hybridization. A Practical Approach, 2nd edition, Oxford University Press, Oxford, pp. 69–86.

Simeone, A., Acampora, D., Gulisano, M., Stornaiuolo, A., Boncinelli, E., 1992. Nested expression domains of four homeobox genes in developing rostral brain. Nature 358, 687–690.

Streit, A., Berliner, A.J., Papanayotou, C., Sirulnik, A., Stern, C.D., 2000. Initiation of neural induction by FGF signalling before gastrulation. Nature 406, 74–78.

Tam, P.P., Steiner, K.A., 1999. Anterior patterning by synergistic activity of the early gastrula organizer and the anterior germ layer tissues of the mouse embryo. Development 126, 5171–5179.

Thomas, P., Beddington, R.S.P., 1996. Anterior primitive endoderm may be responsible for patterning the anterior neural plate in the mouse embryo. Curr. Biol. 6, 1487–1496.

Varlet, I., Collignon, J., Robertson, E.J., 1997. Nodal expression in the primitive endoderm is required for specification of the anterior axis during mouse gastrulation. Development 124, 1033–1044.

Walther, C., Gruss, P., 1991. Pax-6, a murine paired box gene, is expressed in the developing CNS. Development 113, 1435–1449.

Wassarman, K.M., Lewandoski, M., Campbell, K., Joyner, A.L., Rubenstein, J.L.R., Martínez, S., Martin, G.R., 1997. Specification of the anterior hindbrain and establishment of a normal mid/hindbrain organizer is dependent on Gbx2 gene function. Development 124, 2923–2934.

Weinstein, D.C., Ruiz i Altaba, A., Chen, W.S., Hoodless, P., Prezioso, V.R., Jessell, T.M., Darnell Jr., J.E., 1994. The winged-helix transcription factor HNF-3 beta is required for notochord development in the mouse embryo. Cell 78, 575–588.

Wurst, W., Bally-Cuif, L., 2001. Neural plate patterning: upstream and downstream of the isthmic organizer. Nat. Rev. Neurosci. 2, 99–108.

Xu, C., Liguori, G., Persico, M.G., Adamson, E.D., 1999. Abrogation of the Cripto gene in mouse leads to failure of postgastrulation morphogenesis and lack of differentiation of cardiomyocytes. Development 126, 483–494.

Yan, Y.T., Liu, J.J., Luo, Y.E.C., Haltiwanger, R.S., Abate-Shen, C., Shen, M.M., 2002. Dual roles of Cripto as a ligand and coreceptor in the nodal signaling pathway. Mol. Cell. Biol. 22, 4439–4449.